Resource Allocation for Coordinated Multipoint Joint Transmission System and Received Signal Strength Based Positioning in Long Term Evolution Network

Thesis submitted in accordance with the requirements of

the University of Liverpool for the degree of Doctor in Philosophy

By

Yang Li

September 2017

Declaration

The work in this thesis is based on research carried out at the University of Liverpool. No part of this thesis has been submitted elsewhere for any other degree or qualification and it is all my own work unless referenced to the contrary in the text.

Yang Li

Liverpool, United Kingdom

Abstract

The Long-Term Evolution Advanced (LTE-A) system are expected to provide high speed and high quality services, which are supported by emerging technologies such as Coordinated Multipoint (CoMP) transmission and reception. Dynamic resource allocation plays a vital role in LTE-A design and planning, which is investigated in this thesis. In addition, Received Signal Strength (RSS) based positioning is also investigated in orthogonal frequency division multiplexing (OFDM) based wireless networks, which is based on an industry project.

In the first contribution, a physical resource blocks (PRB) allocation scheme with fuzzy logic based user selection is proposed. This work considers three parameters and exploit a fuzzy logic (FL) based criterion to categorize users. As a result, it enhances accuracy of user classification. This work improves system capacity by a ranking based PRBs allocation schemes. Simulation results show that proposed fuzzy logic based user selection scheme improves performance for CoMP users. Proposed ranking based greedy allocation algorithm cut complexity in half but maintain same performance.

In the second contribution, a two-layer proportional-fair (PF) user scheduling scheme is proposed. This work focused on fairness between

CoMP and Non-CoMP users instead of balancing fairness in each user categories. Proposed scheme jointly optimizes fairness and system capacity over both CoMP and Non-CoMP users. Simulation results show that proposed algorithm significantly improves fairness between CoMP and Non-CoMP users.

In the last contribution, RSS measurement method in LTE system is analyzed and a realizable RSS measurement method is proposed to fight against multipath effect. Simulation results shows that proposed method significantly reduced measurement error caused by multipath. In RSS based positioning area, this is the first work that consider exploiting LTE's own signal strength measurement mechanism to enhance accuracy of positioning. Furthermore, the proposed method can be deployed in modern LTE system with limited cost.

Acknowledgement

Firstly, I would like to express my sincere gratitude to my supervisor Dr. Xu Zhu, for the continuous support of my Ph.D. study, for her great patience and immense knowledge. Her guidance helped me in all the time of research and life. I also appreciate warm helps from Prof. Yi Huang.

I am grateful to everyone in the Wireless Communication and Smart Grid group: Dr. Yufei Jiang, Mr. Teng Ma, Mr. Chaowei Liu, Dr. Chao Zhang, Dr. Jun Yin, Mr. Kainan Zhu, Mr. Qinyuan Qian, Dr. Zhongxiang Wei, Dr. Linhao Dong, for all the support and encouragement, research views, the greatest dishes and dinner parties.

I would like to thank Ms. Zhenzhen Song for the constant support and encouragement. I couldn’t make it without you.

Finally, my gratitude is dedicated to my parents. I love you.

Contents

List of Figures

List of Tables

Abbreviations

2G	second generation
3G	third generation
3GPP	3rd generation partnership project
ANN	artificial neural network
AOA	angle-of-arrival
CDF	cumulative distribution function
CDMA2000	code division multiple access 2000
CIR	channel impulse response
CoMP	coordinated multipoint
CS/CB	coordinated scheduling or beamforming
DCEM	dynamic circle expanding mechanism
eNB	eNodeB
EV-DO	evolution-data optimized
EXP-PF	exponential proportional fair
FL	fuzzy logic
FP	fingerprinting
GPS	global positioning system
GSM	global system for mobile communications

HSPA	high speed packet access
ICI	inter-cell interference
ISI	inter-symbol interference
JP	joint processing
LLS	linear least square
LMU	location measurement unit
LS	least square
LTE	long term evolution
LTE-A	long term evolution advanced
ML	maximum likelihood
M-LWDF	modified largest weighted delay first
NLLS	non-linear least square
OFDM	orthogonal frequency division multiplexing
PAPR	high peak-to-average power ratio
PF	proportional-fair
PL	path loss
PLE	path loss exponent
PLES	path loss exponent searching
PRB	physical resource blocks
QoE	quality of experience
QoS	quality of service
RA	resource allocation

RN	reference nodes
RS	reference signal
RSRP	reference signal received power
RSS	received signal strength
SDP	semi-definite programming
SINR	interference and noise ratio
SMEGUS	simplified mean enhanced greedy
ST	simplified trilateration
TDMA	time-division multiple access
UE	user equipment
UMTS	universal mobile telecommunications system
USRG	user selection ranking greedy
WiMax	worldwide interoperability for microwave access

Mathematical Notations

$log_{10}(x)$	Logarithmic of *x* with base 10.
$E(\cdot)$	Statistical expectation.
$\sum$	Sum operator.
$\prod$	Multiplication operator.
e^x	Exponential function of *x*.
$exp(x)$	Exponential function of *x*.
$\bar{x}$	Average of *x*.
$\otimes$	Convolution.
$x \in \mathbf{X}$	*x* is an element of set **X**.
$\forall x \in \mathbf{X}$	*x* can be any element of set **X**.
$arg\ min/max$	Arguments of the minima/maxima
var(x,y,z)	Variance of elements in a list.

Chapter 1

Introduction

1.1 Motivation

In the past decades wireless communications have made a leap forward [1, 2]. Plenty of research activates have been carried out to improve system capacity [3], system coverage [4], quality of service (QoS) [5], and power consumption [6]. Long term evolution (LTE) network has been deployed globally, over 2 billion LTE subscriptions recorded due to early 2017 [7]. In some region LTE-Advanced network has been marketed. Although various techniques have been proved successful in last generation networks, as technology has advanced, much more effective methods of combating the previous problems have gained support [8].

As the fast developing of wireless communication market, the importance of inter-cell interference (ICI) attracts attention [7]. Coordinated Multipoint (CoMP) transmission and reception technologies, including Joint Processing (JP) and Coordinated Scheduling or Beamforming (CS/CB) has been consider as an advanced solution to

combating ICI in LTE-A network. With dynamic coordination of multiple geographically separated eNodeBs (eNB), the interference is reduced by being utilized constructively rather than destructively [8]. In addition, coordinated eNBs are able to enhance user equipment's (UE) received power and connection quality [9]. Meanwhile adaptive resource allocation (RA) and user scheduling plays important roles in multi-carrier based wireless networks [10-13]. System capacity can be improved significantly with optimal dynamic resource allocation algorithms. User scheduling is essential to ensure fair quality of service [14]. Therefore, resource allocation and user scheduling are critical in CoMP system.

User selection is the first challenge in CoMP system. CoMP users require resource from multiple eNBs. With limitation of system resource, CoMP user selection must be accurate to ensure good service quality for both CoMP and Non-CoMP users. Power allocation had been discussed in many works, but frequency resource allocation for CoMP system didn't get much attention. Frequency resource occupied by CoMP users cannot be used by Non-CoMP users in same cluster. Therefore, fairness among CoMP and Non-CoMP users is another challenge.

Location based service (LBS) is now widely deployed with mass popularity of smart phones. Global position system (GPS) becomes regular accessory of modern cellphones. However, it only operates in open area and energy consumption is high [15]. Network based positioning had been

discussed to assist GPS to improve its positioning performance. Received signal strength (RSS) based positioning is the most convenient and cheapest method. User's distance from base station can be calculated from RSS. With RSS data from multiple base station, user's location can be determined. The main challenge is that RSS data is affected by many factors. One of the most critical factors is multipath effect [16, 17].

1.2 Research Contributions

In this thesis, a physical resource blocks (PRB) allocation scheme with fuzzy logic (FL) based user selection is presents in the first. By applying this low-complexity scheme UE which locate at cell edge gain an improvement on network performance. After this, a two-layer proportional-fair user scheduling scheme is proposed to maximize CoMP system capacity and maintain fairness between users. In addition, a low-complexity received signal strength (RSS) based positioning algorithm is proposed for an industry project. An analysis of received signal strength measurement in LTE is presented in the end, in which a realizable measurement method is proposed to enhance accurate of RSS based positioning.

The research contributions during this PhD study is presented as the following:

- A physical resource blocks allocation scheme with fuzzy logic based user selection is proposed. This work is different from existing researches in the following aspects. First, instead of classifying users by single threshold, this work considers three parameters and exploit a fuzzy logic based criterion to categorize users. As a result, it enhances accuracy of user classification. Second, instead of investigating power control scheme to explore capacity potential, this work improves system capacity by a ranking based PRBs allocation schemes. Simulation results show that proposed fuzzy logic based user selection scheme improves system performance, especially for CoMP users. Proposed ranking based greedy allocation algorithm cut complexity in half but maintain same performance.
- A two-layer proportional-fair user scheduling scheme is proposed. This work is different from existing works in the following aspects. First, fairness between CoMP and Non-CoMP users are focused instead of balancing fairness in each user categories. Second, proposed scheme jointly optimizes fairness and system capacity over both CoMP and Non-CoMP users. Simulation results show that proposed algorithm significantly improves fairness between CoMP and Non-CoMP users without using predetermined PRBs limitation.
- RSS measurement method in LTE system is analyzed and a realizable RSS measurement method is proposed to fight against multipath effect.

The contribution of this work is that, in RSS based positioning area, this is the first work that consider exploiting LTE's own signal strength measurement mechanism to enhance accuracy of positioning. Furthermore, the proposed method is able to be deployed in modern LTE system with limited cost.

1.3 Thesis Organization

The rest of this thesis is organized as follows.

The wireless channels and systems are introduced in Chapter 2. Wireless communication channel models are presented in Section 2.1. In Section 2.2, an overview of wireless communication systems is presented. OFDM technique is also described in Section 2.2.

Literature review on RA of broadband wireless communication systems is presented in Chapter 3. In this chapter, the radio resource in wireless communication are described in Section 3.1. Literature reviews on resource allocation and scheduling are presented in Section 3.2. In Section 3.3, a brief introduction of Fuzzy Logic is presented.

PRB allocation scheme with fuzzy logic user selection and proposed two-layer proportional-fair user scheduling scheme are presents in Chapter 4. Section 4.1 presents the system model. Fuzzy logic based user selection and ranking based PRBs allocation algorithms are presented in Section 4.2.

Two-layer proportional-faire user scheduling is presented in Section 4.3. Section 4.4 presents the summary.

In Chapter 5, low-complexity RSS based positioning algorithm is presented, followed by analysis of proposed RSS measurement method in LTE. The low-complexity positioning method is presented in Section 5.1. The multipath reduced RSS measurement method is presented in Section 5.2. Section 5.3 gives the summary.

Conclusions and future work are presented in the final chapter.

1.4 Publication List

Conference Paper

1. Y. Li, X. Zhu, Y. Jiang, Y. Huang, and E. G. Lim, "Energy-efficient positioning for cellular networks with unknown path loss exponent," *IEEE International Conference on Consumer Electronics - Taiwan*, pp. 502-503, 2015 [18]

Chapter 2

Wireless Communication Channel and System

Wireless communication channel models are presented in Section 2.1. In Section 2.2, an overview of wireless communication systems is presented. OFDM technique is also described in Section 2.2.

2.1 Wireless Communication Channels

2.1.1 Large-Scale Path Loss

When an electromagnetic wave propagates from transmitter to the receiver, its signal strength decreases over distances. This reduction in power density is refereed as large-scale path loss (PL). Normally path loss is caused by diffraction, absorption, and the natural expansion of electromagnetic wave. After travelling the distance d, the received signal power P_r at receiver can be expressed as [19]

$$P_r(d) = \frac{P_t G_t G_r \lambda^2}{(4\pi)^2 d^\alpha L} \tag{2.1}$$

where P_t is transmitted power, G_t and G_r are transmitter and receiver antenna gains, respectively, λ is wavelength of radio wave, L represents system loss which is not related to propagation, α represents path loss exponent. Table 2.1 shows some typical value of PL exponent based on measured data.

Table 2.1: PL Exponent in Different Environments [19]

Environments	PL Exponent
Free space	2
Urban area	2.7 to 3.5
Shadowed urban	3 to 5
In building line-of-sight	1.6 to 1.8
Obstructed in building	4 to 6
Obstructed in factories	2 to 3

The path loss is defined as reduction of signal power between transmitter and receiver, which can be expressed as [19]

$$PL(d) = \frac{P_t}{P_r} = \frac{(4\pi)^2 d^\alpha L}{G_t G_r \lambda^2} \tag{2.2}$$

Rewrite (2.2) in dB,

$$PL(d) = PL_0 + 10\alpha log_{10}(d) \tag{2.3}$$

where $PL_0 = 10log_{10}\frac{(4\pi)^2 L}{G_t G_r \lambda^2}$ [15]. From (2.3), PL is mainly affected by the transmitted distance and PL plays an important role in wireless network planning and design [19].

2.1.2 Small-Scale Fading

Small-scale fading is the small and fast fluctuation of signal after travelling short time or distance. In urban area, receivers are normally blocked by obstruction from transmitter and line-of-sight path is not available for transmitting signal. The radio wave travels along several different paths to receiver with reflection, diffraction and scattering. Therefore, the received signal is a combination of a group of waves with randomly distributed amplitude, phase and delay.

2.1.2.1 Factors of Small-Scale Fading

Let g_i represent the channel gain and τ_i denote the delay of the ith path, the mean excess delay can be expressed as [19]

$$\bar{\tau} = E(\tau) = \frac{\sum_i |g_i|^2 \tau_i}{\sum_i |g_i|^2} \tag{2.4}$$

Then the root-mean-square (RMS) delay spread can be expressed as [19]

$$\mu = \sqrt{E[(\tau - \bar{\tau})^2]} = \sqrt{\overline{\tau^2} - \bar{\tau}^2} \tag{2.5}$$

The RMS delay spread measures the time dispersion of multipath channels. Large RMS value indicates heavy multipath effect.

The coherence bandwidth B_c is a threshold to decide if there is a high possibility of amplitude correlation between two frequency components. Coherence bandwidth Bc can be derived from the RMS delay spread μ, $.e., B_{c,50\%} \approx \frac{1}{5\mu}$ [19].

When relative motion exists between transmitter and receiver, Doppler Effect occurs. Assuming the velocity of this relative motion is v, the Doppler shift f_d is given by [19]

$$f_d = \frac{v}{\lambda} cos\theta \tag{2.6}$$

where θ is the angle between direction of receiver's and transmitter's motions. When receiver and transmitter move in same direction, Doppler shift reaches the maximum, $f_{d,max} = \frac{v}{\lambda}$.

The coherence time T_c is is a threshold to decide if there is a high

possibility of amplitude correlation between two signals [19].The coherence time T_c can be derived from the maximum Doppler shift $f_{d,max}$, $i.e., T_c \approx \frac{9}{16\pi f_{d,max}}$.

2.1.2.2 Types of Small-Scale Fading

There are four different types of small-scale fading, which are distinct with each other in characteristics of transmitted signal and multipath channel. Let T_s denote symbol period and B_s represent signal bandwidth, these four types of small-scale fading are presented in Table 2.2

Table 2.2: Four Types of Small-Scale Fading [19]

Fast Fading	$T_s > T_c$
Slow Fading	$T_s \ll T_c$
Flat Fading	$B_s < B_{c,50\%}$, $T_s > 5\mu$
Frequency Selective Fading	$B_s > B_{c,50\%}$, $T_s < 5\mu$

- Fast fading: The symbol period is longer than the coherence time ($T_s > T_c$). In this case, the channel changes so fast that the signal goes through different channels within one symbol period.
- Slow fading: The symbol period is much less than the coherence time ($T_s \ll T_c$). In this case, the channel remains unchanged over one or

more symbol periods.

- Flat fading: if the symbol period is larger than the RMS delay spread ($T_s > 5\mu$), or the bandwidth of the transmitted signal is smaller than the channel coherence bandwidth ($B_s < B_{c,50\%}$), all the frequency over transmitted bandwidth has almost the same channel gain and linear phase. Flat fading occurs in this case. Flat fading is the most common type described in the literature. The channel gains of flat fading follows different distributions such as Rayleigh fading, Nakagami fading, and Rician fading [19].
- Frequency selective fading: if the symbol period is smaller than the RMS delay spread of a wireless channel ($T_s < 5\mu$), or the bandwidth of the transmitted signal is larger than the channel coherence bandwidth ($B_s > B_{c,50\%}$), previous transmitted symbols could easily cause interference to current transmitted symbols. This interference is called inter-symbol interference (ISI). In the frequency domain, the ISI is presented by a formation that frequency components of the received signal's spectrum undergo different amplitudes. Hence, this fading is referred to as frequency selective fading.

2.1.3 Channel Model

Assuming that there are L paths between the transmitter and receiver, each path is independent in delays, and during transmission each symbol

is transmitted over signal bandwidth B_s during symbol period T_s, the channel impulse response (CIR) is given by [19]

$$g(t) = \sum_{i=0}^{L-1} g_i \delta(t - \tau_i) \tag{2.7}$$

where $\delta(\cdot)$ is the impulse function. When $L = 1$, this channel becomes a flat fading channel.

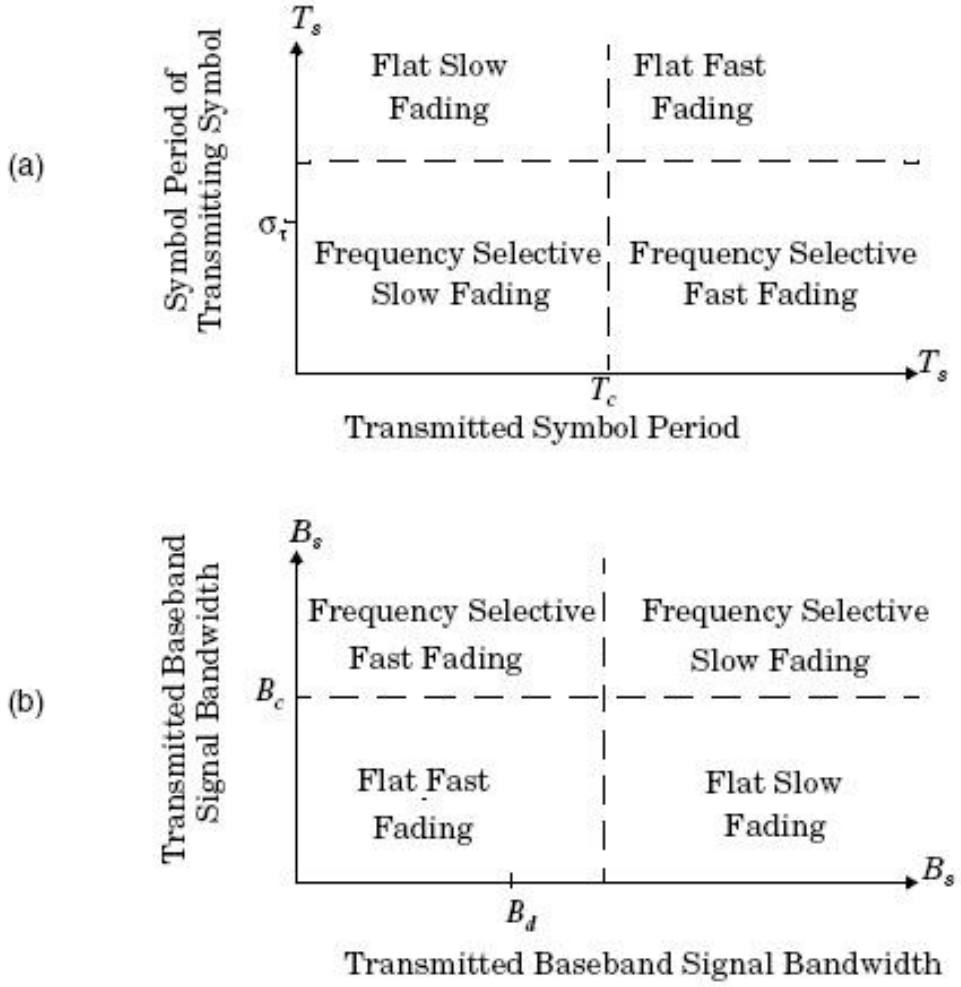

Figure 2.1: Four types of small-scale fading according to several parameters [19].

Assuming that g_i is an independent zero mean complex Gaussian random variable, with a variance of the following discrete exponential power delay profile [19]:

$$\boldsymbol{E}[|g_i|^2] = b \cdot exp\left(-\frac{\tau_i}{\mu}\right) \tag{2.8}$$

where b is the normalizing factor. Normally $|g_i|$ follows the Rayleigh distribution with a probability density function [19]:

$$p(|g_i|) = \frac{|g_i|}{V^2} exp\left(-\frac{|g_i|^2}{2V^2}\right), \qquad 0 \leq |g_i| < \infty \tag{2.9}$$

where V represents the RMS voltage value of the received signal, and V^2 is the time averaged power of the received signal.

Let $f(t)$ denote the pulse shape with the effects of the transmit and received filters, the overall CIR is the convolution of the physical CIR $g(t)$ and $f(t)$, which is expressed as [19]

$$h(t) = f(t) \otimes g(t) = \sum_{i=0}^{L-1} g_i f(t - \tau_i) \tag{2.10}$$

2.2 Wireless Communication Systems

2.2.1 Overview of Wireless Communication Systems

The first wireless communication experiment was conducted by Guglielmo Marconi in 1897. He built a radio station at Isle of Wright and started an era of using wireless communication [20]. Following his step, many inventors joined the world of wireless communication. In 1948, AT&T established the first commercialized mobile telephone service [21]. In 1960s, Richard H. Frenkiel proposed frequency reuse and handoff scheme, which is considered as the early model of modern cellular network [22].

The first cellular network “Advanced Mobile Phone System” was deployed in North America in 1978. In the early 1990s, thanks to the contribution of very-large-scale integration technologies on computer industry, the wireless technology came into the digital era.

In 1991 the first second generation (2G) wireless communication network, Global System for Mobile Communications (GSM) system, was launched in Finland. Until 2007, over 2 billion customers around the world had enjoyed service from GSM [2]. Even now GSM is still the main cellular network service in some region. In early 2000s Universal Mobile Telecommunications System (UMTS) [23] and Code Division Multiple Access 2000 (CDMA2000) [24] were deployed as the third generation (3G) network. Since that wireless communication network started to provide

various data services.

Within years the dramatic increasing demands of data services couldn't be satisfied by UMTS and CDMA2000. In 2003 and 2005 Evolution-Data Optimized (EV-DO) [25] and High Speed Packet Access (HSPA) [26], which are regarded as 3.5G standards, were launched to the market. The maximum download speeds for HSPA and EV-DO are 14.4 Mbit/s and 4.9×N Mbit/s, respectively, and their maximum upload speeds are 5.76 Mbit/s and 1.9×N Mbit/s, respectively, where N is the number of 1.25 MHz spectrum chunk used in EV-DO systems. The updated version of HSPA, which is called as HSPA+ [26], was proposed to improve the system capacity. The downlink and uplink peak data rates of HSPA+ are 42×N and 11×N, respectively, where N is the number of 5 MHz carriers employed.

Now in North Europe, Asia and America, Worldwide Interoperability for Microwave Access (WiMax) and Long-Term Evolution (LTE) systems have been deployed. Based on the IEEE 802.16 protocol, WiMAX can provide broadband access with downlink and uplink speeds up to 75 Mbit/s and 25 Mbit/s, respectively. Meanwhile, the current LTE, which belongs to 3rd generation partnership project (3GPP) release 8, offers up to 326.4 Mbit/s and 86.4 Mbit/s as the peak downlink and uplink data rates [27]. In 2010, WiMAX had been given up due to competition with LTE. LTE-Advanced were proposed in 2011 as the 4G standards to support peak

downlink data rate up to 1 Gbit/s and peak uplink data rate up to 500 Mbit/s [28]. In LTE-Advanced systems, relay and coordinated multipoint (CoMP) techniques are adopted to help improve the cell-edge performance [8, 28]. All the aforementioned wireless communication techniques are summarized in Table 2.3.

2.2.2 OFDM Technique

Orthogonal Frequency-Division Multiplexing (OFDM) was proposed in 802.11a as the modulation scheme to combat with frequency selective fading [28]. OFDM uses a group of orthogonal sub-carriers to carry data. The original data is transformed into several parallel data streams on each subcarrier. Then the sub-carriers are modulated with a conventional modulation scheme at a low symbol rate. Total data rate remains same to

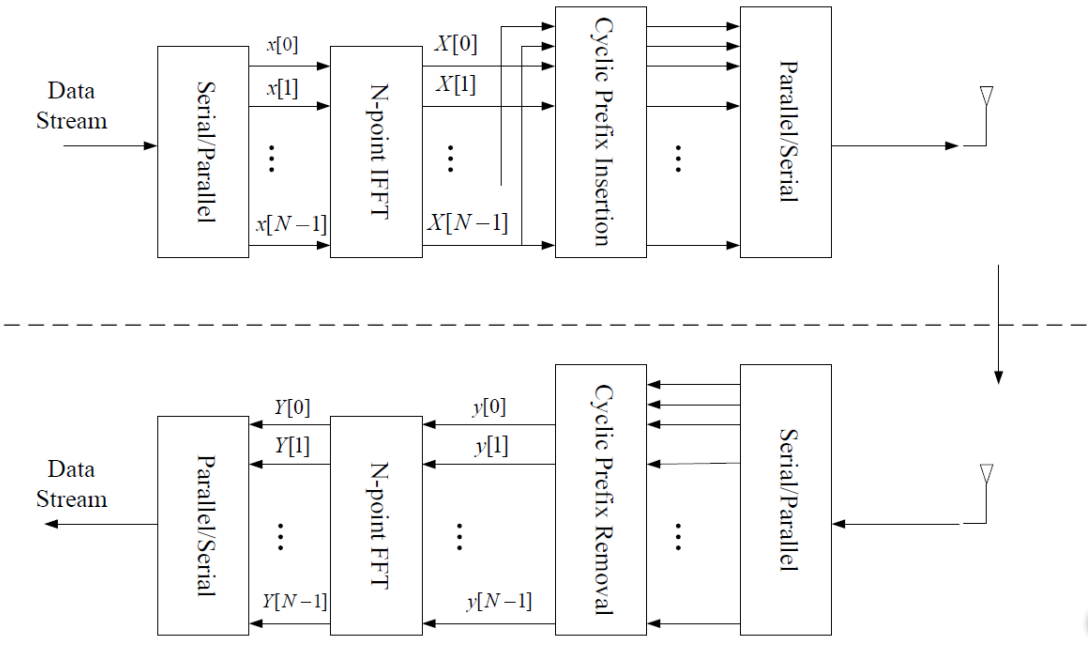

Figure 2.2: Block diagram of the OFDM transmission system [29]

Table 2.3: Comparison of mobile telephony standards

Family	Standard	Channel Bandwidth (MHz)	Peak Data Rates (Mbps)	Radio Tech
3GPP2	CDMA2000	1.25	0.307(DL) 0.307(UL)	CDMA
	EV-DO Rev.B	1.25·*N*	4.9·N(DL) 1.9·N(UL)	TDMA(DL) CDMA(UL)
	UMB	1.25·*N*	18.7·N(DL) 4.3·N(UL)	OFDMA MIMO
3GPP	UMTS	5	2(DL) 2(UL)	WCDMA
	HSPA	5	14.4(DL) 5.76(UL)	WCDMA
	HSPA+	5·*M*	42·N(DL) 11·N(UL)	WCDMA MIMO
	LTE	Up to 20	300(DL) 75(UL)	OFDMA(DL) SC-FDMA(UL) MIMO
	LTE-Advanced	Up to 100	1000(DL) 500(UL)	OFDMA(DL) SC-FDMA(UL) MIMO Relay CoMP
IEEE	WiMAX	5, 7, 8.75, 10	128(DL) 66(UL)	SOFDMA MIMO
	WiMAX 2	5 to 20	300(DL) 135(UL)	SOFDMA MIMO Relay

N =number of carriers, max. 15
M =number of carriers, max. 4

conventional single-carrier modulation schemes in the same bandwidth. The OFDM streams can be regarded as slowly-modulated narrow-band signals. Figure 2.3 shows Block diagram of OFDM in a communication system, where $x[n]$ $(n = 0, \dots, N-1)$ are the source symbols, and N is the number of sub-carriers. The cyclic prefix (CP) is designed to eliminate

the multipath effect when the OFDM symbols arrive at the receiver. The transmitted symbols after the inverse fast Fourier transform (IFFT) can be expressed as [29]

$$X[n] = \sum_{i=0}^{N-1} x[i] e^{j\frac{2\pi}{N}in}, n = 0, \dots, N-1 \qquad (2.11)$$

The received signals can be expressed as [29]

$$y[n] = h[n] \otimes X[n] + z[n], n = 0, \dots, N-1 \qquad (2.12)$$

where $h[n]$ is CIR and $z[n]$ is AWGN noise. The recovered signal can be expressed as [29]

$$\begin{aligned} \hat{x}[n] &= \sum_{i=0}^{N-1} y[i]\, e^{-j\frac{2\pi}{N}in}, n = 0, \dots, N-1 \\ &= FFT(h[n] \otimes X[n] + z[n]) \\ &= H_n x[n] + Z[n] \end{aligned} \qquad (2.13)$$

where H_n, $Z[n]$ are the CIR and AWGN noise on the nth sub-carrier in frequency domain.

According to Equation (2.10), the information of symbols has been

spread across N transmission data. Hence, the symbol period in OFDM system becomes NT_s which mitigates ISI. In frequency domain, the frequency range of each symbol is narrowed to B_s/N. Each subcarrier is in flat fading and can be processed independently. The original symbols can be detected by channel equalization method, such as zero-forcing (ZF). With estimation of channel information $\widehat{H}_n$, the result from ZF equalization can be written as [29]

$$\lim_{\widehat{H}_n \to H_n} \hat{x}[n] = \lim_{\widehat{H}_n \to H_n} \left(\frac{H_n x[n]}{\widehat{H}_n} + \frac{Z[n]}{\widehat{H}_n}\right)$$
$$= x[n] + \frac{Z[n]}{\widehat{H}_n} \qquad (2.14)$$

The error of estimated symbol $\hat{x}[n]$ depends on the accuracy of estimated channel information $\widehat{H}_n$ and noise $\frac{Z[n]}{\widehat{H}_n}$.

OFDM technique provide several benefits [29]. First, OFDM streams can be viewed as many slowly-modulated narrow-band signals which are in flat fading. This feature eliminates ISI problem in multipath environments. This feature also provides frequency diversity in OFDM systems, because not all subcarriers suffer fading in a multipath channel. Additionally, each subcarrier can be modulated indecently, which provides a higher spectral efficiency than single-carrier systems under frequency selective channel. OFDM is also computationally efficient by using FFT

techniques to implement the modulation and demodulation functions.

Orthogonal frequency division multiple access (OFDMA) [29] has same modulation scheme as OFDM and has a multiple access scheme that combines TDMA and FDMA. OFDMA allows multiple users to send data on the different subcarrier at the same time. However, OFDMA is highly sensitive to frequency offset. Its high peak-to-average power ratio (PAPR) due to in-phase addition of subcarriers, which is a critical problem for uplink transmission with limited power storage. To overcome this drawback, single carrier FDMA (SC-FDMA) is chosen as uplink method in LTE. Besides its lower PAPR, SC-FDMA has similar implementation structure to OFDMA, which is one of the reason that it is selected by LTE.

OFDMA system in cellular networks has been investigated in many literatures. In [30], the joint resource allocation (RA) algorithm with different constraints were proposed to minimize the total transmit power. A chunk-based RA algorithm were proposed in [31-33] to maximize the system throughput under the average bit-error-rate (BER) and total power constraints. In [34], a low-complexity RA algorithm was proposed to make trade-off between energy efficiency and spectral efficiency.

2.2.3 Coordinated Multipoint Transmission and Reception

The cell edges are the most challenging area to achieve high data speed in LTE-A. Not only is the signal lower in strength because of the distance from the base station (eNB), but also interference levels from neighboring eNBs are higher [8]. Coordinated multipoint requires coordination between a group of geographically separated eNBs, dynamically coordinate to provide joint scheduling and transmissions and reception. In this way, a user equipment (UE) at the edge of a cell can be served by two or more eNBs to improve signals reception / transmission and increase throughput particularly under cell edge conditions. CoMP techniques falls into two major categories:

- Joint processing (JP): Joint processing occurs where there is coordination between multiple entities - base stations - that are simultaneously transmitting or receiving to or from UEs.
- Coordinated scheduling or beamforming (CS/CB): CS/CB is a form of coordination where a UE is transmitting with a single transmission or reception point - base station. However, the communication is made with an exchange of control among several coordinated entities.

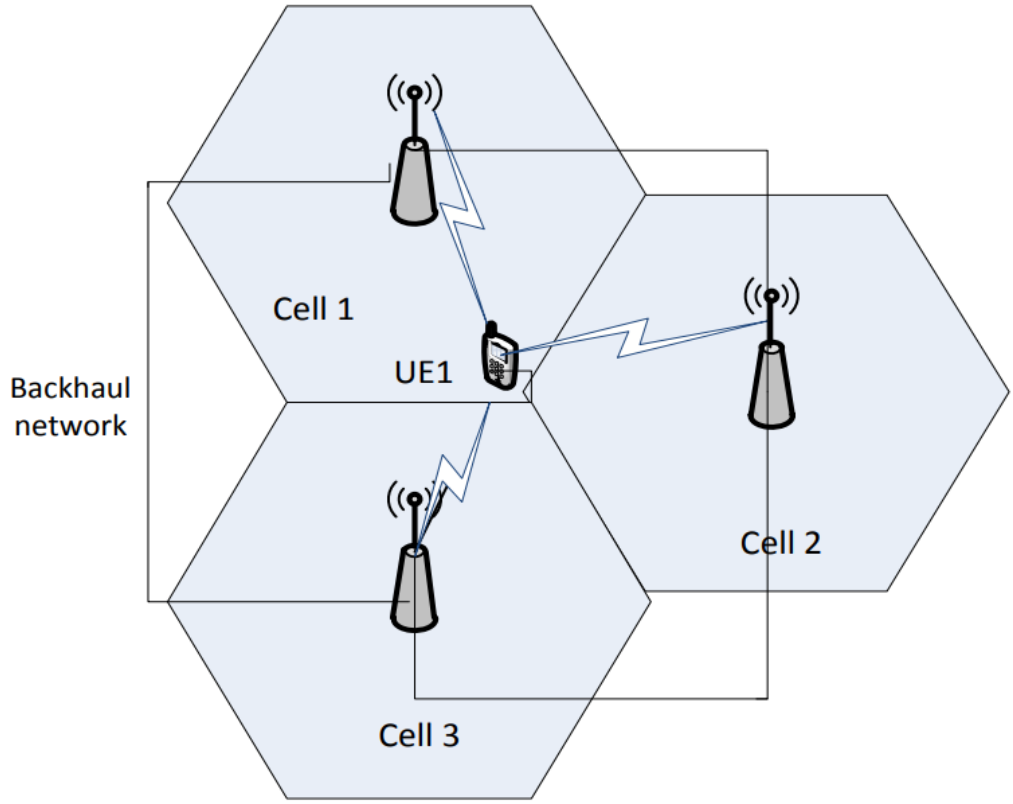

Figure 2.3: Coordinated Multipoint system in JP mode

In JP mode, eNBs share all transmit data and channel state information (CSI) of users through the backhaul links. Multiple BSs transmit data to one user simultaneously on the same frequency [3, 6]. Many CoMP-JP schemes were proposed in literatures. In [35], eNB power constraint and various transmission schemes were discussed. Authors in [36] proposed a block diagonalization method to maximizing the weighted sum-rate of all UEs in the downlink transmission with eNB power constraint. In [37], a cluster constructing strategy was proposed to reduce inter-cluster interference. In JP mode, both the CSI and users' data have to be shared among the coordinated eNBs, which is only valid for centralized networks.

In [38-40], authors proposed various techniques to address the practical issue, such as backhaul limitation, complexity of encoding and decoding. In practice, although coordinated eNBs can exchange information over the backhaul, such as X2-interfaces in LTE-A [41], complete coordination is not achievable due to the backhaul overhead and computational complexity.

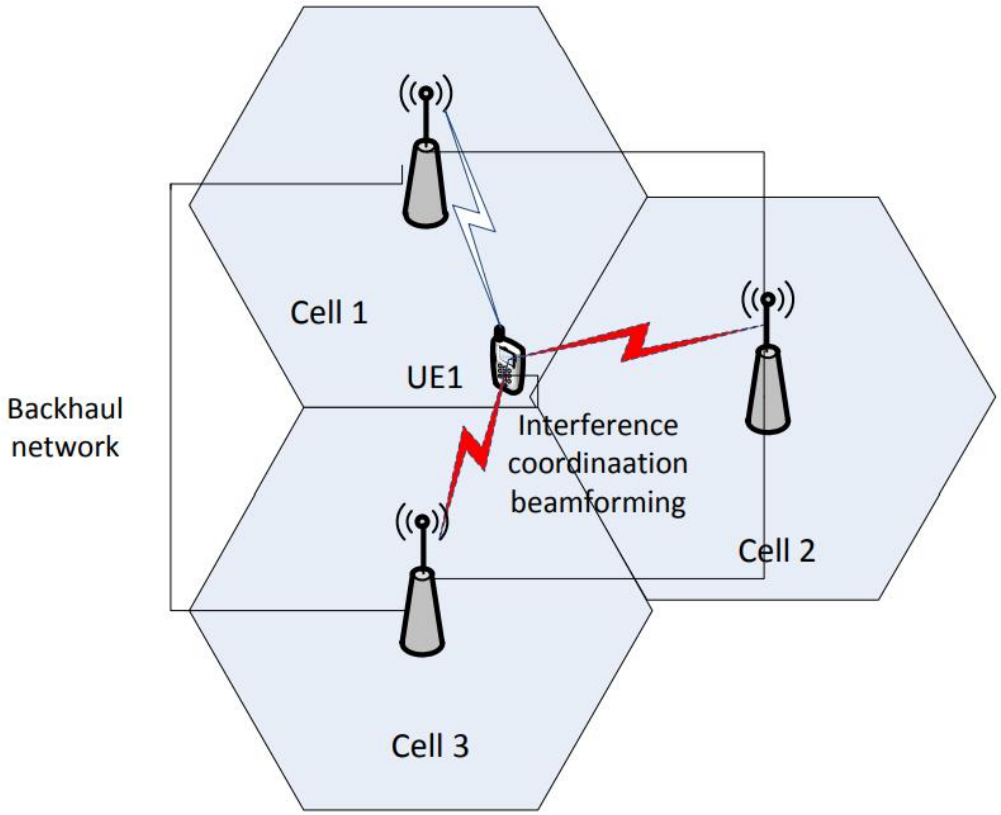

Figure 2.4: Coordinated Multipoint system in CS/CB mode

In CS/CB mode, signal for a UE is transmitted from only one single transmission point but the scheduling decision are coordinated among the coordinated eNBs [42, 43]. Transmit beamforming weight of each UE can reduce the interference from each other. CS/CB mode is more practical than JP mode because only partial information needed to be exchanged

over backhaul. Precoding matrix index (PMI) reporting algorithm was proposed in [44]. It mitigates the interference based on the report of a restricted or recommended PMI, which can provide a potential precoder at an interfering eNB. The CoMP UEs calculate and report the restricted or recommended PMIs to their serving cell and the PMIs are used as a precoder in interfering eNBs to improve performance. Zero-forcing beamforming was proposed in [45] to compute a new transmit filter based on the CSI feedback from serving and interfering eNBs to force the interference to be zero. In [46], a joint leakage suppression (JLS) filter was discussed by maximizing the signal-to-leakage-plus-noise ratio (SLNR) or the US served by the reference eNB. ZFBF and JLS based CB has more flexibility in system design than PMI reporting algorithm, but requiring more computational complexity, CSI accuracy and backhaul overhead.

Chapter 3

Overview of Resource Allocation for Broadband Wireless System

In this chapter, the radio resource in wireless communication are described in Section 3.1. Literature reviews on resource allocation and scheduling are presented in Section 3.2. Fuzzy Logic is introduced in Section 3.3.

3.1 Radio Resources in OFDM based Broadband Wireless Systems

Radio resources are usually referred to carrier frequency resource and transmit power. In multiuser wireless communication systems, channels condition is independent across each user. Channel condition is affected by many factors, i.e. user's position. Therefore, when the channel is in heavy fading for a user, it may be in a good condition for another user. In this scenario, the system can always choose the user with good channel

condition to transmit data to achieve a higher system capacity.

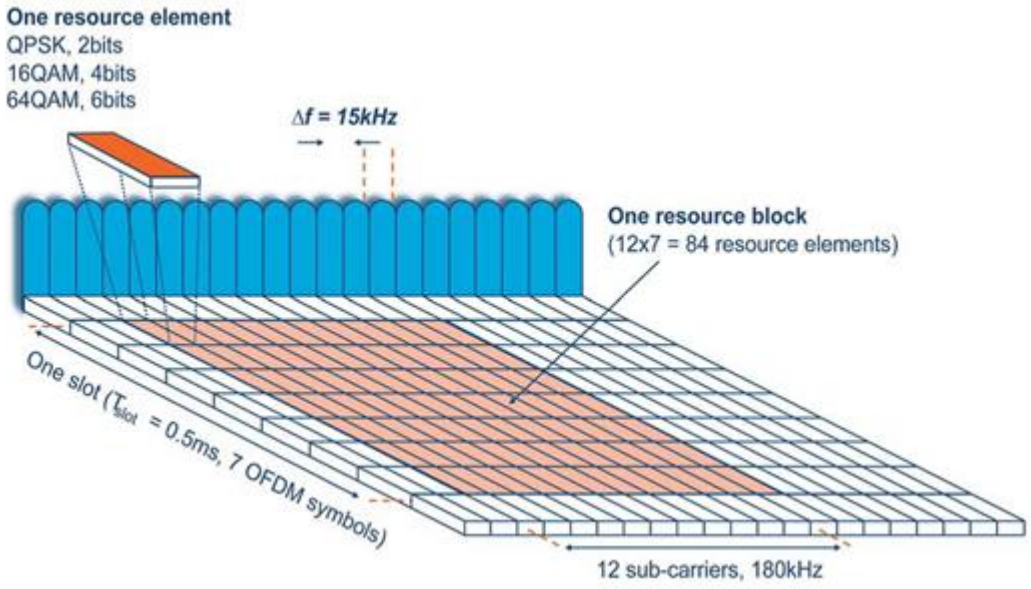

Figure 3.1: Physical resource block

In LTE standard [41], the time-frequency resource is divided into resource blocks. One PRB consists of 12 consecutive subcarriers for one slot. PRB is the smallest element of resource allocation. Allocation of PRBs is handled by a scheduler at the 3GPP eNB. PRB structure is shown in Figure 3.1.

To be detected from attenuation and noise, signals must maintain a certain level of signal power at the receiver. Hence the transmit power should be large enough. Ideally the transmitted power is expected as large as possible. However, this is not realistic in practical. One reason is that when wave form has a high PAPR, transmit power should be low to avoid nonlinear distortion. The other limitation is from standards. To keep

network stable, standards usually provide determined transmit power range. Concept of green communication also suggest taking full use of transmit power. It is also an industry requirement [41].

3.2 Resource Allocation in OFDM based Broadband Wireless System

Since frequency and transmit power management plays vital role in wireless system, resource allocation is essential to utilize frequency diversity and multiuser diversity to enhance system performance

3.2.1 Physical Layer Resource Allocation

OFDM system usually contains a large number of subcarriers, which provide large multiuser diversity in resource allocation [27]. In frequency selective fading channels some subcarriers may be in heavy fading for certain user. However, it is unlikely that all users experience deep fading on the same subcarrier, because the channel characteristics are independent for each user. Therefore, by assigning each subcarrier to the user with the best channel condition on that subcarrier, system performance is enhanced.

Many research have been carried out on adaptive RA schemes for OFDM systems to maximize the system sum capacity [47, 48], minimize the sum transmit power [30], guarantee fairness [49] and determine the

modulation level order [50]. In [51, 52], low-complexity algorithms that use iterative methods have been presented. Heuristic algorithms such as genetic algorithms (GA) [53] and particle swarm optimization [54] have also been proposed. However, heuristic algorithms are not suitable for real-time application because their performance and complexity depend on many parameters. The aforementioned algorithms don't adhere to the LTE standard, which require subcarriers to be allocated in blocks.

Considering LTE standard, in [55], three dynamic PRB allocation algorithms were proposed and significantly outperform two-dimensional PRB allocation algorithms. In [56], proposed PRB allocation algorithm ranked users' utilities with multiple criteria and provides a near optimal performance. Author in [4] proposed an asymmetric resource allocation scheme and achieved optimal system capacity for the downlink wireless multidestination relay system.

In broadband wireless communication systems different frequency normally have different channel characteristics. Hence, uniform power allocation may cause degradations of system performance. In OFDM based wireless communication system, transmit power on each subcarrier can be assign separately [2]. The adaptive power on each subcarrier enhances provides better throughput and robustness of data transmission [57].

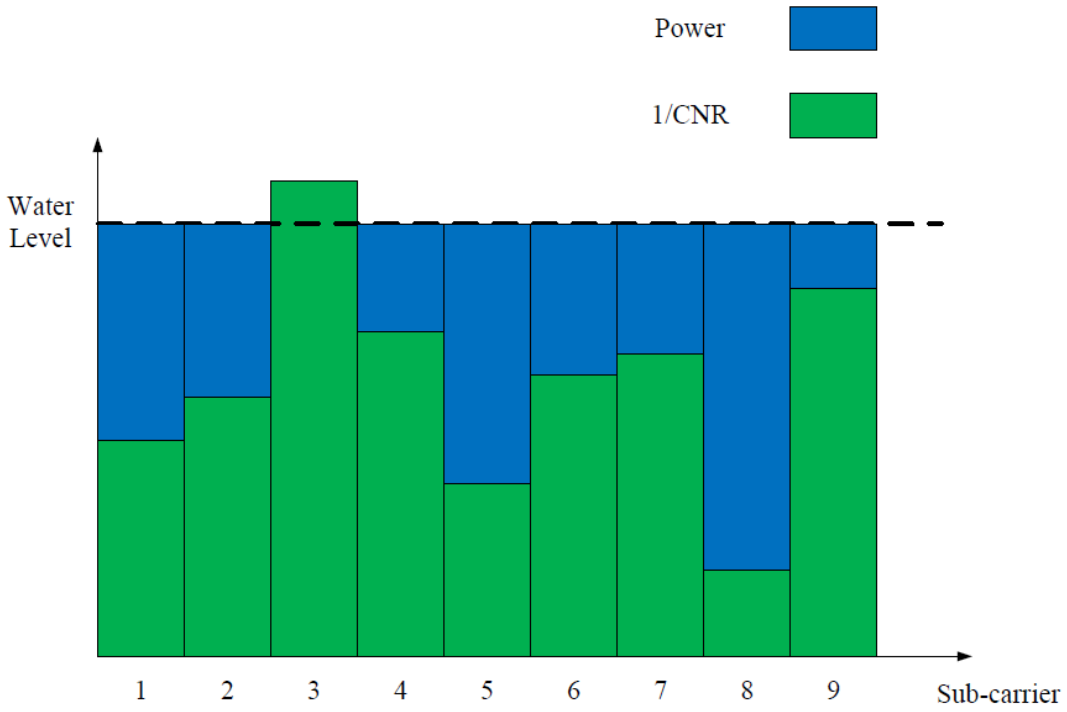

Figure 3.2: Water-filling algorithm

The water-filling algorithm [58] is the most widely applied power allocation algorithm. Figure 3.2 illustrates the idea of water-filling algorithm. Limited volume of water is poured into a pool with the bottom that has different level. The blue bars represent allocated power p_n on each subcarrier. The green parts are determined by channel-to-noise ratio (CNR) γ_n. The water-filling problem can be expressed as follow [58]:

$$\begin{cases} p_n = \left(\varepsilon - \frac{1}{\gamma_n}\right)^+, for\ n = 1, \dots, K \\ \sum_{n=1}^{K} p_n = P, \\ \varepsilon \geq 0 \end{cases} \tag{3.1}$$

where $(x)^+ = \max\{0, x\}$. ε is the water level chosen to satisfy the power sum constraints. With CSI from UEs, system can find the water level and calculate transmit power for each subcarrier.

3.2.2 Cross-Layer Optimization

With different data streaming services, user has different requirements, which are not related to physical resource of wireless networks. For example, video streaming normally disregards data lag due to buffer mechanism, meanwhile real-time video chatting service highly depends on latency. Since these requirements don't need extra physical resource, it is possible to satisfy them through cross-layer scheduling. These requirements are described as Quality of Service (QoS). General QoS parameters include data rate, packet loss ratio, and packet head of line (HoL) delay, fairness etc. [59].

Fairness-aware scheduling rules designed for single carrier systems such as proportional fair (PF) [60] , modified largest weighted delay first (M-LWDF) [59], and exponential proportional fair (EXP-PF) [61] can be adapted for OFDMA system by calculating these rules on each resource.

M-LWDF takes account of the delay requirement in services and utilizes it with PF to support multiple real-time data users. EXP-PF can support both real-time and non-real-time service and enhance the priority of real-time flows. According to [62] M-LWDF is the best scheduling rule for delay-sensitive applications in term of fairness and efficiency. However, for delay-sensitive traffic, above scheduling rules are not sufficient to avoid delay violation of flows having lower channel quality.

PF assigns resources according to current channel quality and previous throughput of users, which is regarded as very good scheduling algorithm for non-real-time traffic. In [63], authors evaluated the effect of various parameters on the throughput of the PF scheduler through the numerical analysis in CDMA2000 system. Authors in [64] evaluated PF scheduling performance at the flow level and considered a dynamic network setting with random sized service demands. Multiuser scheduler with PF scheduler was proposed in [65] to provides a superior fairness performance with a modest loss in throughput. However, it requires that user average SINRs are uniform, which indicates the importance of RA procedure.

CoMP system faces many challenges in consideration of QoS and overhead and backhaul limitation are two of them. Limit number of CoMP user in cluster is popular method to reduce backhaul data and uplink overhead. In [66] authors addressed joint design of transmit beamformers

and user data allocation at BSs to minimize the backhaul data transfer. CoMP user are pre-selected in [67], according to their different QoS requirement. In [9] and [68], distributed user selection and resource allocation are proposed to avoid uplink load.

3.3 Fuzzy Logic

Computer's logic block usually only understands precise input and produces Boolean logic values TRUE or FALSE, which is equivalent to human's YES or NO logic. By contrast, humans' logic often operates in fuzzy evaluations in everyday situation. A decision made by human contains a range of possibilities between YES and NO, including "certainly yes", "possibly yes", "hard to say", "possibly no" and "certainly no" for example. Fuzzy logic (FL) is a method that resembles human reasoning.

Figure 3.3 shows architecture of fuzzy logic systems. Input variables usually take numerical values, which are called "Crisp value" in FL. A fuzzifier module transforms the crisp input into linguistic variables (fuzzy set) by using fuzzy membership function. Membership function quantify linguistic term and represent a fuzzy set graphically. Each crisp value is mapped to a value between 0 to 1, which is called membership value or membership degree [69]. A membership function for a fuzzy set A on the crisp value sets X is defined as:

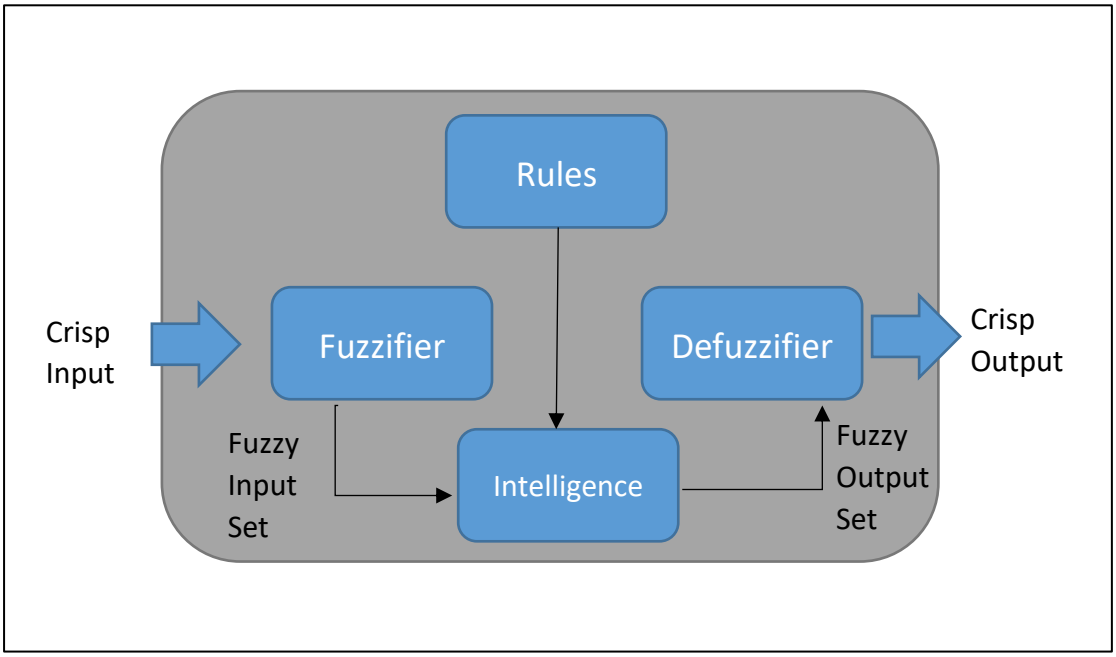

Figure 3.3: Fuzzy logic system architecture

$$\mu_A : \mathrm{X} \rightarrow [0, 1] \tag{3.2}$$

Figure 3.4 shows frequently-used fuzzy membership. Their names are recorded in Table 3.1. Normally the choice of membership function depends on empirical experience, or result from comparison of different functions. Researchers also can build their own membership function according to their works [69].

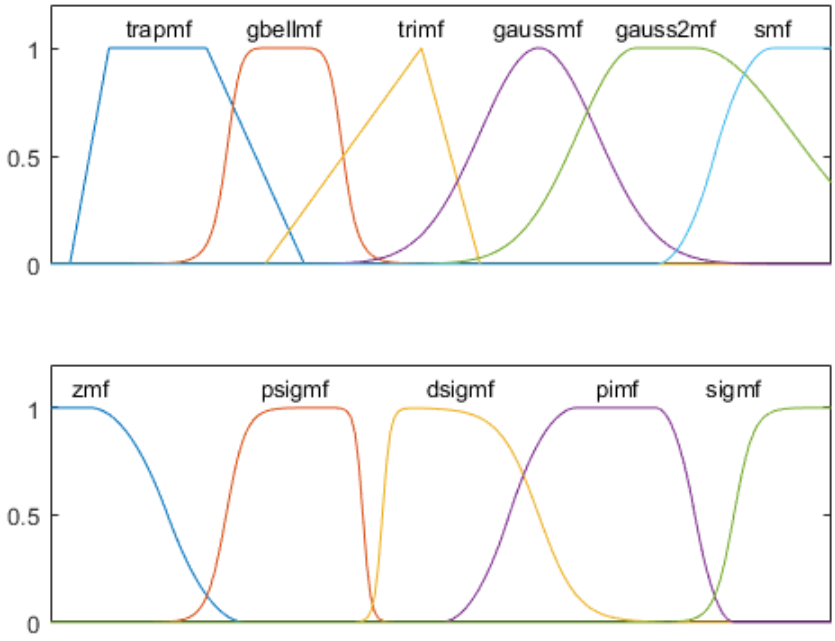

Figure 3.4: Shape of basic membership functions [69]

Table 3.1: Membership Function Name [69]

Code Name	Membership Function Name
trimf	Triangular
trapmf	Trapezoidal
gaussmf	Gaussian distribution
gauss2mf	
gbellmf	Generalized bell
sigmf	Sigmoidal
zmf	Z curve
smf	S curve
pimf	Pi curve

In Figure 3.5, the meanings of the expressions “short”, “medium” and “long” are represented by Trapezoidal membership functions mapping a distance scale. A distance value has three linguistic values according to the three functions. Let’s take a distance with normalized crisp value x=0.45 as example. According to Figure 3.4, this x=0.45 distance may be interpreted as “not long”, “fairly medium” or “kind of short”, with membership degree 0, 0.8, 0.2 respectively.

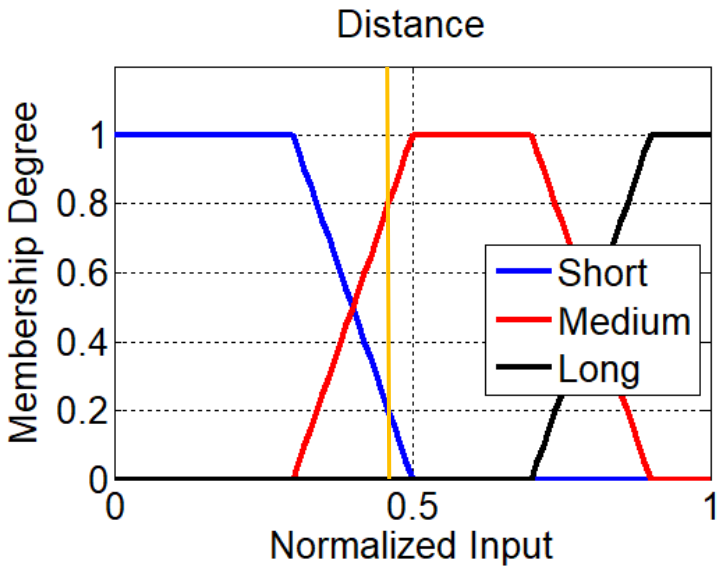

Figure 3.5: Example of fuzzy membership function

After fuzzification, intelligence engine of fuzzy logic block map fuzzy sets to desired output fuzzy sets by applying IF-THEN rules on each fuzzy value. The operations used for OR and AND are MAX and Min respectively. Combine all results of evaluation to form a final result $\mu_A(x)$.

Defuzzification converts a fuzzy output in to crisp output. The frequently-used defuzzification methods are described below [69]:

- Max-Membership Method

This method is limited to peak output functions and also known as height method. This method is the simplest but only useful in special case.

$$\mu_A(x^*) > \mu_A(x) \quad for\ all\ x \in X \tag{3.3}$$

where $x^*$is the defuzzified crisp output.

- Centroid Method

This mehod is also known as the center of gravity method, which is the most popular and physically appealing of all the defuzzification methods [70]

$$x^* = \frac{\int \mu_A(x) \cdot x dx}{\int \mu_A(x) \cdot dx} \tag{3.4}$$

- Weighted Average Method

In this method, each membership function is weighted by its maximum membership value. Valid for symmetrical output membership functions.

$$x^* = \frac{\sum \mu_A(\overline{x_\iota}) \cdot \overline{x_\iota}}{\sum \mu_A(\overline{x_\iota})} \tag{3.5}$$

where $\overline{x_\iota}$ indicates the middle position of membership shape.

- Mean-Max Membership Method

This method is also known as the middle of the maxima method.

$$x^* = \frac{\sum_{i=1}^{N} \overline{x_\iota}}{N} \tag{3.6}$$

Chapter 4

Resource Allocation for LTE System with Coordinated Multipoint

CoMP (Coordinated Multipoint) transmission and reception is introduced in the 3GPP LTE-Advanced standard to enhance system throughput. This technique has been widely studied in recent years because throughput of cellular networks are heavily limited by intercell interference [8]

Power control schemes have been widely investigated to solve CoMP resource allocation problems. In [3, 57, 71], power allocation maximized system throughput with restricted transmit power. Required data rate was applied to be constraints to minimize total transmit power in [6, 66, 72, 73]. In [74], game theoretic method was introduced to solve Quality of Experience (QoE) based power allocation problem. Physical Resource Block (PRB) was randomly allocated in above algorithms. However, PRB allocation strongly affects system throughput [55]. In [75], author proposed

to set two fixed groups of PRBs for CoMP and Non-CoMP and perform PRB allocation respectively. In a network with CoMP technique, users are divided into two categories: normal users and CoMP users. As CoMP has influence on system capacity and user fairness, a tradeoff is required in user selection. In [6], backhaul link capacity was considered to establish selection threshold for JP transmission. A zero-force beamforming method was proposed with user selection for CB transmission in [73]. In most literature, channel gain is the major parameter to select transmission mode because it contains effect of both distance and interference condition. In CoMP system, maximum throughput scheduler can maximize the sum throughput of the network but the cell-edge users' throughput will be extremely low due to their low competitive power. Max-min fairness scheduler improves cell-edge user's throughput. However, system throughput cannot be guaranteed. Proportional Fairness (PF) algorithm provides a good trade-off between system throughput and cell-edge throughput [76]. Classical PF algorithm is not suitable for CoMP resource allocation.

In this chapter, a Fuzzy Logic (FL) based user selection algorithm is proposed, following with simplified mean enhanced greedy PRBs allocation algorithm, to maximize system capacity, then a ranking based greedy allocation algorithm is proposed to reduce computational complexity. This work is different from existing researches in the following

aspects. First, instead of classifying users by single threshold, this work considers three parameters and exploit a fuzzy logic process to categorize users. As a result, measurement errors from single parameter are reduced. Users at edge of threshold are classified more accurate. Second, instead of investigating power control scheme to explore capacity potential, this work improves system capacity by a ranking based PRBs allocation schemes. Simulation results show that proposed fuzzy logic based user selection scheme improves system performance, especially for CoMP users. Proposed ranking based greedy allocation algorithm cut complexity in half but maintain same performance.

Following that, user fairness in CoMP PRBs allocation is investigated and a two-layer proportional-fair user scheduling scheme is proposed. This work is different from existing works in the following aspects. First, fairness between CoMP and Non-CoMP users are focused instead of balancing fairness in each user categories. Second, a modified PF algorithm is proposed to jointly optimize fairness and system capacity. Simulation results show that proposed algorithm significantly improves user fairness.

The rest of this chapter is organized as the follows. Section 4.1 presents the system model. Fuzzy logic based user selection and ranking based PRBs allocation algorithms are presented in Section 4.2. Two-layer proportional-faire user scheduling is presented in Section 4.3. Section 4.4

presents the summary.

4.1 System Model

We consider downlink MIMO-OFDMA LTE network with Joint Transmission (JT/JP) CoMP. The CoMP cell cluster is composed of B cells, indicated by $\mathcal{B} = \{1,2, \dots, b, \dots, B\}$, serving U user equipment (UE), which are uniformly distributed in coverage area. Furthermore, each transmitter is assumed to have N_t transmit antennas to support U users with N_r received antennas per user. CoMP cells can communicate with each other via backhaul link. Frequency reuse factor is 1, number of PRBs is K, and number of subcarriers is M, each PRB is composed of N subcarriers, indicated by $M = KN$.

The received signal of uth user on the mth subcarrier can be expressed as

$$\boldsymbol{Y}_u^m = \sum_{b \in \mathcal{B}} \boldsymbol{H}_u^{mb} \boldsymbol{x}_u^m + \sum_{v \neq u} \sum_{c \neq b} \boldsymbol{H}_v^{mc} \boldsymbol{x}_v^{mc} + \boldsymbol{Z}_u^m \tag{4.1}$$

The first part of Equation (4.1) indicates desired signal from CoMP cells. For a Non-CoMP UE, its CoMP cells group $\mathcal{B}$ only has one serving cell. The second part represents inter-cell interference, where $\boldsymbol{x}_u^m$ is the $l \times 1$ transmitted symbol vector, where l is the length of data symbol. $\boldsymbol{H}_u^{mb}$ is

the $N_t \times N_r$ channel matrix from cell b to user u on subcarrier m. In this work, each user is equipped with a single receiving antenna. $\boldsymbol{Z}_u^k$ is an additive white Gaussian noise (AWGN) with zero mean and variance σ.

The signal to interference and noise ratio (SINR) of uth user on the mth subcarrier can be expressed as

$$\Gamma_u^m = \frac{\left|\sum_{b\in\mathcal{B}} \boldsymbol{H}_u^{mb}\right|^2}{\sum_{v\neq u}\left|\sum_{c\neq b} \boldsymbol{H}_v^{mc}\right|^2 + \sigma^2} \tag{4.2}$$

Then the date rate of uth user on the mth subcarrier can be expressed as

$$T_u^m = BW \cdot \log_2(1 + \Gamma_u^m) \tag{4.3}$$

where BW is bandwidth of subcarrier.

The date rate of uth user on the kth PRB can be expressed as

$$T_u^k = \sum_{kN-N+1}^{kN} T_u^m \tag{4.4}$$

4.2 PRB Allocation with Fuzzy Logic based User Selection

4.2.1 Problem Formulation

The objective is to allocate PRBs to each user, so that the instantaneous system throughput is maximized. The problem can be expressed as below:

$$maximize: J_c = \sum_{u=1}^{U} \sum_{k=1}^{K} T_u^k \cdot S_u^k \tag{4.5}$$

Subject to

$$S_u^k \in \{0,1\} \tag{4.6}$$

$$S_u^k = Sc_u^k + S1_u^k + S2_u^k + \cdots + Sb_u^k + \cdots + SB_u^k \tag{4.7}$$

$$\forall b \in \mathcal{B}: \sum_{k=1}^{K} Sc_u^k + Sb_u^k = 1 \tag{4.8}$$

$$\forall b \in \mathcal{B}: \sum_{u=1}^{U} Sc_u^k + Sb_u^k = 1 \tag{4.9}$$

$$\forall b \in \mathcal{B}: \sum_{u=1}^{U} Sb_u^k \leq 1 \tag{4.10}$$

$$\forall b \in \mathcal{B}: \sum_{k=1}^{K} Sb_u^k \leq 1 \tag{4.11}$$

When *k*th PRB is allocated to the *u*th user $S_u^k = 1$, otherwise $S_u^k =$

0. When kth PRB is allocated to the uth user is a CoMP user $Sc_u^k = 1$, otherwise $Sc_u^k = 0$. When kth PRB is allocated to the uth user is a Non-CoMP user of cell b, then $Sb_u^k = 1$, otherwise $Sb_u^k = 0$. Equation (4.8) and (4.9) indicates that PRB occupied by a CoMP user cannot be allocated to any other users. Equation (4.10) and (4.11) describes that in each cell one PRB can only allocated once. From Equation (4.6) - (4.10), though Non-CoMP users don't affect Non-CoMP users in other cells, PRBs occupied by Non-CoMP user cannot be allocated to CoMP user anymore. In consideration of this constraint, CoMP UEs $\mathcal{R}c$ should be firstly allocated PRBs.

The optimization problem is nonlinear and nonconvex due to the coupled interference among different receivers. With a pre-determined user allocation, the weighted sum rate maximization problem reduces to the conventional sum rate maximization. Weighted sum rate maximization with linear precoding was claimed to be solved by the algorithm in [77]. However, convergence of the optimum solution strongly depends on the initialization. An iterative algorithm based on a repeated transformation from the duel multiple access channel was proposed in [78]. In [79] successive solution of geometric programming problems as proposed. However, aforementioned algorithms only considered a full-coordinated UE group. Resource allocation and fairness balancing among CoMP and Non-CoMP users hadn't been studied.

4.2.2 CoMP User Selection with PRBs Limitation

Cell-edge UE usually receives heavy interference from neighbor cells. Before deploying CoMP to system, it is essential to determine which users are in CoMP mode or Non-CoMP mode. Two threshold based methods are mostly mentioned in literatures: expected SINR based and distance based methods.

With allocated PRBs, the differentiation between CoMP UE and Non-CoMP UE can be made based on the received SINR in Non-CoMP mode at the UE. The mode selection criterion can be expressed as

$$if\ \Gamma n_u^k < \Gamma_{threshold}, user\ u\ is\ in\ CoMP\ mode \tag{4.12}$$

$\Gamma_{threshold}$ is a predetermined threshold. According to literature [80] it can be set to 3dB. Distance based selection criterion can be expressed similarly as

$$if\ \hat{d}_u > d_{threshold}, user\ u\ is\ in\ CoMP\ mode \tag{4.13}$$

$d_{threshold}$ can be set to 0.8-0.9 of maximum coverage range of serving cell [9].

The main constraint in user selection is the limited PRB resources. In JT CoMP, a CoMP user occupies same frequency of all cells in the CoMP

cluster and this frequency cannot be used by any other users in the cluster, no matter CoMP or Non-CoMP users. When there are a large number of CoMP users, system throughput may increase but many Non-CoMP users have delay due to limited frequency resource. Threshold based user selection method, like Equation (4.12) and (4.13), only divided users into CoMP and Non-CoMP user groups. When number of CoMP user is limited, thresholds must adaptively change.

In addition, cells in same cluster may have different number of Non-CoMP user, which should also be considered in user selection constraint. For a CoMP cluster $\mathcal{B} = \{1,2,\dots,b,\dots,B\}$, , number of all users, CoMP users and Non-CoMP users in each CoMP cell are indicated respectively by $\mathcal{U} = \{U_1, U_2, \dots, U_b, \dots, U_B\}$, $\mathcal{U}c = \{Uc_1, Uc_2, \dots, Uc_b, \dots, Uc_B\}$ and $\mathcal{U}n = \{Un_1, Un_2, \dots, Un_b, \dots, Un_B\}$, where $U_b = Uc_b + Un_b$. To fully exploit PRBs resource of the cluster, maximum total number of CoMP users in the cluster can be expressed as

$$UC_{max} = K - \max(Un_1, Un_2, \dots, Un_b, \dots, Un_B) \tag{4.14}$$

A ranking based user selection is proposed with constraint of PRBs limitation. According to ranking criterion, users are sorted in order and some top users are chosen as CoMP user according to limited PRB. The algorithms are show in Algorithm 4.1.

The ranking criterion RC_u can be estimated distance $\hat{d}_u$ or Non-

CoMP PRB SINR Γn_u^k. It needs to be noticed that Γn_u^k is pre-allocated PRB SINR in Non-CoMP mode. Because in this work PRBs will be allocated dynamically, the mean PRB SINR is used instead of pre-allocated PRB SINR, which is given by:

$$RC_u^{\Gamma} = -\frac{\sum_{k=1}^{K} \Gamma n_u^k}{K} \tag{4.15}$$

Algorithm 4.1 *Ranking Based CoMP User Selection with Constraint*

Initialization: calculate Ranking Criterion RC_u^{Γ} for all users in the cluster $\mathcal{B} = \{1,2,\dots,b,\dots,B\}$, number of users in each CoMP cell $\mathcal{U} = \{U_1, U_2, \dots, U_b, \dots, U_B\}$, number of Non-CoMP users in each CoMP cell $\mathcal{U}n = \mathcal{U}$, number of CoMP users in each CoMP cell $\mathcal{U}c = \{Uc_1, Uc_2, \dots, Uc_b, \dots, Uc_B\}$, $where\ \ Uc_b = U_b - Un_b$. Maximum total number of CoMP users UC_{max} is set to 0. Data set for *u*th user is $D_i(u, RC_u^{\Gamma}, b, mode)$, where *b* is serving cell index of *u*th user, *i* is *u*th user's ranking order. The parameter $mode = 0$ indicates user is a Non-CoMP user.

1. Rank all data set *D* in the cluster by descending order of RC_u:
   $Rank = \{D_1, D_2, \dots, D_u, \dots, D_U\}$, where $RC_u^{\Gamma}(D_i) \geq RC_u^{\Gamma}(D_{i+1})$
2. From the front to the end of the *Rank*, set user to be CoMP user one by one, and iteratively check if allocated PRBs overflow:

```
for i = 1:U
    if UC_max < K − max(Un_1, Un_2, ..., Un_b, ..., Un_B)
        Uc_{b^{D_i}} = Uc_{b^{D_i}} + 1;  % Update number of CoMP in serving cell
        Un_{b^{D_i}} = Un_{b^{D_i}} − 1;  % Update number of Non-CoMP
        UC_max = ∑{Uc};      % Update maximum number of CoMP
        mode^{D_i} = 1;  % Set user to CoMP mode.
    else
        mode^{D_i} = 0;  % Set user to Non-CoMP mode.
    end if
end for
```

3. Then the CoMP users set is $\mathcal{R}c = \{u, where\ mode^u = 1\}$, Non-CoMP user set is $\mathcal{R}n = \{u, where\ mode^u = 0\}$.

In ranking of Non-CoMP SINR, because the user with less SINR

should be more likely chosen as CoMP user, a minus operation is added in Equation (4.15) to meet descending ranking in algorithm.

Distance is an empirical criterion to select user, which is accepted to separate CoMP users and Non-CoMP users. However, as a ranking criterion, due to small-scale fading, distance cannot provide enough information in consideration of system throughput. Expected SINR directly considers channel variance, but, also due to fading and shadowing, many cell-center users may be chosen and it may increase mode switching times. To overcome their drawbacks, a criterion based on fuzzy logic is proposed to perform ranking selection in following section.

4.2.3 Fuzzy Logic based Ranking Criterion

To fight with the time variant nature of wireless communication systems, intelligent control methodologies are required for robust and cost-effective design. Many applications of fuzzy logic have been applied in wireless communication research area. Fuzzy logic offers flexible designs channel estimation [81, 82], handover [83-85], interference management [86, 87] in LTE networks. An iterative fuzzy tracking method was applied to track channel coefficients in [81]. In [82], fuzzy logic was applied to estimating channel parameters with pilot reference signal in OFDMA system. From [83-85], fuzzy logic showed powerful ability for auto-tuning parameters, but delay and handover failure ratio increased. Authors proposed game

theory and fuzzy logic inference system based self-optimized power allocation algorithm in [86]. Fuzzy logic was applied to minimize information exchange among eNB. In [87] fuzzy logic was designed to control transmit power for device-to-device communication system. In this work, fuzzy logic is applied to divided users into CoMP and Non-CoMP groups.

A. Fuzzy Inputs

The distance $\hat{d}_u$ and mean PRB throughput $T_u^{mean} = (\frac{1}{K}) \sum_{k=1}^{K} T_u^k$ are two of inputs of proposed fuzzy logic algorithm. In addition, the reference signal received power (RSRP) is the other potential input. RSRP is the received signal strength indicator in LTE. It is valid to assume that the strongest RSRPs are from UE's potential cooperative cluster. If their RSRPs are close to each other, the UE is more likely in heavier inference area. So standard deviation of RSRPs is selected as one criterion $VRSRP$. User with less $VRSRP$ is more likely chosen to be in CoMP mode. The three criteria can reflect UE's position and channel condition, but their measurement errors are affected by different parameters. Combining three criteria by fuzzy logic can improve accuracy of user selection.

$$VRSRP_u = var(RSRP_u)$$

$$= E[(RSRP_u^b - \overline{RSRP_u})^2] \qquad (4.16)$$

B. Fuzzification Process

In order to perform the fuzzificaiton process, three inputs and one outputs should be mapped to fuzzy sets, the name of which are as follows:

$$X = VRSRP \in \{small, medium, large\}$$

$$Y = \hat{d} \in \{short, medium, long\}$$

$$Z = T_u^{mean} \in \{bad, medium, good\}$$

$$O = output \in \{verybad, bad, medium, good, verygood\}$$

The fuzzy output set indicates the UE's suitability for CoMP mode in consideration of all three inputs. Since all three inputs change linearly and continuously, the Trapezoidal function is chosen to generate membership function. The trapezoidal curve is a function of a vector x, and depends on four scalar parameters a, b, c, d, as given by

$$f(x; a, b, c, d) = \begin{cases} 0, & x \le a \\ \dfrac{x-a}{b-a}, & a \le x \le b \\ 1, & b \le x \le c \\ \dfrac{d-x}{d-c}, & c \le x \le d \\ 0, & d \le x \end{cases} \tag{4.17}$$

where *a* and *d* are the valleys and *b, c* are the climaxes of the trapezoidal function. This function is mapping *x* to a value between [0,1] and degree of membership $\mu(x)$ is generated.

As there is no experience information of *VRSRP* and T_u^{mean}, their memberships have balanced distribution of three levels. Distance is an empirical parameter for mode selection, as results that its distribution of levels skews to right. The medium level of membership of fuzzy output has more core area, which makes weights of side levels closer to edges and enlarges difference of suitability of CoMP and Non-CoMP UEs.

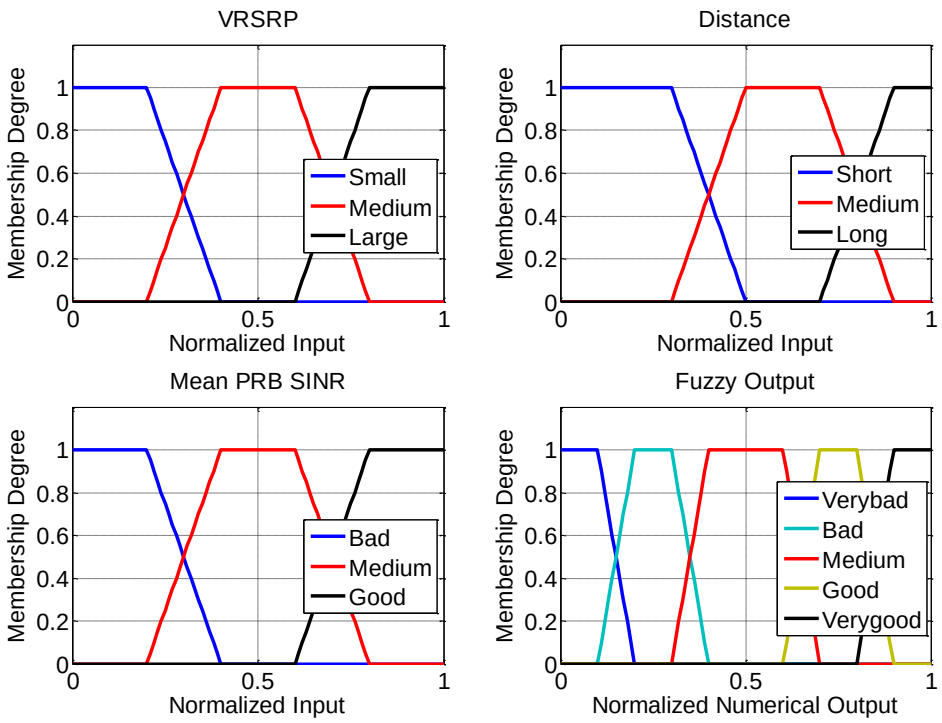

Figure 4.1. Membership functions of inputs and output.

Figure 4.1 shows membership degree of different type of inputs. For one input, membership function generates one membership degree whose value is between 0 to 1, according to the type (small/medium/large etc.) of input. The membership function for the distance is not symmetric.

Normally CoMP users locates in the edge area of cells. Users with short distance to cell center are hardly possible to be a CoMP user. Therefore, the part which represents “short” is larger than “medium” and “long”, which ensure that fewer center users are switched to CoMP mode.

C. Defuzzification Process

With three 3-level inputs, a fuzzy rule base composed of 27 rules [Appendix 1] is generated to map fuzzy inputs to output. This fuzzy rule base indicates different outputs with 27 points of view on inputs. If two or more inputs are at same level, the output is set to same level. If all inputs are at different level, the output is set to medium level. The SINR criteria has slightly more weight in the decision of rules, because throughput of the whole system is the main objective. Since fuzzy rules are established by AND logic, membership of fuzzy output set is given by

$$\mu_O = min(\mu_X, \mu_Y, \mu_Z) \tag{4.18}$$

From Equation (4.18), a fuzzy output membership set, consisting of 27 elements or points of view on inputs, is generated. In order to compare fuzzy output of different users, output membership set should be mapped to numerical outcome or a crisp output. Weighted average defuzzification method [69] is used in this work because membership function is

symmetrical. The crisp output is a numerical value between [0, 1], indicating user's suitability for CoMP mode, given by

$$CO = \frac{\sum(\mu_O \cdot O_M(\mu_O))}{\sum \mu_O} \tag{4.19}$$

where $O_M(\mu_O)$ is middle value of normalized numerical output value of μ_O membership. UE with larger *CO* is more likely to be CoMP UE. After defuzzification, each UE has own crisp output CO_u. Then fuzzy logic based ranking criterion is given by:

$$RC_u^{fuzzy} = CO_u \tag{4.20}$$

4.2.4 PRBs Allocation Algorithms in CoMP

4.2.4.1 Simplified Mean Enhanced Greedy

Simplified Mean Enhanced Greedy (SMEGUS) algorithm applies SMEG separately to each user groups (CoMP group, Non-CoMP group in each cell). CoMP user group is allocated PRBs firstly to ensure that available PRBs are enough for CoMP use. Then the rest of PRBs are allocated in each cell for Non-CoMP user. User selection processing only provides division of user group. The procedure of SMEGUS is showed as below:

Algorithm 4.2 *Simplified Mean Enhanced Greedy with User Selection*

1. For all UEs $\mathcal{R} = \{1,2, \dots, u, \dots, U\}$, calculate mean PRBs throughput of T_u^{mean}. For CoMP UE set $\mathcal{R}c = \{u, where\ mode^u = 1\}$, rank CoMP users by their T_u^{mean}.
2. From top to bottom of the rank, for each user:
   a) Allocate the best PRB $k^* = arg\max_k T_u^k$ to user u^*
   b) Set $T_{u*}^k = 0\ and\ T_u^{k*} = 0$, where $k = 1,2, \dots, K, u = 1,2, \dots, U$, so that a CoMP user do not share PRB with any other users according to Equation (4.8) and (4.9)
3. For Non-CoMP UE set $\mathcal{R}n = \{u, where\ mode^u = 0\}$, T_u^{mean} is divided into Tb_u^{mean} according to different cells, and rank users in cell b by their Tb_u^{mean} for all cells.
4. From top to bottom of the rank, for each user in each cell:
   a) Allocate the best PRB $k^* = arg\max_k Tb_u^k$ to user u^*
   b) Set $Tb_{u*}^k = 0\ and\ Tb_u^{k*} = 0$, where $k = 1,2, \dots, K, u = 1,2, \dots, U$, so that a Non-CoMP user do not share PRB with Non-CoMP user in same cell according to Equation (4.10) and (4.11)

4.2.4.2 Proposed User Selection Ranking Greedy

Proposed User Selection Ranking Greedy (USRG) algorithm takes use of ranking order in user selection process. Comparing to SMEGUS, ranking of mean PRB performance is absent. Actually, USRG PRB allocation can be performed with user selection processing according to algorithm structure. In other word, USRG can jointly do user selection and PRB allocation. The procedure of USRG is showed as below:

Algorithm 4.3 *User Selection Ranking Greedy (USRG)*

1. For all UEs $\mathcal{R} = \{1,2,\dots,u,\dots,U\}$, rank all users by their Ranking Criterion RC_u
2. From top to bottom of the rank, for each user:
   If number of CoMP users doesn't reach maximum:
   a) Allocate the best PRB $k^* = arg\max_k T_u^k$ to user u^*
   b) Set $T_{u*}^k = 0\ and\ T_u^{k*} = 0$, where $k = 1,2,\dots,K, u = 1,2,\dots,U$, so that a CoMP user do not share PRB with any other users according to Equation (4.8) and (4.9)
   If CoMP user slots are full:
   a) Allocate the best PRB $k^* = arg\max_k Tb_u^k$ to user u^*
   b) Set $Tb_{u*}^k = 0\ and\ Tb_u^{k*} = 0$, where $k = 1,2,\dots,K, u = 1,2,\dots,U$, so that a Non-CoMP user do not share PRB with Non-CoMP user in same cell according to Equation (4.10) and (4.11)

4.2.5 Simulation Results

The simulation setup is shown in Table 4.1. From Figure 4.2 – 4.17, proposed Fuzzy-SMEGUS and Fuzzy-USRG algorithms have almost same performance in respect of average spectral efficiency of edge users, system throughput, distribution of users' spectral efficiency. In Figure 4.18, D-USRG and SINR-USRG have much lower cell-edge performance because their allocation orders are determined by distance/SINR criterion. These results indicate that ranking criterion generated from FL user selection procedure is a reliable data to support the following resource allocation procedure. Results of FL user selection can be used to determine a fixed user allocation order. Additional ranking criteria such as mean PRB gain is no longer necessary.

Table 4.1. Simulation Setup

Parameters	Value
Cluster Model	3-cell
System bandwidth	20MHz
distance between BSs	500m
Carrier frequency	2GHz
Subcarrier interval	15kHz
Size of each RB	180kHz
Number of RBs	100
Transmit power of BS	43dBm
Shadow fading	10dB
Noise power spectral density	-67dB

The impacts of number of users **U** and number of CoMP users **C** are investigated in simulations. Proposed Fuzzy based algorithms have better cell-edge performance than D/SINR based algorithms according to Figure 4.2 – 4.9. D/SINR based algorithms have improved cell edge performance when number of users are much less than number of PRBs, meanwhile FL based algorithms don't have this feature. This is because CoMP users chosen by FL are more suitable for CoMP mode. They may locate nearer to cell edge, or suffer heavier interference from neighbor cells. For D/SINR

based methods, fewer number of users provides more possibility to assign better channel to their CoMP user, which leads an improvement in this situation. When proportion of CoMP users increases to 80%, performance of all the algorithms draw closer. The reason is that in this case results calculated from different user selection algorithms tend to similar. However, FL based algorithms still provide a bit better performance in high-speed users according to Figure 4.8, 4.9.

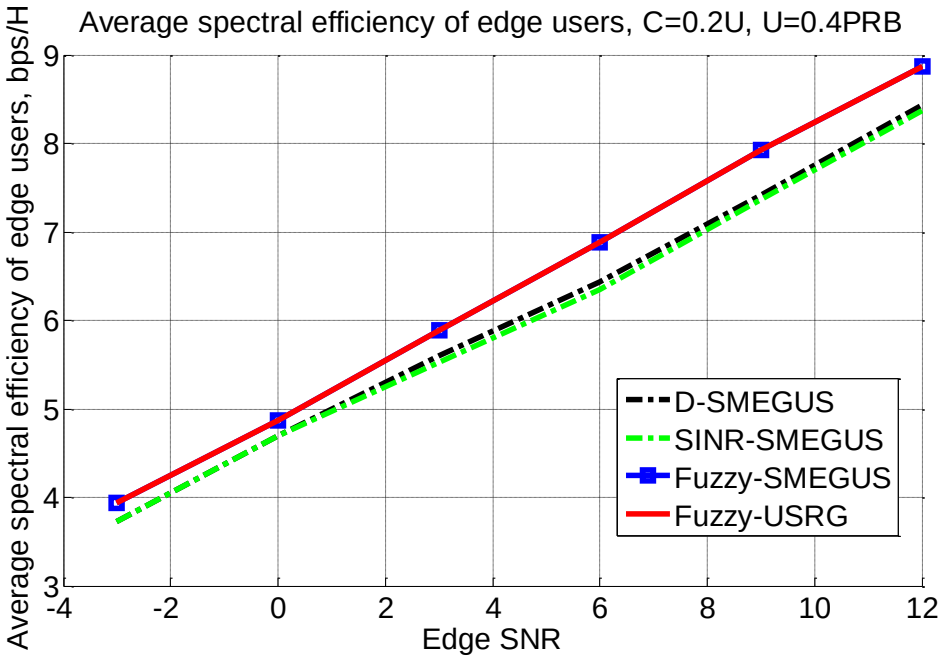

Figure 4.2: Average spectral efficiency of edge users, 20% of users are CoMP user, U=0.4*K

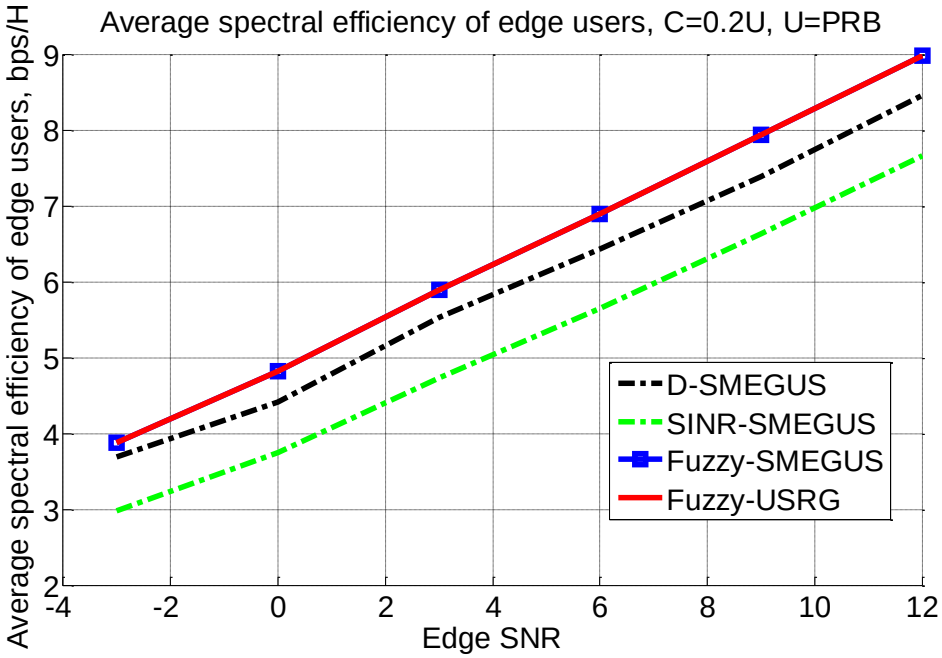

Figure 4.3: Average spectral efficiency of edge users, 20% of users are CoMP user, U=K

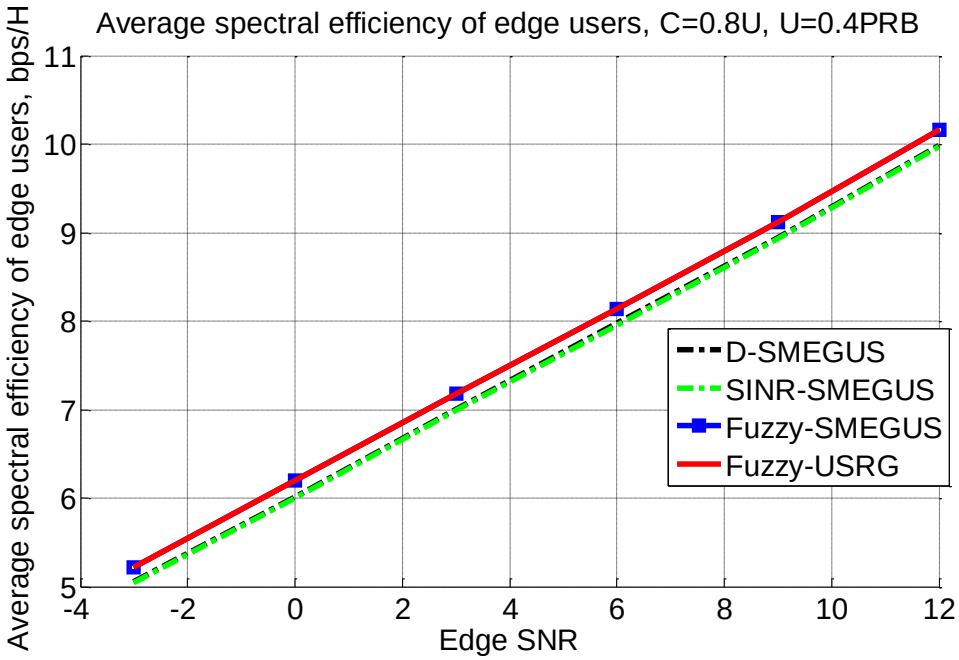

Figure 4.4: Average spectral efficiency of edge users, 80% of users are CoMP user, U=0.4*K

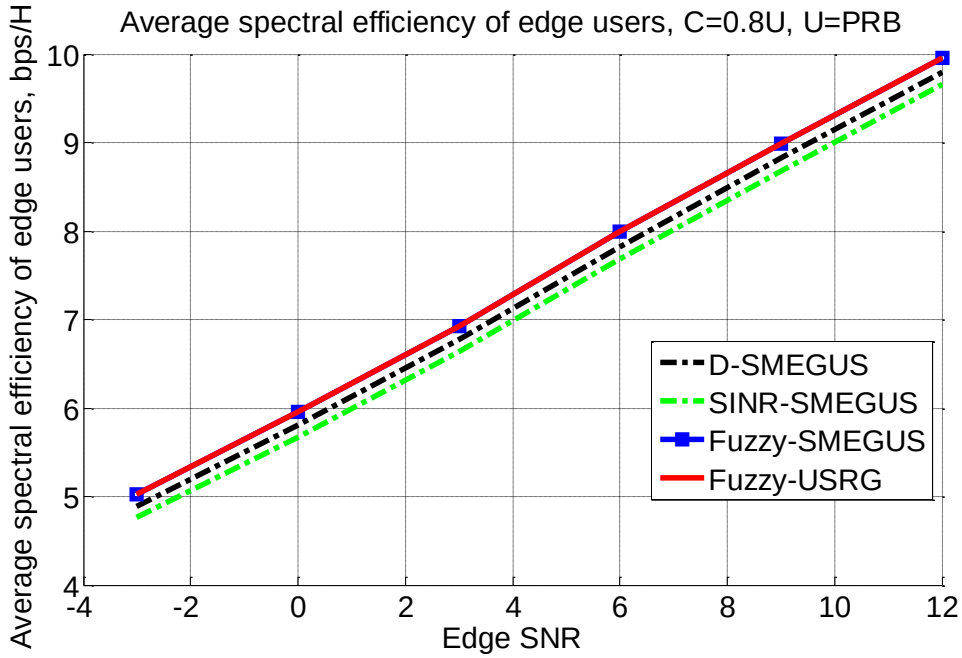

Figure 4.5: Average spectral efficiency of edge users, 80% of users are CoMP user, U=K

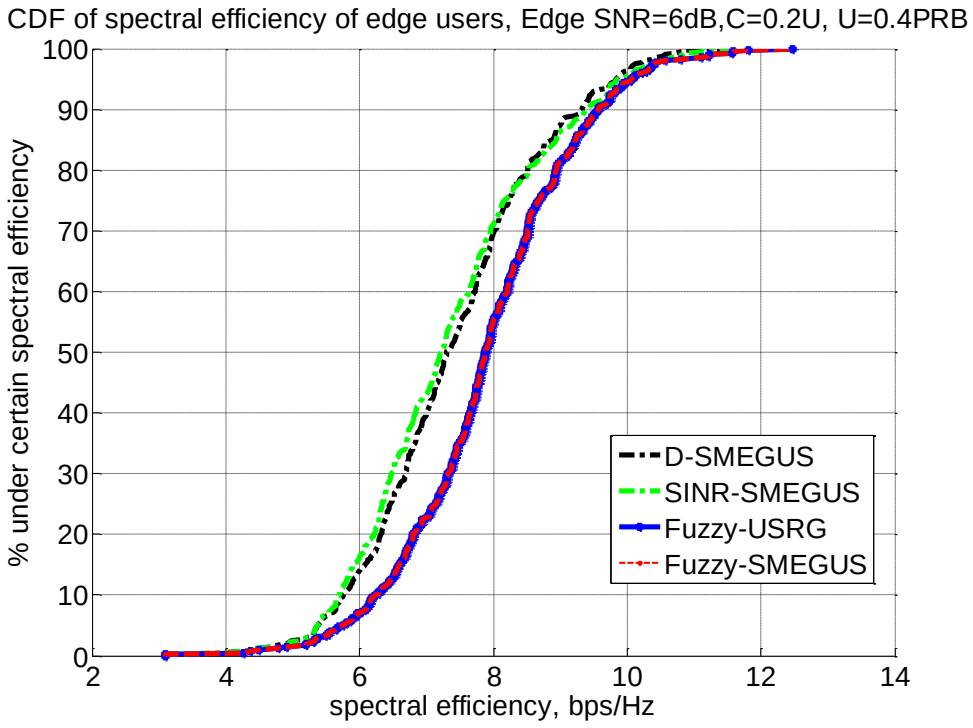

Figure 4.6: CDF of spectral efficiency of edge users, with SNR=6dB, 20% of users are CoMP user, U=0.4*K

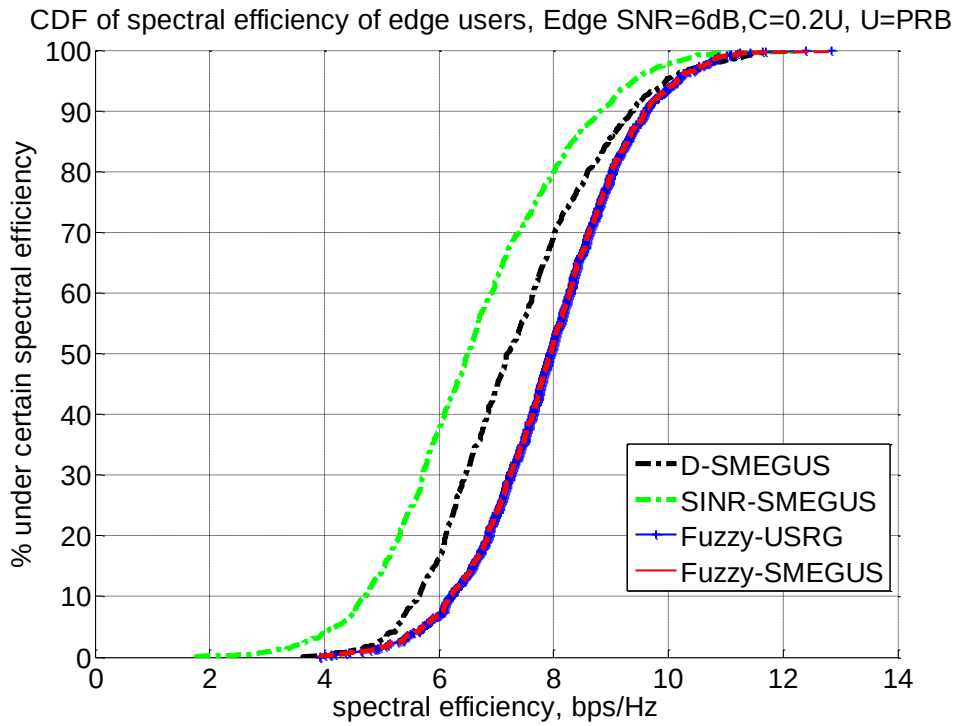

Figure 4.7: CDF of spectral efficiency of edge users, with SNR=6dB, 20% of users are CoMP user, U=K

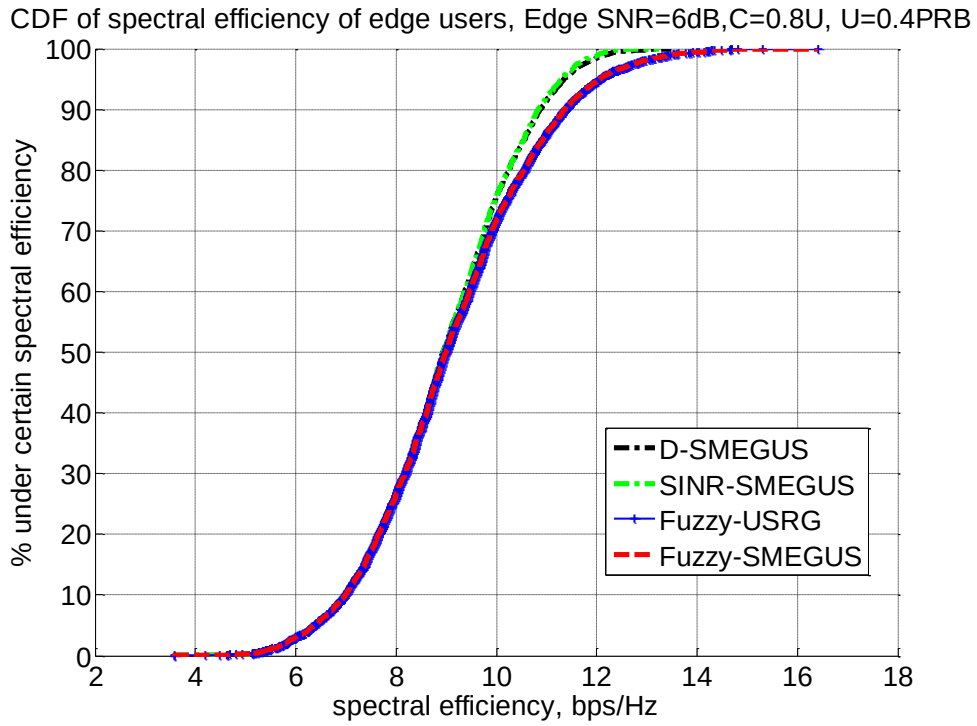

Figure 4.8: CDF of spectral efficiency of edge users, with SNR=6dB, 80% of users are CoMP user, U=0.4*K

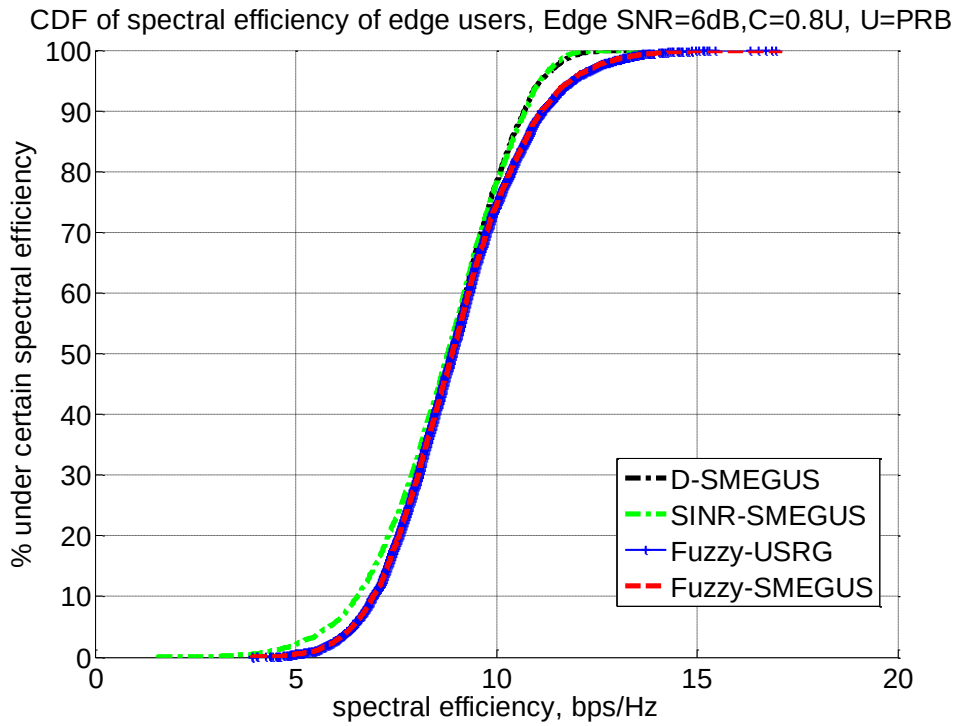

Figure 4.9: CDF of spectral efficiency of edge users, with SNR=6dB, 80% of users are CoMP user, U=K

Figure 4.10 – 4.18 show performance of the whole system. FL based algorithms have very similar system performance with D/SINR based algorithms. When proportion of CoMP users is small, system performance is mainly determined by resource allocation on Non-CoMP users, which is proved by Figure 4.14 – 4.15. There is only a small difference of distribution of users' spectral efficiency between CoMP algorithms and Non-CoMP mode. Comparing with Figure 4.16 – 4.17, the more CoMP users, the more improvement CoMP algorithms provide. In Figure 4.15, FL based algorithms have less high-speed users and less low-speed users. This explains that FL base algorithms have better cell edge performance but still

have similar system performance with D/SINR algorithms.

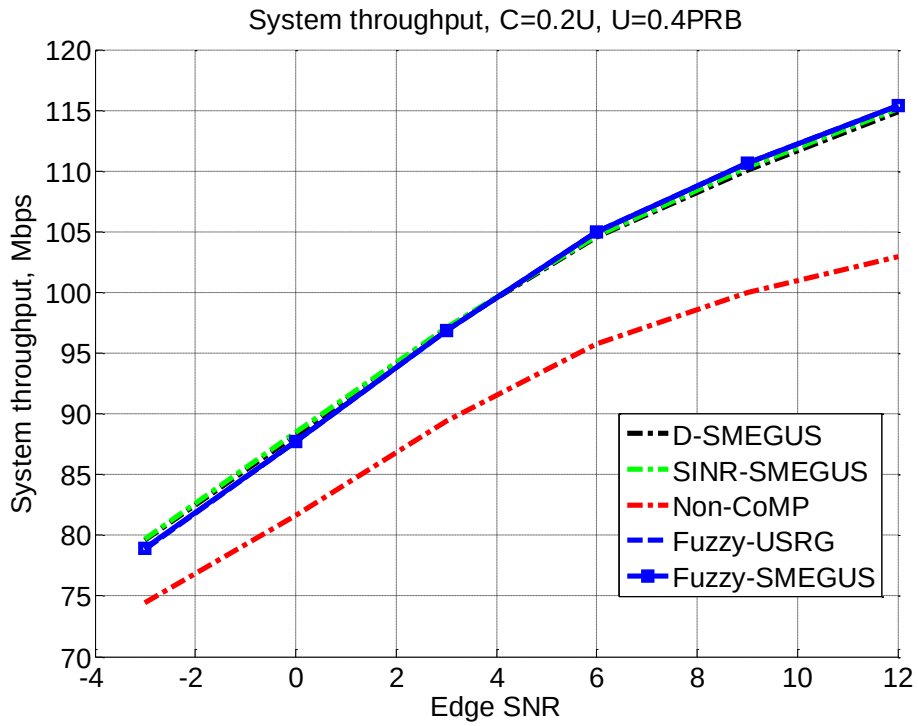

Figure 4.10: System throughput, 20% of users are CoMP user, U=0.4*K

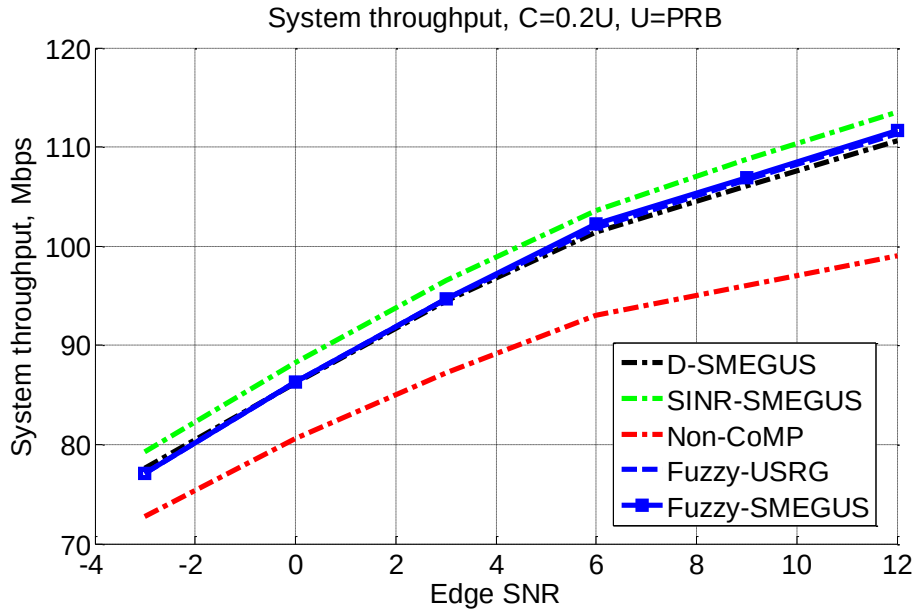

Figure 4.11: System throughput, 20% of users are CoMP user, U=K

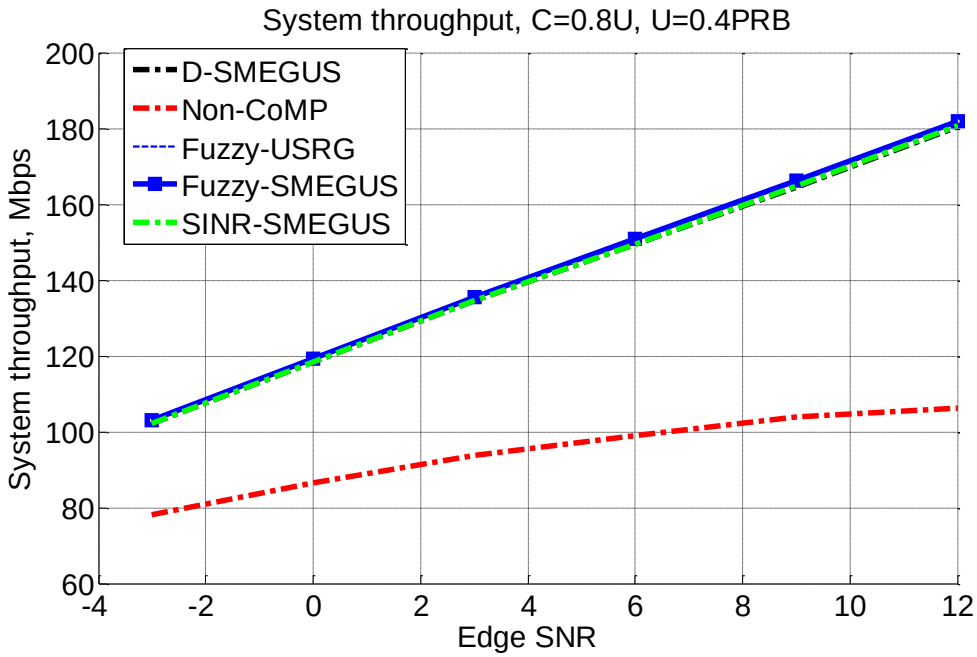

Figure 4.12: System throughput, 80% of users are CoMP user, U=0.4K

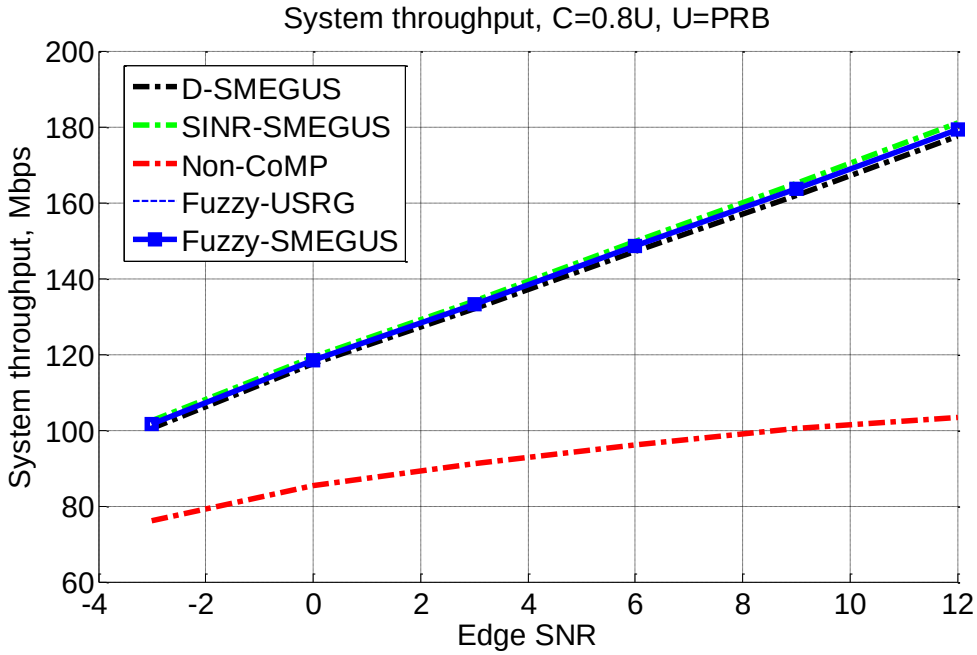

Figure 4.13: System throughput, 80% of users are CoMP user, U=K

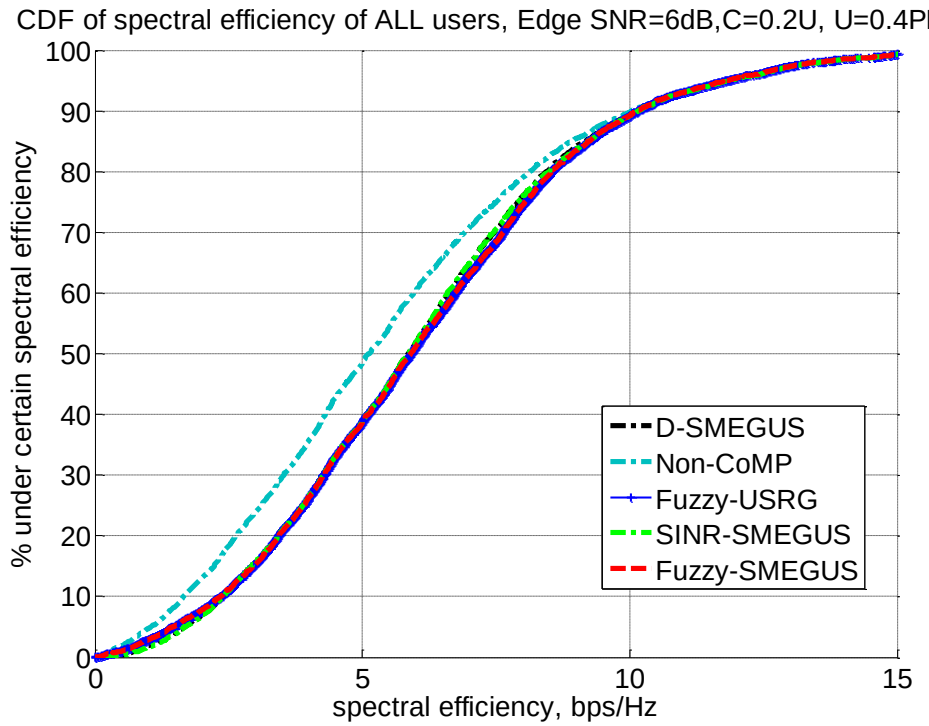

Figure 4.14: CDF of spectral efficiency of all users, with SNR=6dB, 20% of users are CoMP user, U=0.4*K

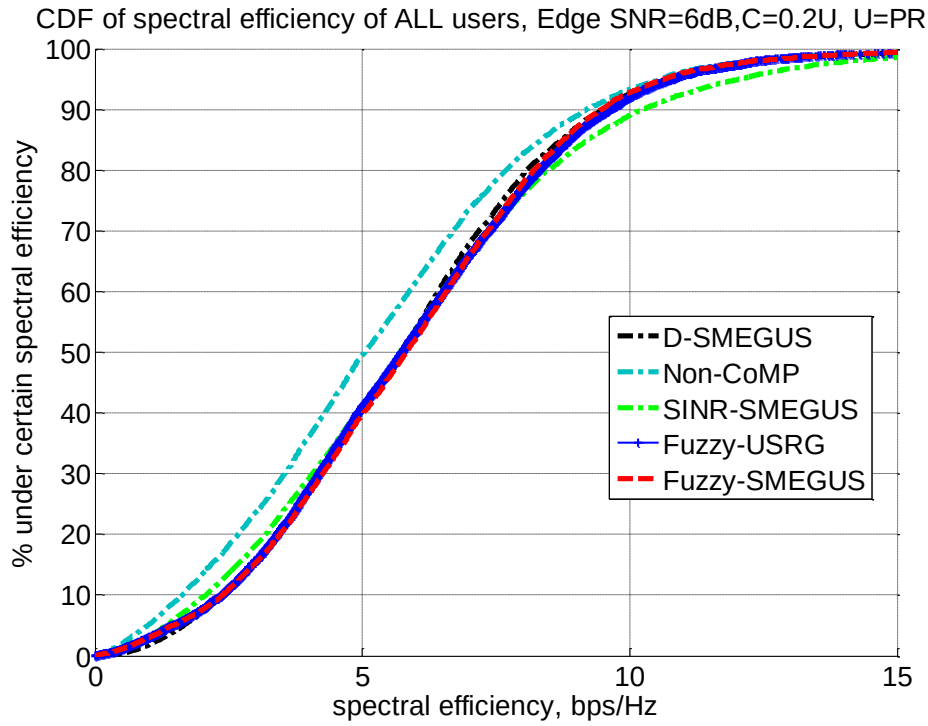

Figure 4.15: CDF of spectral efficiency of all users, with SNR=6dB, 20% of users are CoMP user, U=K

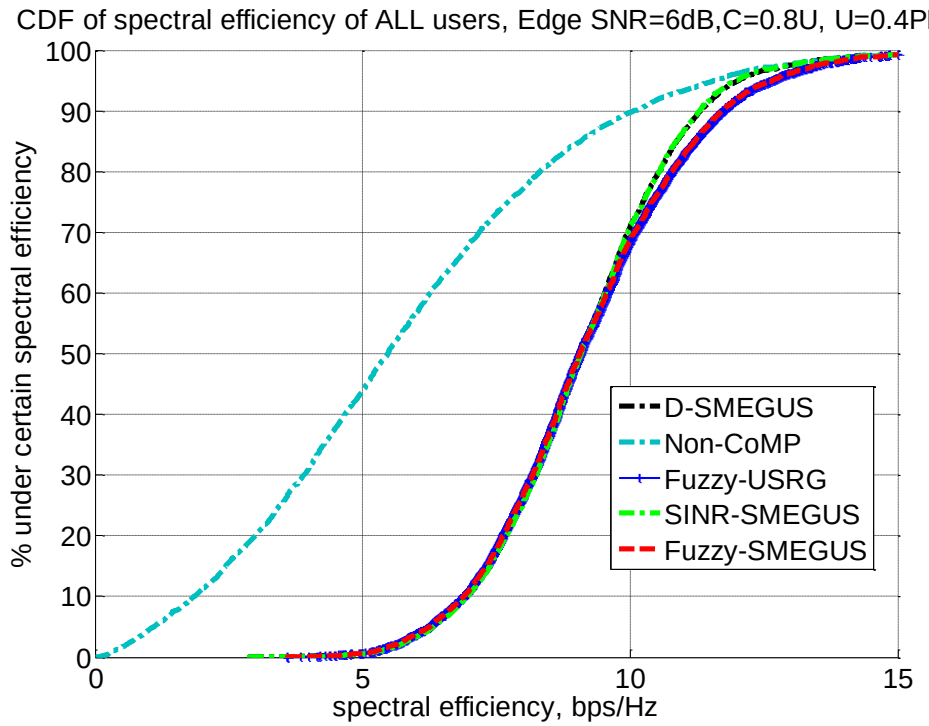

Figure 4.16: CDF of spectral efficiency of all users, with SNR=6dB, 80% of users are CoMP user, U=0.4*K

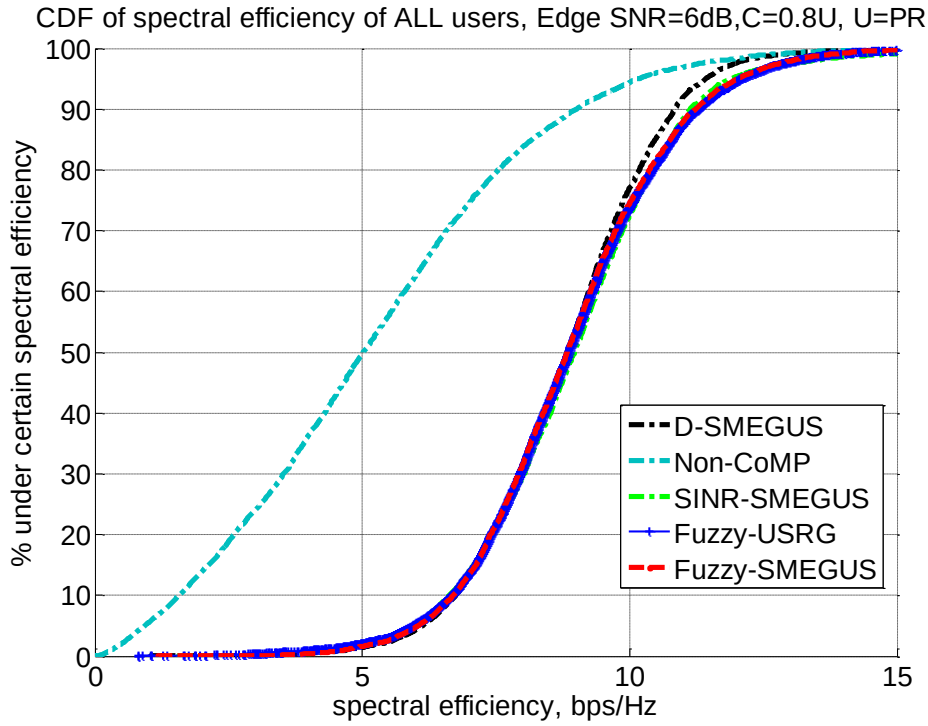

Figure 4.17: CDF of spectral efficiency of all users, with SNR=6dB, 80% of users are CoMP user, U=K

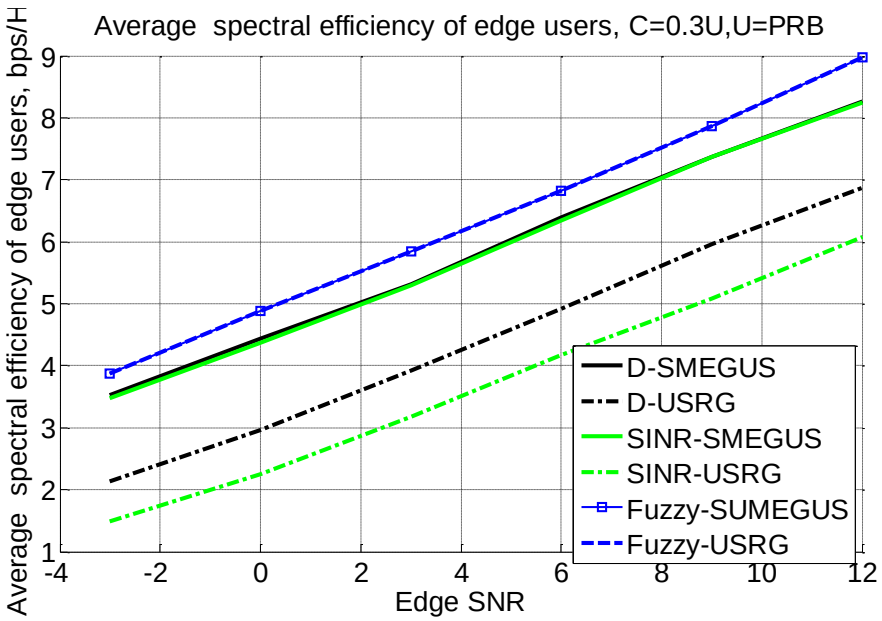

Figure 4.18: Average spectral efficiency of edge users, 30% of users are CoMP user, U=K

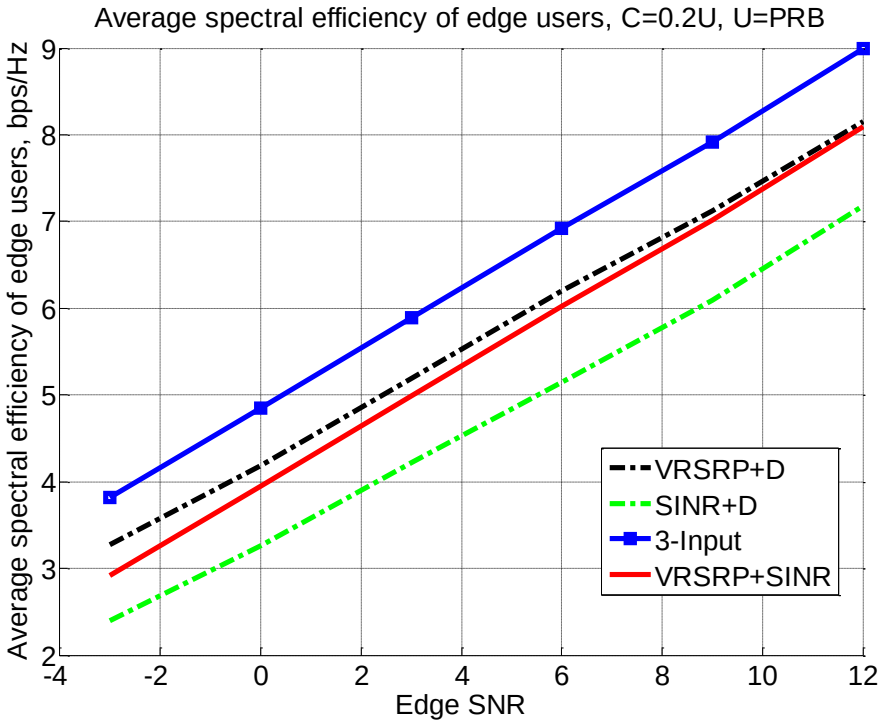

Figure 4.19: Average spectral efficiency of edge users from FL methods with different input combinations, 20% of users are CoMP user, U=K

In Figure 4.19, results of FL methods with different input combinations are shown. With SINR and D as inputs, the result of FL method is the worst in the figure, because distance and SINR are affected by many noises. 3-input FL method has the best average spectral efficiency of edge users since it combines all three inputs to include information as much as possible. In addition, 2-input FL has a rule base of only 9 rules, while 3-input FL has 27 rules. If introducing the 4^{th} 3-level input, it increases to 81 rules, which is much more complex than 3-input. Therefore, 3-input FL method is chosen in this work.

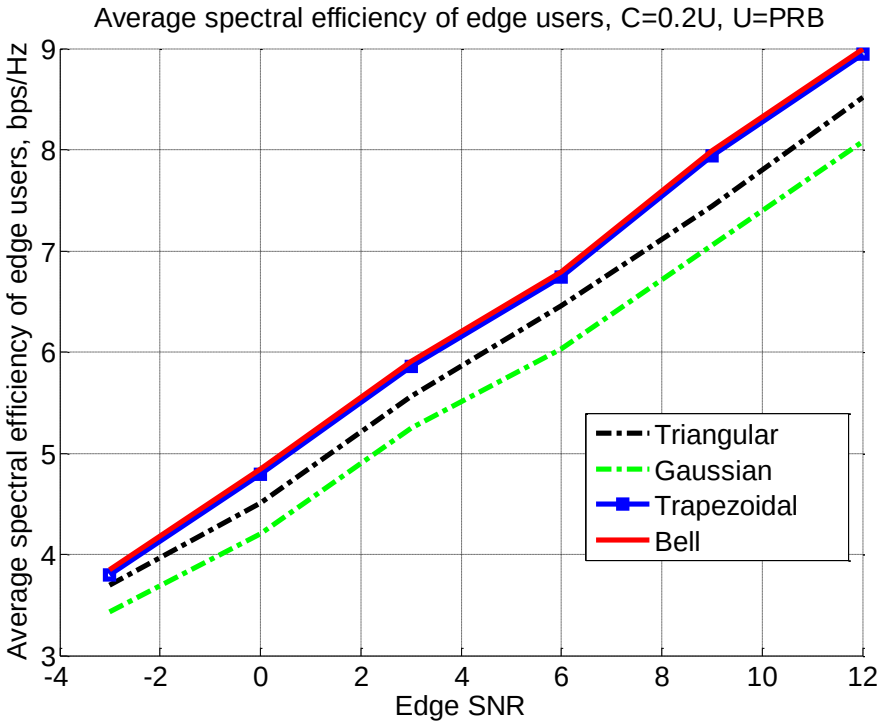

Figure 4.20: Average spectral efficiency of edge users from FL methods with different membership functions, 20% of users are CoMP user, U=K

From Figure 4.20, Trapezoidal membership function shows the same result of Generalized bell function, because Generalized bell function has almost same but smoother version of shape of Trapezoidal function. Gaussian distribution function provides the worst result. The reason is that it is smooth and non-zero at all points. When inputs are all in near-medium level, Gaussian distribution function can't contribute to a precise decision. Triangular function has slightly worse performance since its top-level area is only one point, which makes inputs indistinct. Sigmoidal function is usually used for asymmetric set. For symmetric set, Sigmoidal function performs similarly as Generalized bell. However, as Trapezoidal function consist of only straight lines, it is the least complex function for this problem. Considering complexity and performance, Trapezoidal function is chosen in this work.

Table 4.2 shows computational complexity of algorithms. One calculating operation counts 1 in complexity. It can be noticed that Fuzzy-USRG has about half complexity than other methods because USRG is simpler than SMEGUS. According to Figure 4.2 - 4.18, Fuzzy-USRG has almost same performance of Fuzzy-SMEGUS. The processing time was recorded in multiple times by matlab simulation in 5000 loops. The average execution time doesn't strictly match ratio of complexity of algorithms, because processing time of different type of calculation varies.

With results in Table 4.2, Fuzzy-USRG is outstanding over other

methods on complexity. The reason is that USRG directly takes use of ranking criterion generated by FL, meanwhile SMEGUS has to calculate PRB gain for allocating users. D-SMEGUS and SINR-SMEGUS require same computational complexity because processing distance and SINR has no significant complexity difference. The complexity in this thesis represents the number of calculation of an algorithm. Fuzzy logic based user selection require higher complexity. However, complexity of resource allocation algorithm dominates complexity of the whole algorithm.

Table 4.2. Complexity of CoMP PRB Allocation Algorithms with User Selection

Algorithm	Complexity	Normalized Complexity U=200	Processing Time per 5000 loops.
D-SMEGUS	3U^2+4.5U	1	9.7862s
SINR-SMEGUS	3U^2+4.5U	1	9.7635s
Fuzzy-SMEGUS	3U^2+93.5U	1.15	11.012s
Fuzzy-USRG	1.5U^2+91.5U	0.5	5.8931s

4.3 Two-Layer Proportional-Fair User Scheduling

In this section, fairness aware user scheduling problem has been studied

for downlink CoMP. Due to PRB reusing in a CoMP cluster, traditional fairness aware algorithm cannot be applied. To solve this problem, a two-layer PF scheduling algorithm is proposed. In the first layer, Non-CoMP users compete PRBs with CoMP users. Non-CoMP users compete each other in the second layer to generate Non-CoMP partners and avoid waste of PRBs.

4.3.1 Problem Formulation

To achieve optimal system capacity, user fairness is investigated in a period time. The fairness balance in each time slot is expensive and unnecessary in the view of industry. Therefor the problem formulation is added by time index t. The problem can be expressed as below:

$$maximize: J_c = \sum_{u=1}^{U} \sum_{k=1}^{K} T_u^k S_u^k f_u^k \tag{4.21}$$

Subject to

$$S_u^k \in \{0,1\} \tag{4.22}$$

$$S_u^k = Sc_u^k + S1_u^k + S2_u^k + \cdots + Sb_u^k + \cdots + SB_u^k \tag{4.23}$$

$$\forall b \in \mathcal{B}: \sum_{k=1}^{K} Sc_u^k + Sb_u^k \leq 1 \tag{4.24}$$

$$\forall b \in \mathcal{B}: \sum_{u=1}^{U} Sc_u^k + Sb_u^k = 1 \tag{4.25}$$

$$\forall b \in \mathcal{B}: \sum_{u=1}^{U} Sb_u^k \leq 1 \tag{4.26}$$

$$\forall b \in \mathcal{B}: \sum_{k=1}^{K} Sb_u^k \leq 1 \tag{4.27}$$

f_u^k is the proportional fair weight of user *u* on *k*th PRB, at time slot *t*: $f_u^k(t) = T_u^k(t)/R_u^k(t+1)$, *where* $R_u^k(t+1) = (1 - \frac{1}{t_s})R_u^k(t) + \frac{1}{t_s}T_u^k(t+1)$, R_u^k is the accumulated throughput and t_s is duration of one time slot. Equation (4.24) indicates that some users may not have any resource in certain time slot.

4.3.2 Two-Layer Proportional-Fair Scheduler

Users are divided into two groups in advance: CoMP users and Non-CoMP users. The algorithm is shown in Figure 4.19. All users compete for PRB by their PF priority. At *t* time slot, for the PRB *k*, the user *u* with highest PF priority is chosen to use PRB *k*. this is the first layer of PF scheduling. In JP CoMP, the PRBs occupied by CoMP users can not be used by other user in this cluster, while the PRB occupied by one Non-CoMP user can be used by Non-CoMP user in other cells, who is called Non-CoMP partners in this work.

To maximize PRB usage and increase system throughput, if user *u* is

a Non-CoMP user, all cells in this cluster must select Non-CoMP partners to occupy PRB *k*. The second layer of PF scheduling is performed between Non-CoMP users in each cell to select Non-CoMP partners. If user *u* is a CoMP user, then algorithm moves to PRB *k+1*. Flow chart of proposed algorithm is shown in Figure 4.21.

4.3.3 Simulation Results

In this section, performance of proposed scheduler is compared with another PF based scheduler in [75]. Authors predetermined a proportion of PRBs to serve CoMP users and apply classic PF scheduler in CoMP users group and Non-CoMP users group respectively. The simulation setup is same as Table 4.1. Number of user is set to 200. Fairness and system throughput results are shown against percentage of predetermined PRBs for classic PF. Note that proposed two-layer PF algorithm doesn't need this predetermined parameter, therefore its performance only varies slightly in each figure.

From Figure 4.23, 4.25 and 4.27, system throughputs of classic PF both show the trend of decrease with increase of CoMP PRBs. The reason is that CoMP mode acquires more resource than Non-CoMP mode to improve cell-edge users' performance. With increase of proportion of CoMP PRBs, system resource wastes in unnecessary CoMP mode. Two-layer PF doesn't need to predetermine how many PRBs are for CoMP mode.

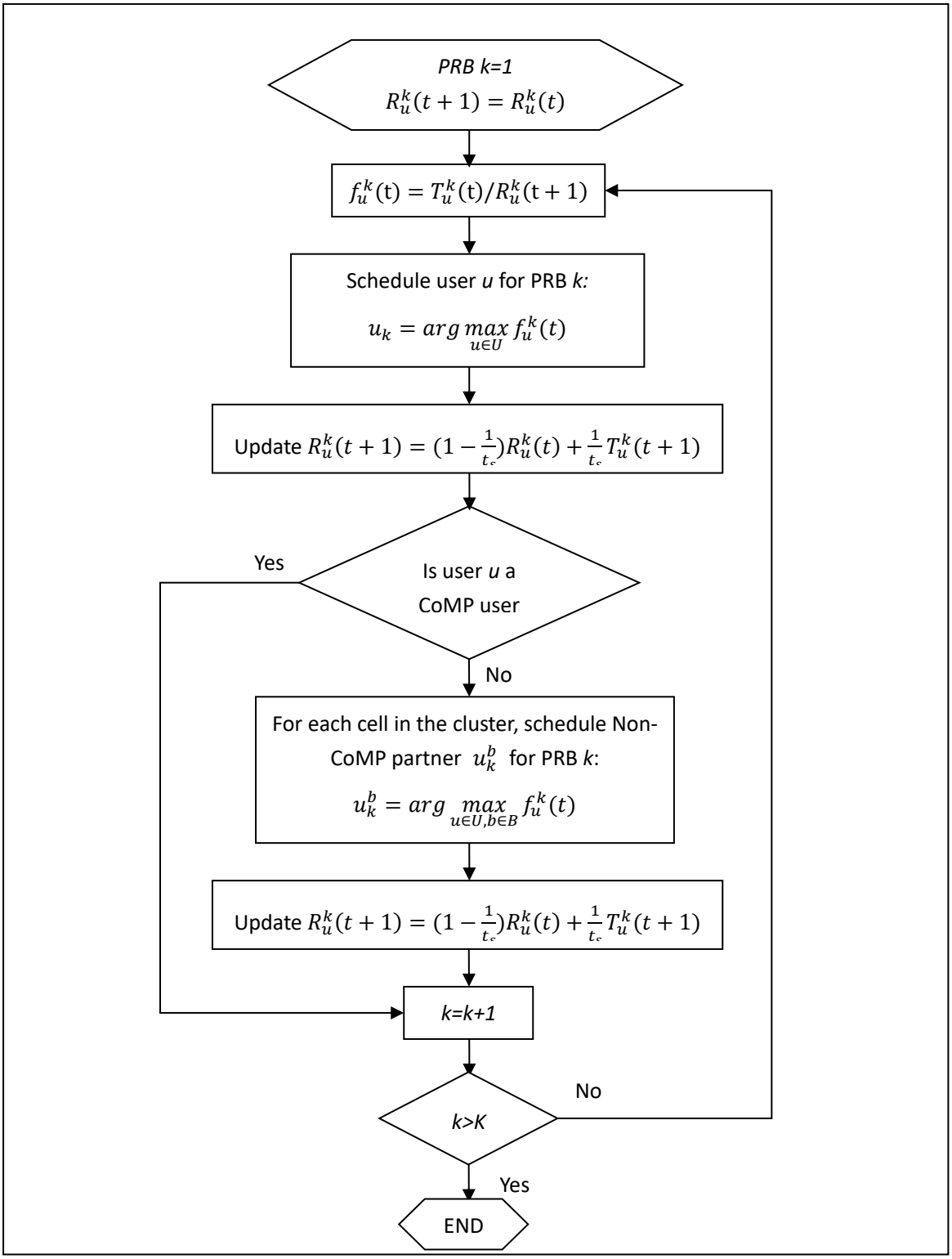

Figure 4.21: Two-layer PF user scheduler

In figures, it maintains a fairly good system performance. The first layer PF of proposed algorithm allows both CoMP and Non-CoMP users to compete PRBs, which results in a dynamic CoMP PRB selection. System performance doesn't depend on proportion of CoMP PRBs.

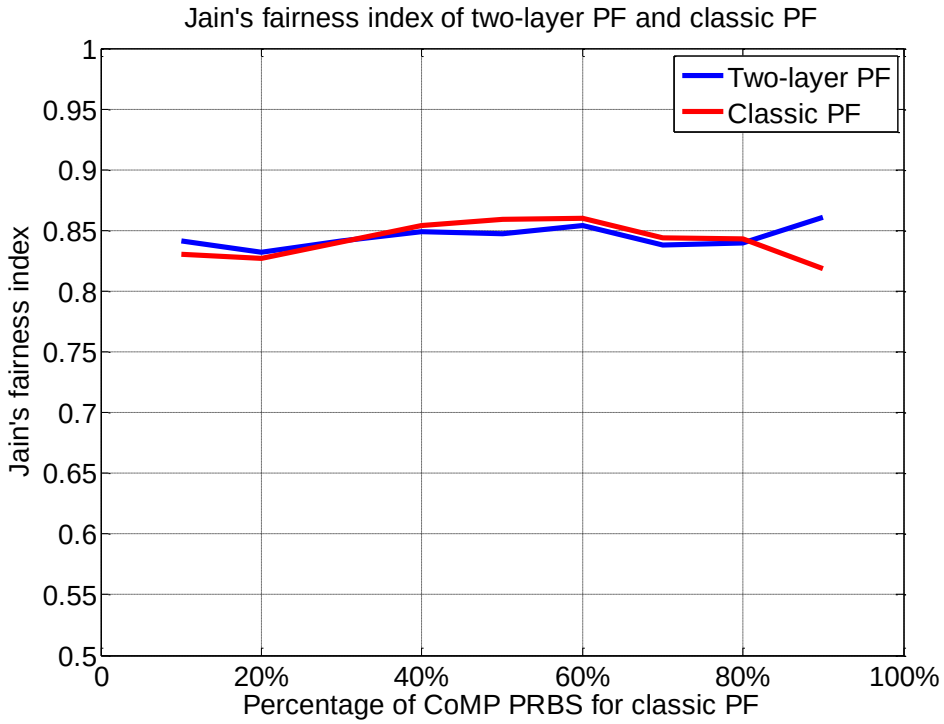

Figure 4.22: Fairness performance of Two-layer PF and classic PF scheduling, when 20% users are CoMP candidates

In Figure 4.22, thought system throughput of classic PF trend to decrease, its fairness doesn't show much fluctuation. This is because only 20% users are CoMP candidates. Its Jain's fairness dominated by large Non-CoMP users group, which are applied PF to ensure inter-group fairness.

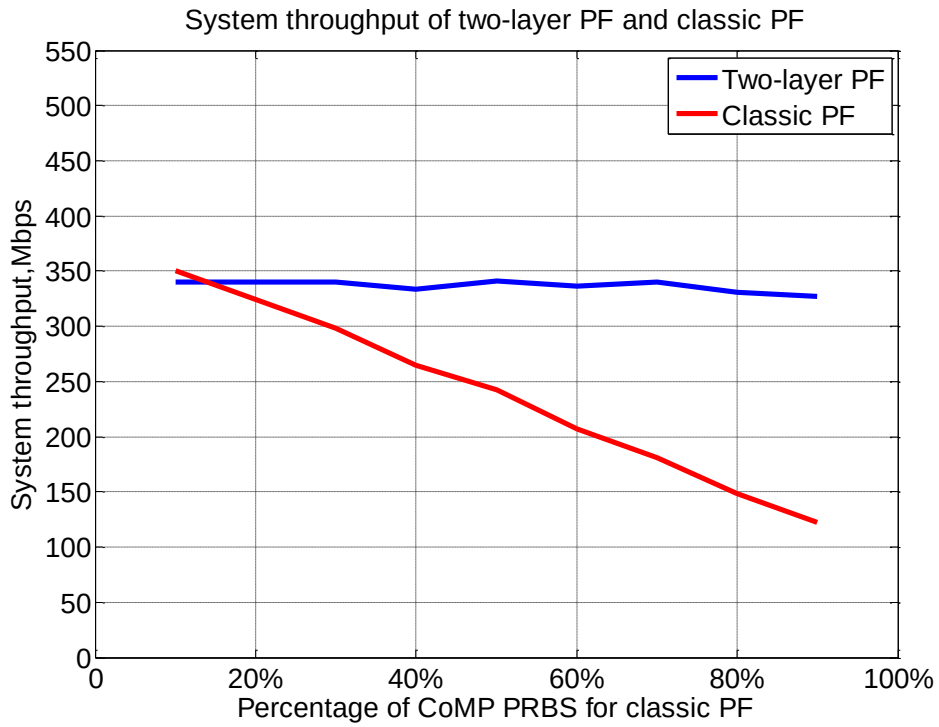

Figure 4.23: System throughput of Two-layer PF and classic PF scheduling, when 20% users are CoMP candidates

However, as shown in Figure 4.24 and 4.26, when number of CoMP candidates increases, balance between CoMP users group and Non-CoMP group is broken. When proportion of CoMP PRBs can't satisfy the requirement of large CoMP user group, as shown at 20% in Figure 4.24 and 4.26 for example, classic PF can't maintain a fairly resource allocation among all users. Non-CoMP users can access most of the system resource, resulting in a high system throughput.

In Figure 4.23, 4.25 and 4.27, system throughput of two-layer PF decreases with increase of CoMP user candidates. When CoMP candidates

are few in the whole users, two-layer PF works like a normal PF scheduler for Non-CoMP users with full system resource, which provides a good system throughput. To maintain fairness between CoMP users group and Non-CoMP users group when CoMP requirement is crucial, more system resource is allocated in CoMP mode, which causes a fall of whole system throughput.

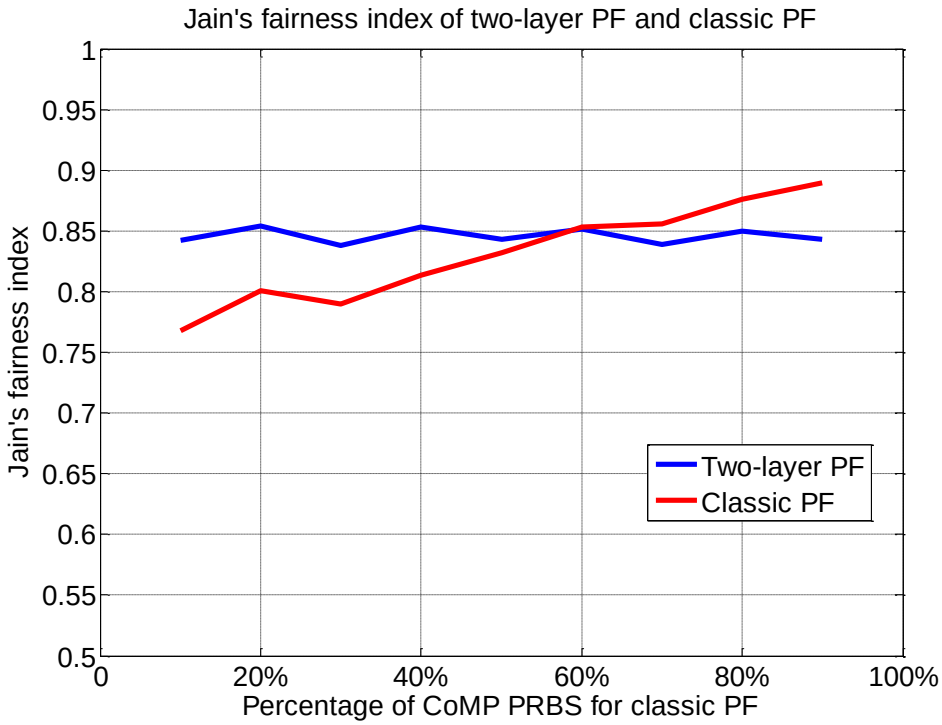

Figure 4.24: Fairness performance of Two-layer PF and classic PF scheduling, when 50% users are CoMP candidates

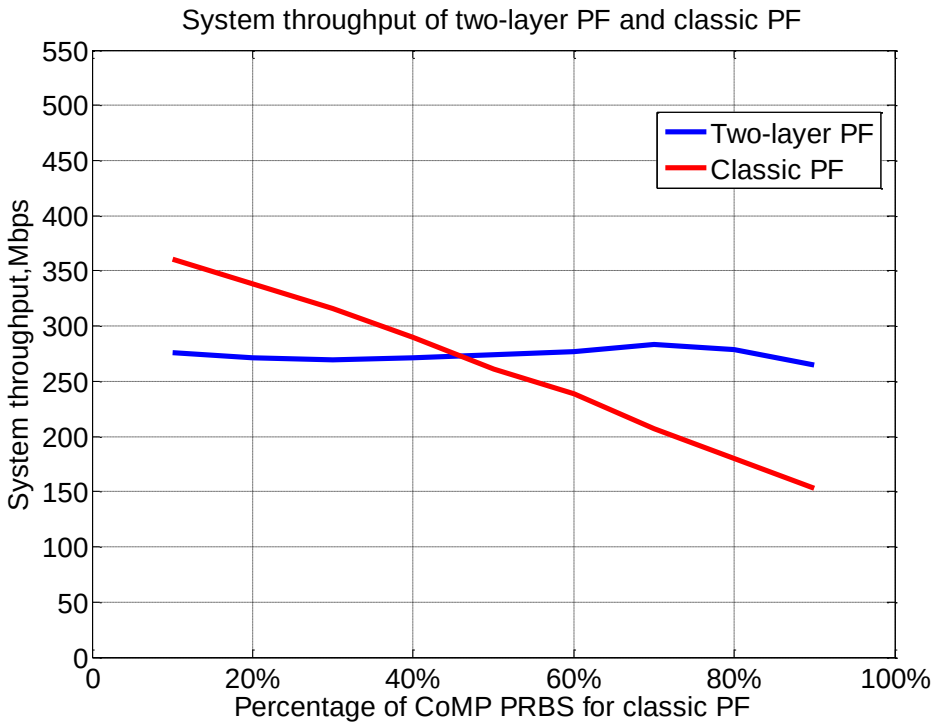

Figure 4.25: System throughput of Two-layer PF and classic PF scheduling, when 50% users are CoMP candidates

Curves of classic PF in figures have intersection point with two-layer PF. These points mean that classic PF achieves similar system throughput and fairness of two-layer PF when predetermined CoMP PRBs proportion matches proportion of CoMP user candidates. Therefore, predetermined CoMP PRBs percentage is crucial for classic PF in CoMP system in term of user fairness. Suggested percentage is 30%-50% [75]. Considering a common scenario, this ratio may be a fairly match of CoMP candidates. However, this predetermined percentage doesn't have flexibility to adopt to various real situation.

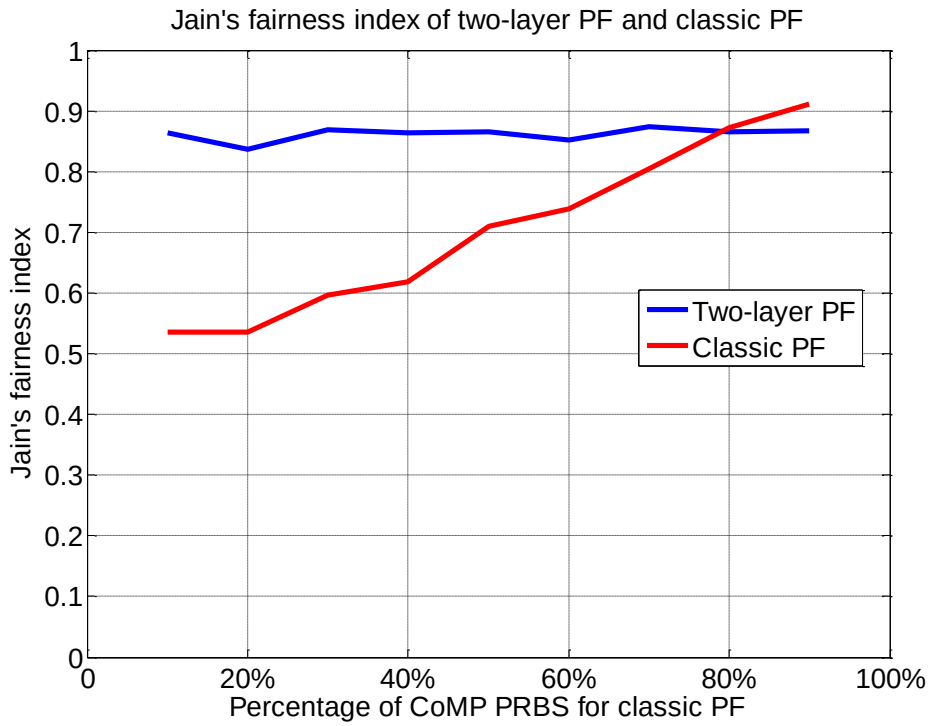

Figure 4.26: Fairness performance of Two-layer PF and classic PF scheduling, when 80% users are CoMP candidates

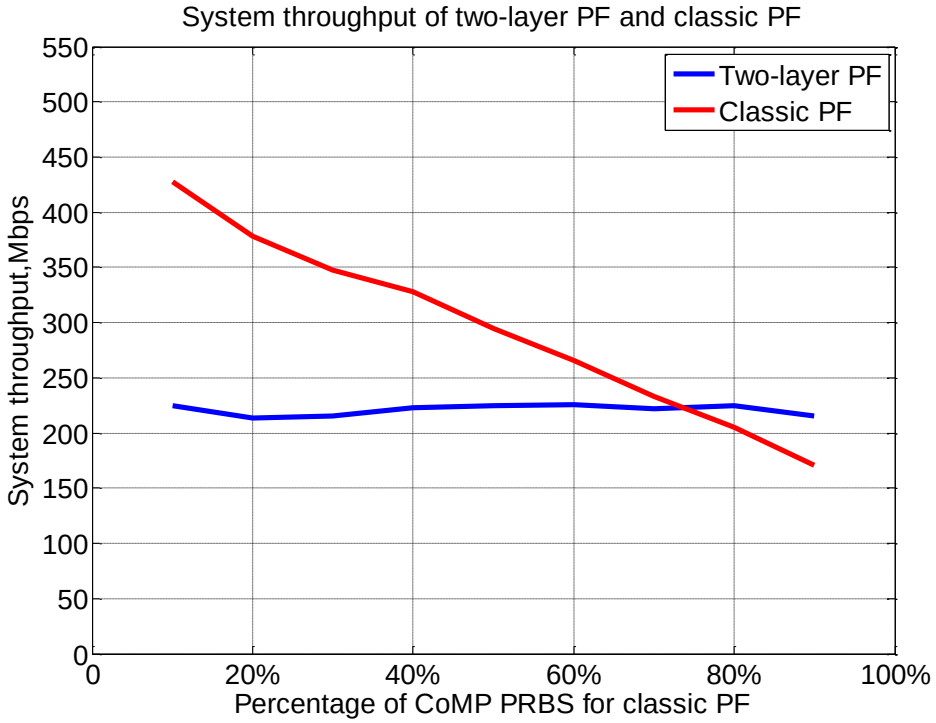

Figure 4.27: System throughput of Two-layer PF and classic PF scheduling, when 80% users are CoMP candidates

Let $\gamma_K = \frac{K_c}{K_c+K_b}$ be preterminal CoMP PRBs ratio, where K_c is number of CoMP PRBs and $K_b = K - K_c$ is number of Non-CoMP PRBs. $U = U_c + U_b \cdot N$ where U_c is number of CoMP candidates, U_b is number of Non-CoMP users in one cell. Assuming cluster has N cells and each cell has U_b Non-CoMP users. Let $\gamma_U = \frac{U_c}{U_c+NU_b}$ be the ratio of CoMP candidates of all users. The complexity of two-layer PF can be expressed as

$$\begin{aligned} &K(3U+6) + NK'(3U_b+6) \\ &= K(3U+6) + NK'(3U - U\cdot\gamma_U + 6) \end{aligned} \tag{4.28}$$

where K' is the number of PRBs belong to Non-CoMP users. Due to natural of PF algorithm, K'can be determined before simulation. And complexity of classic PF in CoMP can be expressed as

$$\begin{aligned} &K_c(3U_c+6) + NK_b(3U_b+6) \\ &= 3NK(U+2) + (2KU\cdot\gamma_K - 3NK)\gamma_U - K(U+N-6)\gamma_K \end{aligned} \tag{4.29}$$

From Equation 4.28, complexity of two-layer PF increases with number of CoMP candidates and is independent to γ_K. Equation 4.29 indicates that complexity of classic PF decreases with increase of CoMP PRBs proportion, since one PRB is only allocated once in CoMP mode but

in Non-CoMP mode every cell must allocate this PRB. Table 4.2 shows numerical results of complexity in form of simulation time. With low γ_K and high γ_U, complexities of two PF algorithm are similar, meanwhile with low γ_U and high γ_K, proposed two-layer PF algorithm has around 3 times as large as classic PF.

Table 4.2: Time of execution of two PF algorithm in simulation

Two-layer PF	$\gamma_U = 20\%$	$\gamma_U = 80\%$
$\gamma_K = 20\%$	0.9263	0.7664
$\gamma_K = 80\%$	0.9419	0.7617

Classic PF	$\gamma_U = 20\%$	$\gamma_U = 80\%$
$\gamma_K = 20\%$	0.7308	0.7140
$\gamma_K = 80\%$	0.3788	0.3794

4.4 Summary

A Fuzzy Logic based user selection algorithm and two PRBs allocation algorithms are proposed. Simulation results show that CoMP users' performance are improved. Proposed ranking based greedy allocation algorithm achieves same system performance with only half complexity. A two-layer proportional-fair user scheduling scheme is proposed to solve fairness problem among the whole users group in CoMP cluseter. Simulation results show that Fairness between CoMP and Non-CoMP users are balanced in a period of time with stable system throughput.

Chapter 5

RSS based Positioning for Cellular Networks

Location based services enables various cell phone applications such as navigation, security and social networking. Therefore, research for positioning techniques with high accuracy and low energy consume has gained huge interest. Global positioning system (GPS) [88] performs well in open areas, however, its performance degradation is significant with non-line-of-sight, and its energy consumption is relatively high. Network-based positioning has very good coverage and consumes few energies.

Time-based positioning techniques [89, 90] require location measurement unit (LMU) devices installed in networks, which is power consuming and expensive in operators' view. Angle-of-arrival (AOA) based positioning techniques [91] also require special hardware to obtain measurement information. On the other hand, received signal strength (RSS) based positioning techniques exploit regular signaling mechanism of cell phone to acquire measurement information without additional

hardware. RSS based methods employs path loss model to estimate distance, or consider distinct characteristic of RSS in different position. The main advantage is its low cost both for operators and users. In wireless communication networks, RSS is a basic data used to determine handover, estimate channel condition etc. therefore it is frequently measured by operator and user's equipment automatically. In dedicated mode (e.g. on phone, data streaming), RSS from at most 6 neighbor base stations are measured every 1 sec; in idle mode, at least every 5 minutes one measurement is performed. Exact measurement time depends on operator [88]. This makes RSS a cheap and popular data resource for network based positioning. According to its feature of auto-measuring, it is also useful in passive tracking, emergency positioning.

Classic RSS based positioning methods consider relationship between RSS and user's distance to base station. Path loss model is essential part in these methods. It is a function of distance and RSS, in which error in RSS measurement must be considered. Trilateration is very basic ranging-based method. Distance to each base station can be calculated from path loss model. With known path loss exponent (PLE), distance can be calculated from RSS by path loss model. Each distance indicates a circle around base station, which is potential user's position. With two or more distances, user's position is marked as the cross point, or intersection of circles when measurement error exists [16, 92]. Normally the center of intersection is

chosen as result. In [16] authors proposed that Dynamic Circle Expanding Mechanism (DCEM) to decrease intersection area. It is based on assumption that the measurement of strongest RSS is the most confident.

The Maximum likelihood (ML) estimator is another popular method. When the statistics of the measurement error are known, the ML estimator is asymptotically optimal [93, 94]. However, due to the nature of the localization problem itself, the formed ML estimator has no closed-form solution, and thus, an iterative solver is required. In addition, the formed ML estimator is non-convex, and thus, its performance highly depends on the initial point [16]. A poor initialization often leads to a very bad estimation. Moreover, also due to the non-convexity, searching for the global minimum of the ML estimator is very difficult [95]. Several researchers have proposed the linear least square (LLS) estimator [95, 96] to overcome disadvantages of ML method. The idea of the LLS estimator is to reorganize and approximate the original nonlinear equations into a set of linear equations and then apply the least square (LS) [96]. Though the LLS estimator is much easier and has an explicit solution, its accuracy is not as good as the ML estimator, particularly when the variance of the measurement noise is high or the geometric condition is not good [93]. Non-linear Least Square (NLLS) estimator is also used as iterative method to do positioning. It is similar to ML and need initial value [95]. In [97] author used LLS's result as a starting estimation for NLLS [98]. In addition,

Bayesian method is also considered to solve positioning problem [99, 100].

In [101] path loss is regarded as a random variable. An Empirical Bayes approach is applied to estimate distance from RSS. Ranging with path loss model is known to be very sensitive to measurement noise, especially when the channel parameters are estimated at run-time, due to the strong non-linearity. Instead, the Bayesian approach is robust but a prior information is needed, which is not realizable in commercial applications. Based on feature of shadowing, Bayesian method can regard path loss as a random variable with zero mean and certain variance. With variance of shadowing increase, accuracy of RSS based positioning decreases. Multipath can produce large bias on RSS measurement, however by only cell phone itself multipath effect is very hard to mitigate. In [102], author provided a joint method to estimate distance of each multipath path and attenuation exponent. But line-of-sight path is essential in this algorithm, which is not achievable.

RSS data can be used to build RSS map, performing Fingerprinting (FP) method [103, 104]; Artificial Neural Network (ANN) method also need a number of RSS data in advance to train network for positioning. Both of them assumed that RSS distribution in certain area is stable, or have certain relationship between each other [105]. Accuracy of FP depends on resolution of FP mapping, while ANN method can reach about 100m accuracy for certain scenario. In [96] author performed experiment

in GSM network in real environment. Artificial Neural Network (ANN) approach is applied. ANN based method normally has less than 100m error. However, it needs offline stage to train network which is not convenient in reality.

The main challenge in RSS based positioning is that raw RSS data is affected by many factors. Shadowing and interference etc. cause estimation error on RSS. Multipath makes RSS changing heavily. Unknown path loss model introduces more ranging error. Most of researches focus on reducing error in path loss model and positioning algorithm. Accuracy of RSS measurement has only few discussion [105, 106]. Accuracy of RSS measurement plays a crucial role. For example least square methods are very sensitive to measurement error [101].

RSS measurement contains several noise and nuisance parameters, including power of background noise, multipath and shadowing. A convenient way to reduce measurement error is averaging RSS samples over time, which can attenuate time variability error. But other errors, including interference, space-dependent variability errors, such as error from shadowing, multipath, are hardly reduced [2]. Normally background noise is simulated as AWGN which can be eliminated by average over time. The shadowing is assumed position-dependent, but almost time invariant [99]. Shadowing components in path loss model is usually a Gaussian zero mean random with certain variance. According to [88] the small-scale

fading (fast fading) due to the multipath can be removed by averaging over time. Most of papers assume the same thing. However, equations in [19] showed that this needs a large amount of sampling to do time averaging, which means this assumption is not achievable in practice.

In this chapter, a RSS based low-complexity approach with unknown PLE for cellular networks is proposed, which requires low computational complexity. The proposed work is different from others in the following aspects. First, the proposed algorithm exploits a PLE searching (PLES) algorithm to estimate unknown parameter. By separating PLE estimation from coordination mapping, complexity of algorithm is reduced. Second, a simplified trilateration (ST) algorithm is proposed to increase weight of reliable raw data and avoid complexity of LS algorithm. Simulation results show that the proposed algorithm has significantly less computational complexity with slightly degradation on accuracy.

Following that, RSS measurement method in LTE system is analyzed and a realizable RSS measurement method is proposed to fight against multipath effect. The contribution of this work is that, in RSS based positioning area, this is the first work that consider exploiting LTE's own signal strength measurement mechanism to enhance accuracy of positioning. The proposed work is different from existing work is that the proposed method has possibility to be deployed in modern LTE system with limited cost.

The rest of the chapter is organized as follows. The low-complexity positioning method is presented in Section 5.1. The multipath reduced RSS measurement method is presented in Section 5.2. Section 5.3 gives the summary.

5.1 Low-complexity Positioning with Unknown Path Loss Exponent

5.1.1 System Model

In cellular network, cell phone regularly measures RSSs and reports up to 6 strongest RSSs from neighbor base stations. These base stations are regarded as reference nodes (RNs). In this paper, we suppose that there are *n* RNs measured by target user's equipment. The *i*th reference node RN_i's position is known and denoted as(x_i, y_i), $1 \le i \le n$, and position of target equipment is denoted as (x, y). The measured RSS from the *i*th reference node RN_i is denoted as RSS_i. Assuming that $PL_i \sim \aleph(\overline{PL}_i, \sigma_{dB}^2)$ is the path lose in dBm unit. The log-distance path loss model describes the relationship between signal power and distance, which can be expressed as [15]

$$\overline{PL}_i = PL_0 - 10\alpha log_{10}\left(\frac{d_i}{d_0}\right) + v \qquad (5.1)$$

where PL_0 is the path loss in dBm unit at distance d_i and reference distance d_0, respectively, α is the PLE, and v represents the shadowing effect which is a random variable with zero-mean Gaussian distribution and standard deviation σ_v. Transmission power P_{ti} can be obtained from operator and RSS_i at RN_i can be expressed as $RSS_i = P_{ti} - PL_i$. Normally, the reference distance d_0 is set to 1m [19]. Therefore, the relationship between RSS and distance can be presented as [15]

$$RSS_i = P_0 + 10\alpha log_{10}(d_i) + v \qquad (5.2)$$

Where P_0 is the signal power at 1m distance away from RN_i, which is assumed to be a fixed parameter for all RN_i. Given Equation (5.1), the density of PL_i is

$$f(PL_i|\overline{PL}_i, \sigma_{dB}^2) = \left(\frac{1}{2\pi\sigma^2}\right)^{n/2} exp\left(-\frac{\sum_{i=1}^{n}(PL_i - \overline{PL}_i)^2}{2\sigma^2}\right)$$

To maximize likelihood,

$$log\left(\mathcal{L}(\overline{PL}_i, \sigma_{dB}^2)\right) = log\left(f(PL_i|\overline{PL}_i, \sigma_{dB}^2)\right)$$

$$= \left(-\frac{n}{2}\right) log(2\pi\sigma^2) - \frac{1}{2\sigma^2}\sum_{i=1}^{n}(RSS_i - P_0 - 10\alpha log_{10}(d_i) - v)^2$$

$$\frac{\partial}{\partial \overline{PL}_i} log\left(\mathcal{L}(\overline{PL}_i, \sigma_{dB}^2)\right) = 0$$

From above derivation, the maximum likelihood (ML) estimator of d_i is expressed as [15]

$$\hat{d}_i = 10^{\frac{RSS_i - P_0}{10\alpha}} \tag{5.3}$$

5.1.2 Simplified Trilateration

When path loss exponent is known, distances from RNs to user's position can be calculated. The distance $\hat{d}_i$ indicates a circle C_i denoting possible position of user around RN_i. A simplified trilateration is proposed to estimate user's position. We assume that the signal with stronger RSS suffer less noise. Then three RNs with strongest RSSs are chosen to apply ST, where $RSS_3 \geq RSS_2 \geq RSS_1$ represent them respectively. Two scenarios are discussed. In the first scenario, C_2 and C_3 have intersection points *A* and *B,* as shown in Figure 5.1 (a). Then the one which is closer to the edge of C_1 is chosen as estimation, which is point A in Figure 5.1 (a). In scenario II, shown as Figure 5.1 (b), C_2 and C_3 have no intersection point. Then according to position of C_1 , the middle point *A* between points *B* and *E* is chosen as estimation, where points *B* and *E* are intersection points of edges and line of centers.

With accurate RSS readings, three circles should have only one intersection point. However, due to multipath effect RSS readings normally contain error, which can't generate the unique intersection point. In ST method, the possible intersection area is roughly estimated by the

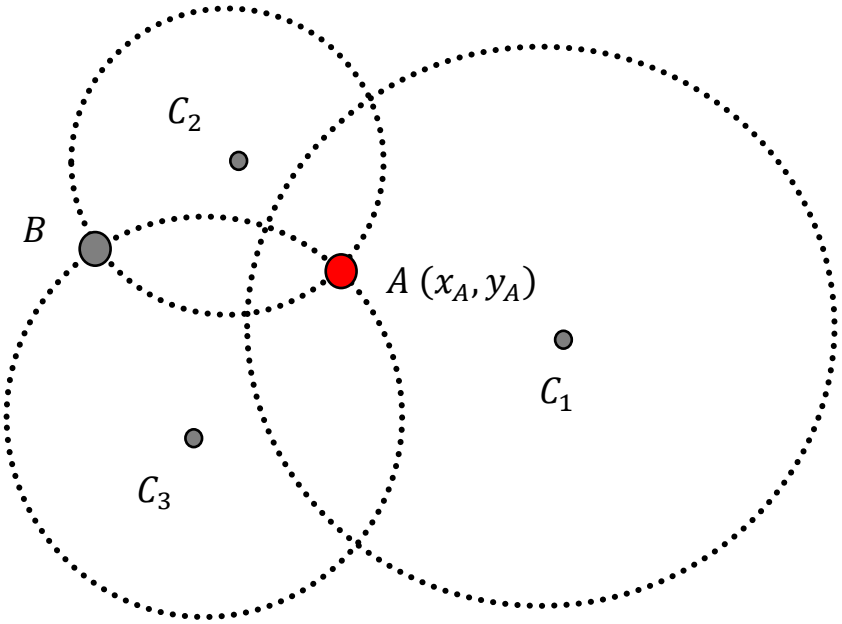

(a)

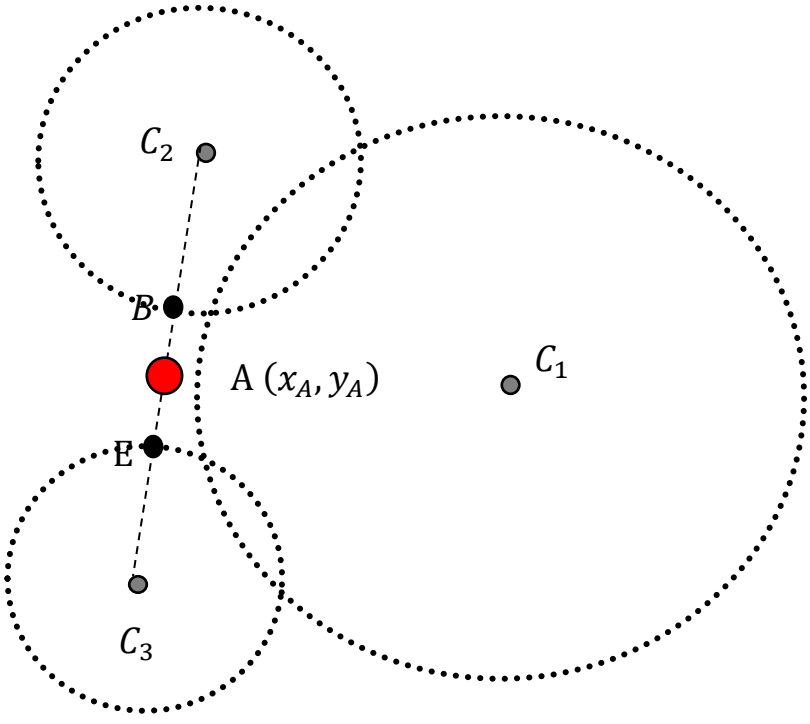

(b)

Figure 5.1: Simplified Trilateration with (a) scenario I; (b) scenario II.

most reliable two RSS readings and the intersection point is determined according to the third reading.

Finally, the estimated user position is given by $(\hat{x}_{SL}, \hat{y}_{SL}) = (x_A, y_A)$, the distance between estimate position and RN_i is expressed as

$$d_{SL,i} = \sqrt{(\hat{x}_{SL} - x_i)^2 + (\hat{y}_{SL} - y_i)^2} \tag{5.4}$$

5.1.3 PLE Searching

In a real environment, PLE α may be changed by terrain or weather. Therefore, a PLE searching algorithm is proposed to estimate α dynamically. For all PLE α_j within constrains $\alpha_{min} \leq \alpha_j \leq \alpha_{max}$ with step of 0.01 empirically regarding to a tradeoff between complexity and accuracy, the ST algorithm can calculate distance $d_{SL,i,j}$, while ML estimator can calculate distances $\hat{d}_{i,j}$. The difference between these two types of distances are calculated and the α_j with smallest matching difference is chosen as the estimated PLE $\hat{\alpha}$.

$$\hat{\alpha} = \arg \min_{\alpha_{min} \leq \alpha_j \leq \alpha_{max}} \sum_{\mathrm{i}=1}^{\mathrm{n}} (d_{SL,i,j} - \hat{d}_{i,j})^2 \tag{5.5}$$

Related position $(\hat{x}_{SL}, \hat{y}_{SL})$ is recorded as user's position estimate. Positioning error ε can be expressed as

$$\varepsilon = \sqrt{(\hat{x}_{SL} - x)^2 + (\hat{y}_{SL} - y)^2} \tag{5.6}$$

5.1.4 Simulation Results

An area containing three fixed RNs is considered in the simulation. The coverage of each RN is set to 800m. Initial values for NLS are randomly generated in the simulation area. Real PLE changes randomly between 2 to 6 at every start of loop. 1000 users' positions are randomly generated in simulation area. Cumulative distribution function (CDF) of positioning error is expressed as $\mathrm{CDF}(err) = \mathrm{p}(\varepsilon \leq err)$, where right-hand side represents the probability that ε the takes on a value less than or equal to error threshold err.

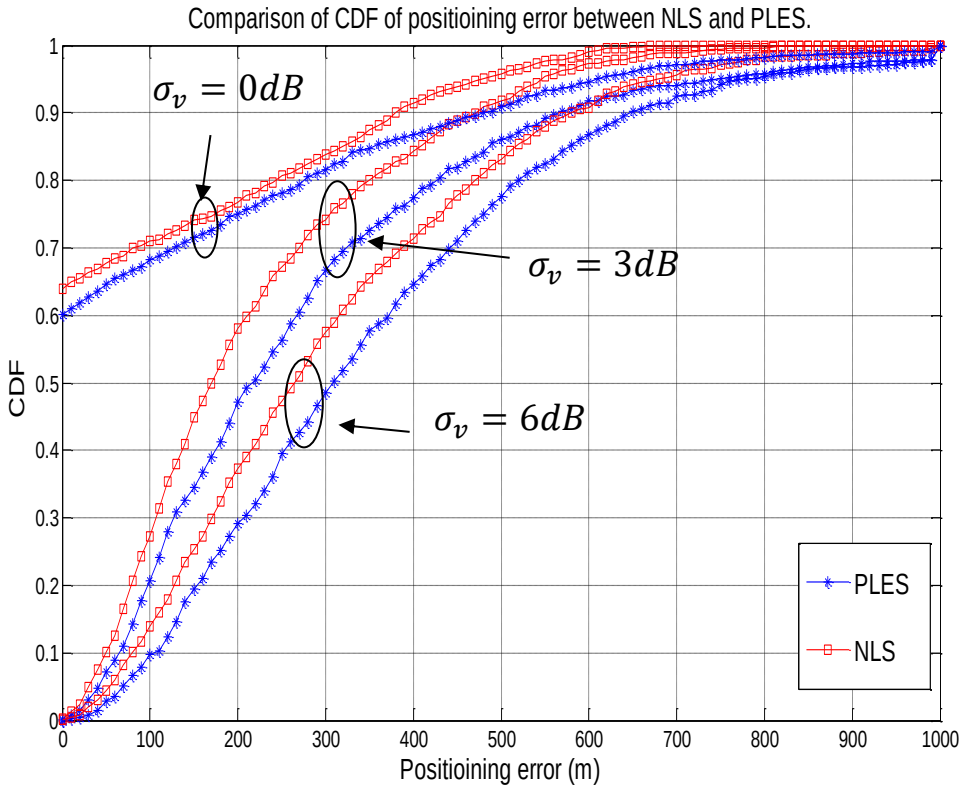

Figure 5.2: CDF performance comparison between NLS and PLES with 0, 3 and 6 dB shadowing.

Figure 5.2 shows that proposed PLES have similar accuracy with NLS. Accuracy of PLES is about 50m worse than NLS. Reason is SL algorithm have worse accuracy than ML estimator. The shapes of CDF of PLES and NLS are similar, indicating that their poisoning results have similar error variance.

Table 5.1 shows that PLES algorithm has only about 1/30 complexity when 3 RNs are available, where the I is number of iteration which is set to 300 in consideration of both convergence and complexity. When the number of available RNs increase, this ratio decreases to 1/40.

Table 5.1: Complexity Comparison

Algorithm	Normalized Complexity			
	n=3	n=4	n=5	n=6
NLS [15], I=300	29	43	61	82
PLES	1	1.33	1.64	2

I is number of iteration.

5.2 Multipath Reduced RSS Measurement in LTE System

5.2.1 System Model

We consider a signal going through multipath channel,

$$y(t) = x(t) \otimes h(t) \tag{5.7}$$

Its baseband form can be expressed as

$$r(t) = \frac{1}{2}\sum_{l=1}^{L} h_l e^{-j\theta_l} \cdot c(t-\tau_l) \tag{5.8}$$

where $\theta_l = 2\pi f_c \tau_l + \phi_l$, L is number of paths, τ_l is delay time of *l-th* path, ϕ_l is phase shift on *l-th* path, h_l is amplitude of *l-th* path. And the instantaneous power can be given by

$$P = |r(t)|^2 = \frac{1}{4}\sum_{l=1}^{L} {a_l}^2 + \frac{1}{2}\sum_{k=1}^{L}\sum_{l=1,l\neq k}^{L} b_{kl} cos(\theta_k - \theta_l) \tag{5.9}$$

$$a_l = h_l c(t-\tau_l), \quad b_{kl} = h_l h_k c(t-\tau_l) c(t-\tau_k) \tag{5.10}$$

Over a small-scale time and distance, we can assume channel impulse response is time invariant. h_l does not change much in small area, but θ_l can vary very much due to time delay and phase shift of each paths. The first part of Equation (5.9) contains time-invariant attenuation in power, including path loss and shadowing effect, which can be regarded as space-dependent factor. The second part indicates multipath effect on signal strength.

5.2.2 Multipath Reduction in RSS Measurement

The received signal strength in LTE is measured by reference signal received power (RSRP), which is the average power of REs carrying reference signal (RS). This measurement is attractive because it is the power of only desire signal, excluding inter-cell interference, thermal noise, control channel etc. therefore RSRP are much more reliable than RSS in past networks. Every resource block has four special REs which contain reference signal. They are spaced by 3 REs and are used to do channel estimation.

Table 5.2 shows a brief signal structure of one PRB. The four red RE, 6, 12, 51 and 57 carry RS in this PRB. RSRP is an averaged value for all the REs for reference signal.

Table 5.2: Physical Resource Block

Symbol:	S0	S1	S2	S3	S4	S5	S6
12 REs	1	13	25	37	49	61	73
	2	14	26	38	50	62	74
	3	15	27	39	51	63	75
	4	16	28	40	52	64	76
	5	17	29	41	53	65	77
	6	18	30	42	54	66	78
	7	19	31	43	55	67	79
	8	20	32	44	56	68	80
	9	21	33	45	57	69	81
	10	22	34	46	58	70	82
	11	23	35	47	59	71	83
	12	24	36	48	60	72	84

Normal RSS processing is to apply time-averaging on received power, which can be expressed as

$$RSS_t = \boldsymbol{E}[P]$$

$$\approx \frac{1}{4}\sum_{l=1}^{L} \boldsymbol{E}[{a_l}^2] + \frac{1}{2}\sum_{k=1}^{L}\sum_{l=1,l\neq k}^{L} \boldsymbol{E}[b_{kl}]\boldsymbol{E}[\cos(\theta_k - \theta_l)] \quad (5.11)$$

if θ_l are uniformly identically and independently distributed over $[0, 2\pi]$, and signal samples are large enough, the second part of Equation (5.11) equals to 0. But in reality, sampling cannot satisfy this requirement.

According to mechanism of measurement of RSRP, if multiple PRBs which are successive in frequency are assigned to the same equipment, its RSS value, which is measured by RSRP is presented as

$$RSS_p = \frac{1}{N}\sum_{n=1}^{N} \boldsymbol{E}[P]_n$$

$$= \frac{1}{N}\sum_{n=1}^{N}\left[\frac{1}{4}\sum_{l=1}^{L}\boldsymbol{E}[{a_l}^2] + \frac{1}{2}\sum_{k=1}^{L}\sum_{l=1,l\neq k}^{L}\boldsymbol{E}[b_{kl}]\boldsymbol{E}[\cos(\theta_k - \theta_l)]\right]$$

$$\approx \frac{1}{4}\sum_{l=1}^{L}\boldsymbol{E}[{a_l}^2] + \frac{1}{2}\sum_{k=1}^{L}\sum_{l=1,l\neq k}^{L}\boldsymbol{E}[b_{kl}]\cdot\boldsymbol{E}[\frac{1}{N}\sum_{n=1}^{N}\cos(\theta_k - \theta_l)] \qquad (5.12)$$

Assuming there are N REs carrying RS and $f_{c+1} = f_c + \Delta f$, which means these signals are spaced by same band width.

$$\frac{1}{N}\sum_{n=1}^{N} cos(\theta_k - \theta_l) = \frac{1}{N}\sum_{n=1}^{N}\cos(2\pi f_0\tau_{kl} + 2\pi n\Delta f\tau_{kl} - \phi_{kl})$$

$$= \left[\frac{sin(N\Delta f\tau_{kl})}{Nsin(\Delta f\tau_{kl})}\right] cos[2\pi f_0\tau_{kl} + 2\pi(N-1)\Delta f\tau_{kl} - \phi_{kl}\,]$$

$$= \boldsymbol{A}cos[2\pi f_0\tau_{kl} + 2\pi(N-1)\Delta f\tau_{kl} - \phi_{kl}\,]$$

$$\approx \boldsymbol{A}cos(\theta_k - \theta_l) \qquad (5.13)$$

where $\boldsymbol{A} = \left[\frac{sin(N\Delta f\tau_{kl})}{Nsin(\Delta f\tau_{kl})}\right]$, which is a periodic sinc function, its derivation is described in [107]. $\boldsymbol{A}$ has a range from 0 to 1, and when N increases, envelope of A goes flatter to 0.

Substituting (5.13) in (5.12), we can get,

$$RSS_p = \frac{1}{4}\sum_{l=1}^{L} \boldsymbol{E}[{a_l}^2] + \frac{1}{2}\sum_{k=1}^{L}\sum_{l=1,l\neq k}^{L} \boldsymbol{AE}[b_{kl}]\boldsymbol{E}[\cos(\theta_k - \theta_l)] \quad (5.14)$$

Compare RSS_t with RSS_p,

$$RSS_t = \boldsymbol{E}[P]$$

$$\approx \frac{1}{4}\sum_{l=1}^{L} \boldsymbol{E}[{a_l}^2] + \frac{1}{2}\sum_{k=1}^{L}\sum_{l=1,l\neq k}^{L} \boldsymbol{E}[b_{kl}]\boldsymbol{E}[\cos(\theta_k - \theta_l)] \quad (5.15)$$

$$RSS_p = \frac{1}{4}\sum_{l=1}^{L} \boldsymbol{E}[{a_l}^2] + \frac{1}{2}\sum_{k=1}^{L}\sum_{l=1,l\neq k}^{L} \boldsymbol{AE}[b_{kl}]\boldsymbol{E}[\cos(\theta_k - \theta_l)] \quad (5.16)$$

We can find,

$$Mean(RSS_p) = Mean(RSS_t) = \boldsymbol{E}\left[\frac{1}{4}\sum_{l=1}^{L} \boldsymbol{E}[{a_l}^2]\right] \quad (5.17)$$

$$Variance(RSS_p) < Variance(RSS_t) \quad (5.18)$$

The second part of RSS_p represents self-interference caused by multipath. Form (5.17) and (5.18), multipath effect on signal strength is reduced. To satisfy the requirement of proposed processing method, target user must have multiple PRBs successive in frequency. This can be

deployed by scheduling when service is required.

5.2.3 Simulation Results

Given fixed location, RSS by time averaging and RSS by proposed processing are shown in Figure 5.3, 5.4, when transmitted power is set to 33dbm. Obviously proposed RSS significantly reduce multipath effect. As number of used frequency increase, RSS by time averaging is slightly closer to real signal power, because number of samples increases with more frequency involved. RSS by proposed multipath reduced method shows trend with increase of used frequency and significant less diversity. To complete proposed method, number N must be continuous integers, which ensure $f_c + N\Delta f$ is carrier frequency of *n-th* signal. This requirement can be supported by LTE.

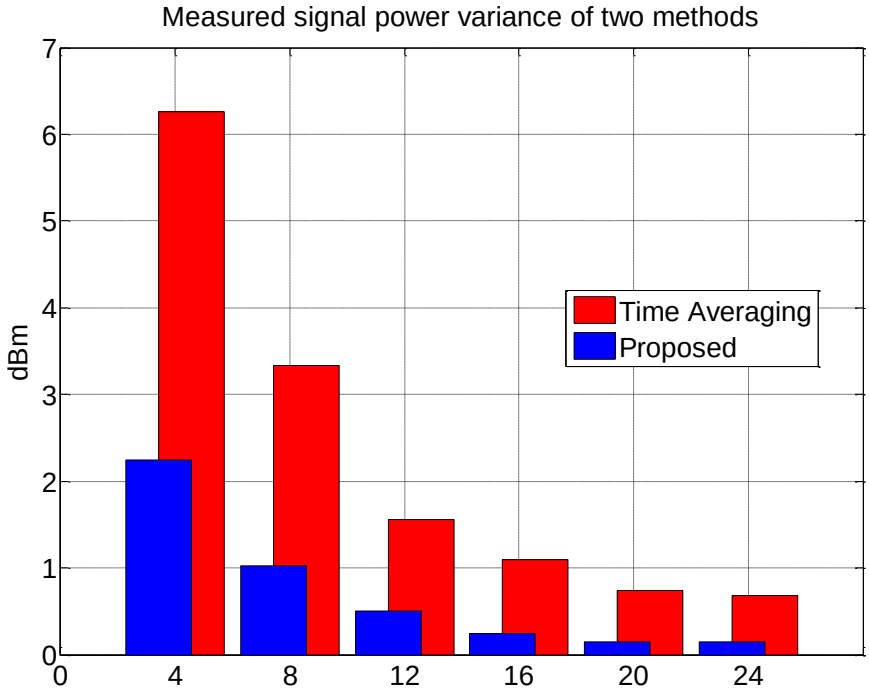

Figure 5.3: Variance of measured signal power of two methods

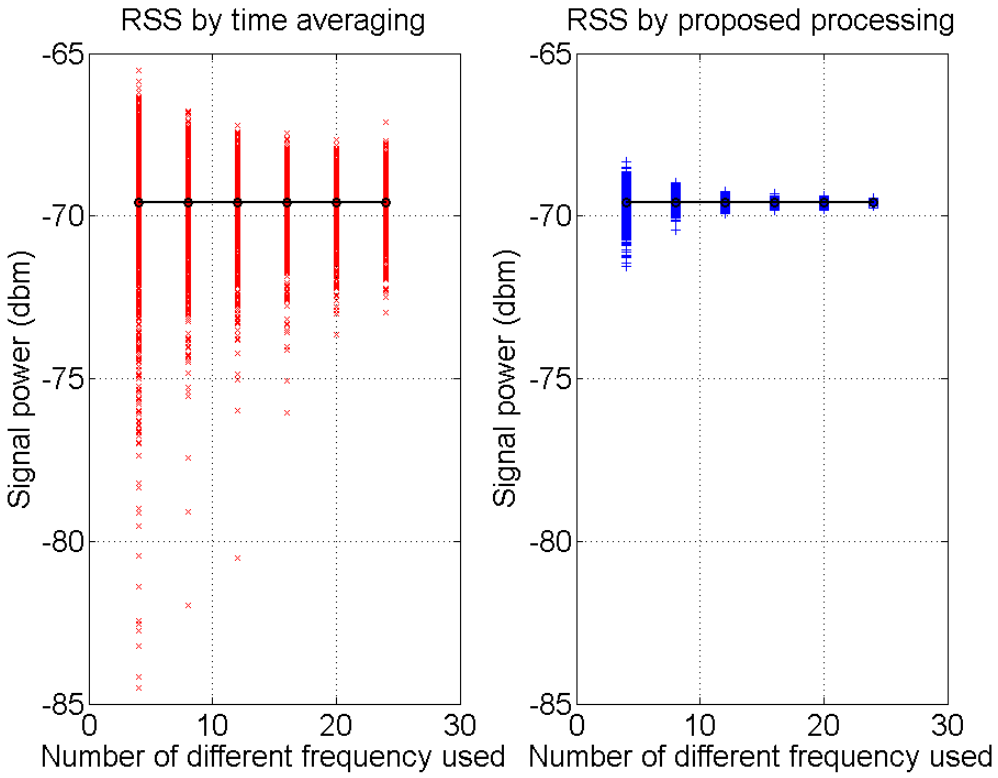

Figure 5.4: Measured signal power diversity of two methods

Given fixed location and PLE, Figure 5.5 presents mean positioning error of two measurement methods. Proposed multipath reduced method provides significantly advantage of accuracy over normal RSS measurement method. With accurate RSS measurement, improvement on performance RSS based positioning is shown in Figure 5.5

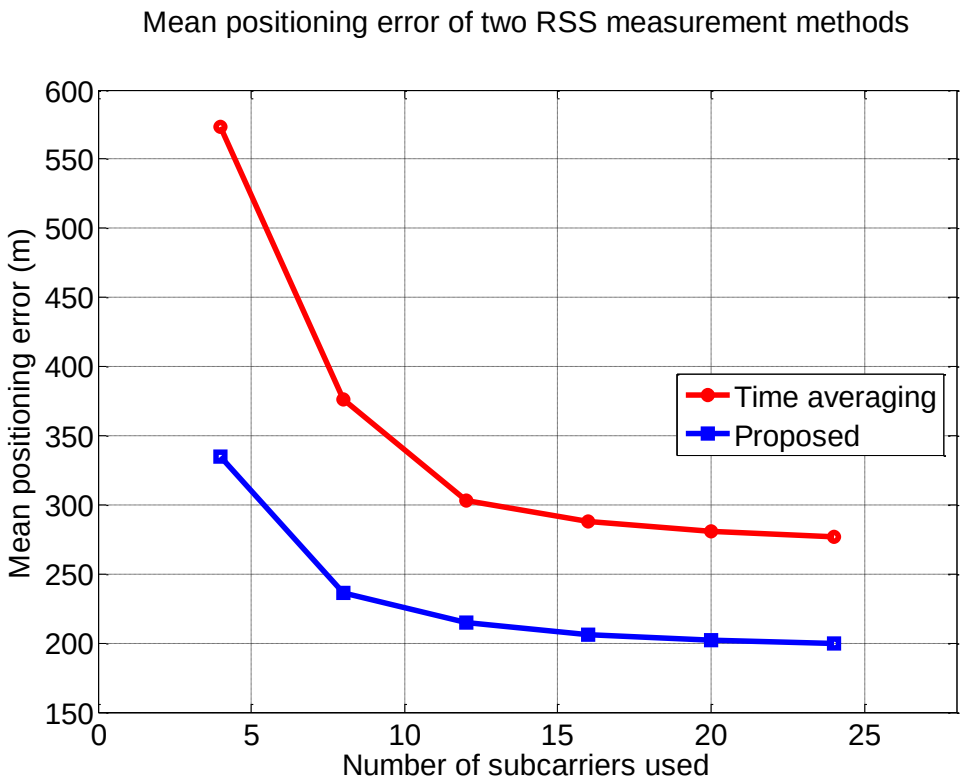

Figure 5.5: Mean positioning error of two RSS measurement methods with known PLE and LS method.

5.3 Summary

A low-complexity positioning algorithm is proposed in the absence of known PLE in Section 5.1, which consists of PLE Searching and Simplified Trilateration. Simulation results show that it achieves a 30-fold complexity reduction over the classic NLS method, with similar positioning accuracy. In Section 5.2, signal structure of LTE system is analyzed and a multipath reduced RSS measurement method is proposed to improve accuracy of raw RSS data. Simulation results shows that

measurement error of RSS causing by multipath effect is significantly reduced by proposed method with mechanism support of LTE system.

Chapter 6

Conclusions and Future work

6.1 Conclusions

In this thesis, resource allocation in LTE network with CoMP has been investigated, including user selection algorithm and user fairness in the whole system. In additional, RSS based positioning with cellular network has been studied, including RSS measurement in LTE network.

In Chapter 4, the PRBs allocation algorithms with user selection have been investigated for CoMP system. the proposed FL based user selection takes distance, SINR and RSRP as input to choose CoMP users and provides a convenient ranking order for following RA process. Simulation results show that proposed FL improves performance of cell edge UEs comparing with D/SINR based algorithms. With USRG RA algorithm, computational complexity is reduced in half. Furthermore, proposed two-layer proportional-fair scheduling algorithm schedules resource to solve fairness problem between CoMP and Non-CoMP users without predetermined

PRBs plan. Simulation results show that proposed PF algorithm outperforms classic PF in [75] in terms of maintaining fairness. The flexibility to achieve promised performance considering various users' setup is also an advantage.

In Chpater 5, low-complexity positioning with unknown path loss exponent has been discussed. Proposed PLES method combines a simplified trilateration and iterative PLE searching method to estimate UE's positioning. Simulation results show that proposed method has slightly worse positioning accuracy but only requires 1/30 computational complexity. In addition, an RSS measurement method aiming multipath reduction for positioning is proposed according to signal structure of LTE system. Simulation results show that variance of measured RSS significantly reduced which benefit RSS based positioning.

6.2 Future Work

In the research on CoMP systems presented in this thesis, it has been assumed that users are randomly distributed in the CoMP cluster. In this case every cell in this cluster has sufficient resource to achieve optimization results. In practice however, users' distribution highly depends on local condition. Furthermore, since this work focus on PRB allocation, only averaged power allocation scheme is considered. With

adapted power allocation scheme, proposed PRB allocation scheme can achieve better results. Hence, the future research topics are summarized as the following:

1. Scenarios with extreme users' distribution will be investigated and proposed allocation scheme will be deployed in.
2. Adapted power allocation scheme will be investigated to coordinate with proposed PRB allocation scheme.

Appendix A

Fuzzy Rule Base

	Criteria			CoMP Suitability
No.	VRSRP	D	CSI	
1	small	short	bad	medium
2	small	short	medium	bad
3	small	short	good	very bad
4	small	medium	bad	good
5	small	medium	medium	medium
6	small	medium	good	medium
7	small	long	bad	very good
8	small	long	medium	very good
9	small	long	good	good
10	medium	short	bad	medium
11	medium	short	medium	bad
12	medium	short	good	very bad
13	medium	medium	bad	good
14	medium	medium	medium	medium
15	medium	medium	good	bad
16	medium	long	bad	very good

17	medium	long	medium	good
18	medium	long	good	medium
19	large	short	bad	bad
20	large	short	medium	bad
21	large	short	good	very bad
22	large	medium	bad	medium
23	large	medium	medium	bad
24	large	medium	good	very bad
25	large	long	bad	good
26	large	long	medium	medium
27	large	long	good	bad

Bibliography

[1] A. F. Molisch, *Wireless Communications, 2nd Edition*. Wiley-IEEE Press, 2011.

[2] K. Q. T. Zhang, *Wireless communications : principles, theory and methodology*. Somerset: Wiley, 2015.

[3] D. Choi, D. Lee, and J. H. Lee, "Resource Allocation for CoMP With Multiuser MIMO-OFDMA," *IEEE Transactions on Vehicular Technology,* vol. 60, no. 9, pp. 4626-4632, 2011.

[4] N. Zhou, X. Zhu, and Y. Huang, "Optimal Asymmetric Resource Allocation and Analysis for OFDM-Based Multidestination Relay Systems in the Downlink," *IEEE Transactions on Vehicular Technology,* vol. 60, no. 3, pp. 1307-1312, 2011.

[5] H. Chen, H. C. B. Chan, C.-K. Chan, and V. C. M. Leung, "QoS-Based Cross-Layer Scheduling for Wireless Multimedia Transmissions with Adaptive Modulation and Coding," *IEEE Transactions on Communications,* vol. 61, no. 11, pp. 4526-4538, 2013.

[6] K. M. S. Huq, S. Mumtaz, J. Bachmatiuk, J. Rodriguez, X. Wang, and R. L. Aguiar, "Green HetNet CoMP: Energy Efficiency Analysis and Optimization," *IEEE Transactions on Vehicular Technology,* vol. 64, no. 10, pp. 4670-4683, 2015.

[7] J. Lee, Y. Kim, Y. Kwak, J. Zhang, A. Papasakellariou, T. Novlan, C. Sun, and Y. Li, "LTE-advanced in 3GPP Rel -13/14: An evolution toward 5G," *IEEE Communications Magazine,* vol. 54, no. 3, pp. 36-42, 2016.

[8] H. L. Ming Ding, *Multi-point cooperative communication systems : theory and applications*. Berlin: Springer 2013.

[9] Q. Zhang and C. Yang, "Transmission Mode Selection for Downlink Coordinated Multipoint Systems," *IEEE Transactions on Vehicular Technology,* vol. 62, no. 1, pp. 465-471, 2013.

[10] A. Kumar, A. Sengupta, R. Tandon, and T. C. Clancy, "Dynamic Resource Allocation for Cooperative Spectrum Sharing in LTE Networks," *IEEE Transactions on Vehicular Technology,* vol. 64, no. 11, pp. 5232-5245, 2015.

[11] H. Zhu, "Radio Resource Allocation for OFDMA Systems in High Speed Environments," *IEEE Journal on Selected Areas in Communications,* vol. 30, no. 4, pp. 748-759, 2012.

[12] M. S. Alam, J. W. Mark, and X. S. Shen, "Relay Selection and Resource Allocation for Multi-User Cooperative OFDMA Networks," *IEEE Transactions on Wireless Communications,* vol. 12, no. 5, pp. 2193-2205, 2013.

[13] N. Zhou, X. Zhu, Y. Huang, and H. Lin, "Low complexity cross-layer design with packet dependent scheduling for heterogeneous traffic in multiuser OFDM systems," *IEEE Transactions on Wireless Communications,* vol. 9, no. 6, pp. 1912-1923, 2010.

[14] S.-H. Moon, C. Lee, S.-R. Lee, and I. Lee, "Joint User Scheduling and Adaptive

Intercell Interference Cancelation for MISO Downlink Cellular Systems," *IEEE Transactions on Vehicular Technology,* vol. 62, no. 1, pp. 172-181, 2013.

[15] C. Gentile, *Geolocation techniques : principles and applications* New York : Springer, 2013.

[16] J. A. Jiang, X. Y. Zheng, Y. F. Chen, C. H. Wang, P. T. Chen, C. L. Chuang, and C. P. Chen, "A Distributed RSS-Based Localization Using a Dynamic Circle Expanding Mechanism," *IEEE Sensors Journal,* vol. 13, no. 10, pp. 3754-3766, 2013.

[17] Z. He, A. Alonazi, Y. Ma, and R. Tafazolli, "A Cooperative Positioning Algorithm in Cellular Networks with Hearability Problem," *IEEE Wireless Communications Letters,* vol. 2, no. 1, pp. 66-69, 2013.

[18] Y. Li, X. Zhu, Y. Jiang, Y. Huang, and E. G. Lim, "Energy-efficient positioning for cellular networks with unknown path loss exponent," *IEEE International Conference on Consumer Electronics - Taiwan,* pp. 502-503, 2015.

[19] K. Q. T. Zhang, *Wireless communications : principles, theory and methodology*. Somerset : Wiley, 2015.

[20] *The History Of Wireless Technology- StoryMap*. Available: http://www.exigentnetworks.ie/the-history-of-wireless-technology-storymap/

[21] P. Hindle. (2015). *History of Wireless Communications*. Available: http://www.microwavejournal.com/articles/24759

[22] R. J. M. Tapan K. Sarkar, Arthur A. Oliner, Magdalena Salazar-Palma, Dipak L. Sengupta, *History of Wireless*. John Wiley & Sons, 2006.

[23] V. Esteve, E. Sanchis-Kilders, J. Jordan, E. J. Dede, and J. A. Carrasco, "UMTS networks," *IEEE Industry Applications Magazine,* vol. 12, no. 2, pp. 36-42, 2006.

[24] V. Chakravarthy, A. S. Nunez, J. P. Stephens, A. K. Shaw, and M. A. Temple, "TDCS, OFDM, and MC-CDMA: a brief tutorial," *IEEE Communications Magazine,* vol. 43, no. 9, pp. 11-16, 2005.

[25] R. Attar, D. Ghosh, C. Lott, M. Fan, P. Black, R. Rezaiifar, and P. Agashe, "Evolution of cdma2000 cellular networks: multicarrier EV-DO," *IEEE Communications Magazine,* vol. 44, no. 3, pp. 46-53 2006.

[26] M. Peng, W. Wang, and H.-H. Chen, "TD-SCDMA Evolution," *IEEE Vehicular Technology Magazine,* vol. 5, no. 2, pp. 28-41, 2010.

[27] C. L. Jean-Gabriel Remy, *LTE standards*. Wiley, 2014.

[28] S. Ahmadi, *LTE-Advanced : a practical systems approach to understanding 3GPP LTE Releases 10 and 11 radio access technologies*. Oxford Elsevier Science, 2014.

[29] S. Ahmadi, *LTE-Advanced : a practical systems approach to understanding 3GPP LTE Releases 10 and 11 radio access technologies*. Oxford : Elsevier Science, 2014.

[30] D. Kivanc, L. Guoqing, and L. Hui, "Computationally efficient bandwidth allocation and power control for ofdma," *IEEE Transactions on Wireless Communications,* vol. 2, no. 6, pp. 1150-1158, 2003.

[31] Z. Huiling and W. Jiangzhou, "Chunk-based resource allocation in OFDMA

systems - part I: chunk allocation," *IEEE Transactions on Communications,* vol. 57, no. 9, pp. 2734-2744, 2009.

[32] V. D. Papoutsis and S. A. Kotsopoulos, "Chunk-Based Resource Allocation in Multicast OFDMA Systems with Average BER Constraint," *IEEE Communications Letters,* vol. 15, no. 5, pp. 551-553, 2011.

[33] H. Zhu and J. Wang, "Chunk-Based Resource Allocation in OFDMA Systems—Part II: Joint Chunk, Power and Bit Allocation," *IEEE Transactions on Communications,* vol. 60, no. 2, pp. 499-509, 2012.

[34] C. Xiong, G. Y. Li, S. Zhang, Y. Chen, and S. Xu, "Energy- and Spectral-Efficiency Tradeoff in Downlink OFDMA Networks," *IEEE Transactions on Wireless Communications,* vol. 10, no. 11, pp. 3874-3886, 2011.

[35] H. Zhang and H. Dai, "Cochannel Interference Mitigation and Cooperative Processing in DownlinkMulticell Multiuser MIMO Networks," *EURASIP Journal on Wireless Communications and Networking,* vol. 2004, no. 2, pp. 222–235, 2004.

[36] R. Zhang, "Cooperative Multi-Cell Block Diagonalization with Per-Base-Station Power Constraints," *IEEE Journal on Selected Areas in Communications,* vol. 28, no. 9, pp. 1435-1445, 2010.

[37] Z. Jun, C. Runhua, J. G. Andrews, A. Ghosh, and R. W. Heath, "Networked MIMO with clustered linear precoding," *IEEE Transactions on Wireless Communications,* vol. 8, no. 4, pp. 1910-1921, 2009.

[38] D. Gesbert, A. Hjørungnes, and H. Skjevling, "Cooperative Spatial Multiplexing with Hybrid Channel Knowledge," *Int. Zurich Seminar on Communications* pp. 22–24, 2006.

[39] B. L. Ng, J. S. Evans, S. V. Hanly, and D. Aktas, "Distributed Downlink Beamforming With Cooperative Base Stations," *IEEE Transactions on Information Theory,* vol. 54, no. 12, pp. 5491-5499, 2008.

[40] H. Zhang, N. B. Mehta, A. F. Molisch, J. Zhang, and H. Dai, "Asynchronous Interference Mitigation in Cooperative Base Station Systems," *IEEE Transactions on Wireless Communications,* vol. 7, no. 1, 2008.

[41] C. L. Jean-Gabriel Remy, *LTE standards*. Wiley, 2014.

[42] S. Bassoy, M. Jaber, M. A. Imran, and P. Xiao, "Load Aware Self-Organising User-Centric Dynamic CoMP Clustering for 5G Networks," *IEEE Access,* vol. 4, pp. 2895-2906, 2016.

[43] J. Uk, S. Hyukmin, P. Jongrok, and L. Sanghoon, "CoMP-CSB for ICI Nulling with User Selection," *IEEE Transactions on Wireless Communications,* vol. 10, no. 9, pp. 2982-2993, 2011.

[44] F. Yang, M. Lv, and X. Liang, "Precoding Matrix Index Estimation Algorithm in LTE-A System," presented at the 2012 Fourth International Conference on Multimedia Information Networking and Security, 2012.

[45] H. Kim, H. Yu, Y. Sung, and Y. H. Lee, "An Efficient Algorithm for Zero-Forcing Coordinated Beamforming," *IEEE Communications Letters,* vol. 16, no. 7, pp. 994-997, 2012.

[46] J. Lee, Y. Kim, H. Lee, B. Ng, D. Mazzarese, J. Liu, W. Xiao, and Y. Zhou,

"Coordinated Multipoint Transmission and Reception in LTE-Advanced Systems," *IEEE Comunications Magazine,* vol. 50, no, 10, pp. 44-50, 2012.

[47] J. Jiho and L. Kwang Bok, "Transmit power adaptation for multiuser OFDM systems," *IEEE Journal on Selected Areas in Communications,* vol. 21, no. 2, pp. 171-178, 2003.

[48] A. Kuhne and A. Klein, " Adaptive Subcarrier Allocation with Imperfect Channel Knowledge Versus Diversity Techniques in a Multi-User OFDM-System," *The 18th Annual IEEE International Symposium on Personal, Indoor and Mobile Radio Communications,* 2007.

[49] S. Zukang, J. G. Andrews, and B. L. Evans, "Adaptive resource allocation in multiuser OFDM systems with proportional rate constraints," *IEEE Transactions on Wireless Communications,* vol. 4, no. 6, pp. 2726-2737, 2005.

[50] Cheong Yui Wong, R. S. Cheng, K. B. Letaief, and R. D. Murch, "Multiuser OFDM with Adaptive Subcarrier, Bit, and Power Allocation," *IEEE Journal on Selected Areas in Communications,* vol. 17, no. 10, 1999.

[51] Keunyoung Kim, Youngnam Han, and Seong-Lyun Kim, "Joint Subcarrier and Power Allocation in Uplink OFDMA Systems," *IEEE Communictaion Letters,* vol. 9, no. 6, 2005.

[52] Cheong Yui Wong, C. Y. Tsui, Roger S. Cheng, and K. B. Letaief, "A Real-time Sub-carrier Allocation Scheme for Multiple Access Downlink OFDM Transmission," *IEEE VTS 50th Vehicular Technology Conference,* 1999.

[53] Yongxue Wang, Fangjiong Chen, and G. Wei, "Adaptive subcarrier and bit allocation for multiuser OFDM system based on genetic algorithm," *2005 International Conference on Communications, Circuits and Systems,* 2005.

[54] I. Ahmed and S. P. Majumder, "Adaptive Resource Allocation Based on Modified Genetic Algorithm and Particle Swarm Optimization for Multiuser OFDM Systems," *5th International Conference on Electrical and Computer Engineering ICECE,* pp. 20-22, 2008.

[55] O. Nwamadi, A. K. Nandi, and X. Zhu, "Dynamic physical resource block allocation algorithms for uplink long term evolution," *IET Communications,* vol. 5, no. 7, pp. 1020-1027, 2011.

[56] O. Nwamadi, X. Zhu, and A. K. Nandi, "Multi-criteria ranking based greedy algorithm for physical resource block allocation in multi-carrier wireless communication systems," *Signal Processing,* vol. 92, no. 11, pp. 2706-2717, 2012.

[57] Q. Zhang, S. Jin, M. McKay, D. Morales-Jimenez, and H. Zhu, "Power Allocation Schemes for Multicell Massive MIMO Systems," *IEEE Transactions on Wireless Communications,* vol. 14, no. 11, pp. 5941-5955, 2015.

[58] P. He, L. Zhao, S. Zhou, and Z. Niu, "Water-Filling: A Geometric Approach and its Application to Solve Generalized Radio Resource Allocation Problems," *IEEE Transactions on Wireless Communications,* vol. 12, no. 7, pp. 3637-3647, 2013.

[59] M. Andrews, K. Kumaran, K. Ramanan, A. Stolyar, P. Whiting, and R. Vijayakumar, "Providing quality of service over a shared wireless link," *IEEE*

Communications Magazine, vol. 39, no. 2, pp. 150-154, 2001.

[60] H. J. Kushner and P. A. Whiting, "Convergence of proportional-fair sharing algorithms under general conditions," *IEEE Transactions on Wireless Communications,* vol. 3, no. 3, pp. 1250-1259, 2004.

[61] J.-H. Rhee, J. M. Holtzman, and D. K. Kim, "Performance analysis of the adaptive EXP/PF channel scheduler in an AMC/TDM system," *IEEE Communications Letters,* vol. 8, no. 8, pp. 497-499, 2004.

[62] H. A. M. Ramli, R. Basukala, K. Sandrasegaran, and R. Patachaianand, "Performance of well known packet scheduling algorithms in the downlink 3GPP LTE system," *IEEE 9th Malaysia International Conference on Communications,* pp. 815-820 2009.

[63] J.-G. Choi and S. Bahk, "Cell-Throughput Analysis of the Proportional Fair Scheduler in the Single-Cell Environment," *IEEE Transactions on Vehicular Technology,* vol. 56, no. 2, pp. 766-778, 2007.

[64] L. Lei, L. Chuang, C. Jun, and S. Xuemin, "Flow-level performance of opportunistic OFDM-TDMA and OFDMA networks," *IEEE Transactions on Wireless Communications,* vol. 7, no. 12, pp. 5461-5472, 2008.

[65] R. Kwan, C. Leung, and J. Zhang, "Proportional Fair Multiuser Scheduling in LTE," *IEEE Signal Processing Letters,* vol. 16, no. 6, pp. 461-464, 2009.

[66] J. Zhao, T. Q. S. Quek, and Z. Lei, "Coordinated Multipoint Transmission with Limited Backhaul Data Transfer," *IEEE Transactions on Wireless Communications,* 2013.

[67] A. Klockar, M. Sternad, A. Brunstrom, and R. Apelfrojd, "User-centric pre-selection and scheduling for coordinated multipoint systems," *International Symposium on Wireless Communications Systems,* pp. 888-894, 2014.

[68] X. Ge, H. Jin, J. Cheng, and V. C. M. Leung, "On Fair Resource Sharing in Downlink Coordinated Multi-Point Systems," *IEEE Communications Letters,* vol. 20, no. 6, pp. 1235-1238, 2016.

[69] T. J. Ross., *Fuzzy logic with engineering applications*. John Wiley and Sons, 2004.

[70] C. C. Lee, "Fuzzy Logic in Control Systems: Fuzzy Logic Controller, Part II," *IEEE Transactions on Systems, Man, and Cybernetics,* vol. 20, no. 2, 1990.

[71] X. Zhang, Y. Sun, X. Chen, S. Zhou, J. Wang, and N. B. Shroff, "Distributed Power Allocation for Coordinated Multipoint Transmissions in Distributed Antenna Systems," *IEEE Transactions on Wireless Communications,* vol. 12, no. 5, pp. 2281-2291, 2013.

[72] Q. Zhang, C. Yang, and A. F. Molisch, "Downlink Base Station Cooperative Transmission Under Limited-Capacity Backhaul," *IEEE Transactions on Wireless Communications* vol. 12, no. 8, pp. 3746-3759, 2013.

[73] J. Liu, X. Feng, C. Wang, and X. Yang, "A novel double-threshold user division method based on channel isolation and scheduling for downlink CoMP," *IEEE Global Communications Conference,* pp. 5026-5031, 2014.

[74] S. Fu, B. Wu, H. Wen, P.-H. Ho, and G. Feng, "Transmission Scheduling and Game Theoretical Power Allocation for Interference Coordination in CoMP,"

IEEE Transactions on Wireless Communications, vol. 13, no. 1, pp. 112-123, 2014.

[75] Z. Li, Y. Liu, Y. Zhang, and W. Wu, "Downlink CoMP resource allocation based on limited backhaul capacity," *China Communications,* vol. 13, no. 14, pp. 38-48, 2016.

[76] S. Mosleh, L. Liu, and J. Zhang, "Proportional-Fair Resource Allocation for Coordinated Multi-Point Transmission in LTE-Advanced," *IEEE Transactions on Wireless Communications,* vol. 15, no. 8, pp. 5355-5367, 2016.

[77] S. Shuying, M. Schubert, and H. Boche, "Rate Optimization for Multiuser MIMO Systems With Linear Processing," *IEEE Transactions on Signal Processing,* vol. 56, no. 8, pp. 4020-4030, 2008.

[78] S. Shi, M. Schubert, and H. Boche, "Downlink MMSE Transceiver Optimization for Multiuser MIMO Systems: Duality and Sum-MSE Minimization," *IEEE Transactions on Signal Processing,* vol. 55, no. 11, pp. 5436-5446, 2007.

[79] M. Chiang, C. W. Tan, D. P. Palomar, D. O'Neill, and D. Julian, "Power Control By Geometric Programming," *IEEE Transactions on Wireless Communications,* vol. 6, no. 7, pp. 2640-2651, 2007.

[80] J. Lee, Y. Kim, H. Lee, B. Ng, D. Mazzarese, J. Liu, W. Xiao, and Y. Zhou, "Coordinated Multipoint Transmission and Reception in LTE-Advanced Systems," *IEEE Comminication Magazine,* vol. 50, no. 11, pp. 44-50, 2012.

[81] A. Niemi, J. Joutsensalo, and T. Ristaniemi, "Fuzzy Channel Estimation in Multipath Fading CDMA Channel," *11th IEEE International Symposium on Personal Indoor and Mobile Radio Communications,* vol. 2, pp. 1131 - 1135, 2000.

[82] M. Morelli and U. Mengali, "A Comparison of Pilot-Aided Channel Estimation Methods for OFDM Systems," *IEEE Transactions on Signal Processing,* vol. 49, no. 12, pp. 3065 - 3073, 2001.

[83] W. Zhang, "Handover Decision Using Fuzzy MADM in Heterogeneous Networks," *2004 IEEE Wireless Communications and Networking Conference,* vol. 2, pp. 653 - 658, 2004.

[84] C. Werner, J. Voigt, S. Khattak, and G. Fettweis, " Handover Parameter Optimization in WCDMA using Fuzzy Controlling," *The 18th Annual IEEE International Symposium on Personal, Indoor and Mobile Radio Communications,* pp. 1 - 5, 2007

[85] P. Munoz, R. Barco, and I. de la Bandera, "On the Potential of Handover Parameter Optimization for Self-Organizing Networks," *IEEE Transactions on Vehicular Technology,* vol. 62, no. 5, pp. 1895-1905, 2013.

[86] Y. Wang, D. Wang, J. Pang, and G. Shen, "Self-optimization of Downlink Transmission Power in 3GPP LTE-A Heterogeneous Network," *2012 IEEE Vehicular Technology Conference* pp. 1 - 5, 2012.

[87] W. Wei, Z. Li, L. Zhuoming, and S. Xuejun, "Fuzzy Logic Power Control of Device to Device Communication underlay TD-LTE-A System," *2013 3rd International Conference on Consumer Electronics, Communications and*

Networks, pp. 320 - 323, 2013.

[88] C. Gentile, *Geolocation techniques : principles and applications* New York: Springer, 2013.

[89] J. Huang and Q. Wan, "Analysis of TDOA and TDOA/SS based geolocation techniques in a non-line-of-sight environment," *Journal of Communications and Networks* vol. 14, no. 5, pp. 533-539 2012.

[90] H. Soganci, S. Gezici, and H. Poor, " Accurate positioning in ultra-wideband systems," *IEEE Wireless Communications Letters,* vol. 18, no. 2, pp. p19-p27, 2011.

[91] K. Yu and Y. J. Guo, "Statistical NLOS Identification Based on AOA, TOA, and Signal Strength," *IEEE Transactions on Vehicular Technology,* vol. 58, no. 1, pp. 274-286, 2009.

[92] R. W. Ouyang, A. K. S. Wong, and L. Chin-Tau, "Received Signal Strength-Based Wireless Localization via Semidefinite Programming: Noncooperative and Cooperative Schemes," *IEEE Transactions on Vehicular Technology,* vol. 59, no. 3, pp. 1307-1318, 2010.

[93] S. D. Chitte, S. Dasgupta, and Z. Ding, "Distance Estimation From Received Signal Strength Under Log-Normal Shadowing: Bias and Variance," *IEEE Signal Processing Letters,* vol. 16, no. 3, pp. 216-218, 2009.

[94] A. Coluccia, "Reduced-Bias ML-Based Estimators with Low Complexity for Self-Calibrating RSS Ranging," *IEEE Transactions on Wireless Communications,* vol. 12, no. 3, pp. 1220-1230, 2013.

[95] N. Salman, A. H. Kemp, and M. Ghogho, "Low Complexity Joint Estimation of Location and Path-Loss Exponent," *IEEE Wireless Communications Letters,* vol. 1, no. 4, pp. 364-367, 2012.

[96] M. Borenovic, A. Neskovic, and N. Neskovic, "Vehicle Positioning Using GSM and Cascade-Connected ANN Structures," *IEEE Transactions on Intelligent Transportation Systems,* vol. 14, no. 1, pp. 34-46, 2013.

[97] K. Li, P. Jiang, E. L. Bodanese, and J. Bigham, "Outdoor Location Estimation Using Received Signal Strength Feedback," *IEEE Communications Letters,* vol. 16, no. 7, pp. 978-981, 2012.

[98] R. M. Vaghefi, M. R. Gholami, R. M. Buehrer, and E. G. Strom, "Cooperative Received Signal Strength-Based Sensor Localization With Unknown Transmit Powers," *IEEE Transactions on Signal Processing,* vol. 61, no. 6, pp. 1389-1403, 2013.

[99] Q. Li, Z. Feng, W. Li, and T. A. Gulliver, "A New Multicast Scheduling Scheme for Cellular Networks," *IEEE Wireless Communications Letters,* vol. 3, no. 1, pp. 26-29, 2014.

[100] G. Wang, H. Chen, Y. Li, and M. Jin, "On Received-Signal-Strength Based Localization with Unknown Transmit Power and Path Loss Exponent," *IEEE Wireless Communications Letters,* vol. 1, no. 5, pp. 536-539, 2012.

[101] S. Savazzi, M. Nicoli, F. Carminati, and M. Riva, "A Bayesian Approach to Device-Free Localization: Modeling and Experimental Assessment," *IEEE Journal of Selected Topics in Signal Processing,* vol. 8, no. 1, pp. 16-29, 2014.

[102] C. Zhang, P. Liu, W. Qi, and L. Wei, "Multipath cancellation by frequency diversity: a training-free and analytical approach to accurate RSS ranging in ground-deployed wireless sensor networks," *Electronics Letters,* vol. 50, no. 6, pp. 471-473, 2014.

[103] K. Li, J. Bigham, E. L. Bodanese, and L. Tokarchuk, "Outdoor Location Estimation in Changeable Environments," *IEEE Communications Letters,* vol. 17, no. 11, pp. 2072-2075, 2013.

[104] K. Li, J. Bigham, and L. Tokarchuk, "Validation of a Probabilistic Approach to Outdoor Localization," *IEEE Wireless Communications Letters,* vol. 2, no. 2, pp. 167-170, 2013.

[105] R. Malaney, "Nuisance Parameters and Location Accuracy in Log-Normal Fading Models," *IEEE Transactions on Wireless Communications,* vol. 6, no. 3, pp. 937-947, 2007.

[106] R. K. Martin, A. S. King, J. R. Pennington, R. W. Thomas, R. Lenahan, and C. Lawyer, "Modeling and Mitigating Noise and Nuisance Parameters in Received Signal Strength Positioning," *IEEE Transactions on Signal Processing,* vol. 60, no. 10, pp. 5451-5463, 2012.

[107] M. R. Spiegel, *Schaum's outline of theory and problems of complex variables : with an introduction to conformal mapping and its applications*. New York : McGraw-Hill, 1964., 1964.